Studies on Photocatalysis by Silica and Silica - Based Materials(Dissertation_全文)

AUTHOR(S):

Yoshida, Hisao

Studies on Photocatalysis by Silica and Silica-Based Materials

HISAO YOSHIDA

1997

Preface

The development of the science of catalysis, which offers a key technology for tomorrow human life, is supported by discoveries of new catalytic systems and understanding of the principles governing the phenomena. Needless to say, new catalytic systems are always desired; so many catalytic systems have been discovered and innovated, and each one has afforded a great impact to chemical industry and preservation of the environment. Among them, nowadays photocatalysis attracts a great deal of attention as a seed of a new clean technology since the photocatalysts work by solar energy in principle.

In this thesis, the author compiles his studies being focused on "silica" that is one of the most familiar materials to catalysis researchers, and some interesting new discoveries about the photocatalytic function of "silica and silica-based materials" are shown; most attractive topics would be those concerning photometathesis of olefins and photoepoxidation of propene over bare silica.

At first, the photoepoxidation of propene by gaseous oxygen was found in course of testing the photooxidation activity of magnesium oxide supported on silica. The discovery was very delightful because the epoxidation of propene by molecular oxygen on a heterogeneous catalyst has been desired for a long time. When the activity was successively tested without gaseous oxygen as a blank test, photometathesis reaction of propene taking place on the sample was found. We were surprised at the fact that metathesis occurred on such a material, since the metathesis reaction is believed to proceed only over transition metal complexes in heterogeneous and homogeneous systems. Moreover, we carried out the investigation about the activity of bare silica without magnesium oxide, leading the discovery of photometathesis of propene over the bare silica. We were excited by the discovery since the silica was usually regarded as an inert material for catalytic action. These phenomena had been unexpected until we

discovered them. Here a new group of photocatalysts were created. The investigation of their details are in progress even now. We believe that this discovery should have contributed to the development of science in catalysis.

The development of silica-based catalysts is very hopeful since the modification of silica would be possible by adding suitable other elements. When a small amount of heteroatoms was loaded on silica surface, the local structure of the heteroatom oxide would be affected by the silica matrix and a new function would be arisen by an interaction with silica as shown in this thesis. Silica materials would have great potentiality to create new catalysis. We hope that the concept presented in this thesis would become a basis of the new silica-photocatalysts family.

The present thesis is a collection of the studies which have been carried out at the Department of Molecular Engineering, Graduate School of Engineering, Kyoto University during 1991 - 1995 under supervision of Professor Satohiro Yoshida, and have been continued under the suggestion of Professor Tadashi Hattori at the Department of Applied Chemistry, Graduate School of Engineering, Nagoya University since 1995. This work was partially supported by the Fellowships of the Japanese Society for the Promotion of Science (JSPS) for Japanese Junior Scientists from 1993 to 1995.

The author wishes to express his sincere gratitude to Professor Satohiro Yoshida for his guidance and valuable discussions and suggestions. The author would like to make a grateful acknowledgment to Professor Tadashi Hattori in Nagoya University for his constructive suggestions and helpful encouragement. Special acknowledgment is made to Professor Takuzo Funabiki for his instructive discussions and continual encouragement. The author is deeply grateful to Professor Tsunehiro Tanaka for his fruitful discussions and strict but heartwarming advice and encouragement throughout this work. Hearty thanks should be made to Assistant Professor Atsushi Satsuma for his kind help to complete this thesis.

The author is grateful to Professor Masaharu Nomura for his advice in recording XAFS spectra and also to the staffs of Photon Factory at KEK for making the beam available. Hearty thanks are made to Professor Nobuhiro Kosugi, Dr. Yasutaka Takata and Dr. Jun-ichi Adachi of UVSOR at Institute for Molecular Science for their helpful suggestion for measurements of XAFS spectra and also to Associate Professors Masao Kamada, Toyohiko Kinoshita, Messrs. Osamu Matsudo and Jun-ichiro Yamazaki and the staffs of UVSOR for the assistance in XAFS measurements. Acknowledgment is made to Professor Sadao Hasegawa and Mr. Masahiko Morooka at Tokyo Gakugei University for his collaboration in Mg K-edge XAFS experiments. The author acknowledges Professor Masahide Yamamoto at Department of Polymer Chemistry, Graduate School of Engineering, Kyoto University for his help in luminescence experiment. The authors would like to thank Professor Masao Kitamura at Graduate School of Science, Kyoto University for his kindness to offer some reference samples. The author thanks Mr. Yoshiharu Honda at Environment Preservation Center, Kyoto University, for XRF analysis. Grateful acknowledgment is made to Shinji Inagaki and Dr. Yoshiaki. Fukushima at Toyota Central R & D Labs., Inc., for their help in the preparation of samples.

Hearty thanks are made to all the members of the group of catalysis research led by Professor Satohiro Yoshida, specially to Dr. Yasuo Nishimura, Messrs. Takeshi Hiraiwa, Hirokatsu Hayashi, Toshio Waku, Hiroyuki Nojima, Yasutaka Nagai, Hiroaki Nakagawa, Kazuhiro Nakatsuka, Sakae Takenaka, Dr. Hirofumi Aritani, Messrs. Hiroyuki Hirano, Takahiro Nagase, Muneshige Yamamoto, Hiroki Hayashi, Takaki Hatsui, Shigehiro Matsuo, Tamio Yamazaki for the collaborations. Thanks must be made to all the members of the group of catalysis research led by Professor Tadashi Hattori for their exciting discussions and continual encouragement, specially to Messrs. Koji Nishi, Ken-ichi Shimizu, Koichi Kimura, Tatsuya Abe, Yoshitaka Inaki, Yuko Kato for the collaborations. Grateful acknowledgment is made to Dr. Kohki Ebitani at Osaka Univesity for his hearty encouragement.

The Data Processing Center of Kyoto University is acknowledged for generous use of the FACOM M1800 computer system to perform the numerical calculations. The X-ray absorption experiments were performed under the approval of the Photon Factory Program Advisory Committee. The soft X-ray absorption experiments were supported by the Joint Studies Program of UVSOR of the Institute for Molecular Science.

The author sincerely thanks his parents Sachio and Akiko for their understanding and continual encouragement. The author deeply thanks his sister Chiaki and Hanada family for their helpful encouragement. Finally, the author thanks from the bottom of his heart his wife Dr. Tomoko Yoshida for her collaboration, fruitful discussion and hearty encouragement throughout this work.

Hisao Yoshida

Nagoya

December, 1997

Contents

General Introduction

To keep the global environment safe, we have to make an all-out effort for reduction of environmental disruption. To produce energy to support our modern life style, we consume huge fossil fuels day by day and release exhaust gases, wastes and chemical pollutants. For the present and coming generations, we should consider the issues. Since we cannot help to consume huge energy to maintain our modern life styles, we had better turn our attention to renewable clean energy. A bright solution is utilization of the solar energy; day after day, the sun provides abundant sunlight to us.

Catalysis is a key technology for solving problems in modern and future world. Catalysts promote chemical processes under milder condition than in the case without them; they can reduce consumption of energy. Catalysts make new reaction pathways; they can avoid to produce undesirable chemicals and can cut down unnecessary reactants and energy. Although heat is necessary to activate catalysts, it is significant that the catalysts function without needless and extra heat. If they function with solar energy, no energy for heating is needed. Photocatalysts function with photoenergy. Photocatalysts which works by sunlight consumes no petroleum and other energy sources to work. In these days, the evolution of photocatalysts is strongly desired.

Although the origin of photocatalysis in history is not certain, since "Honda-Fujishima effect" in water decomposition over electrode of semiconductors was found,[1, 2] the catalytic conversion of photoenergy to chemical energy by powder of semiconductor has attracted a great deal of attention. Many studies for heterogeneous photocatalysis followed "Honda-Fujishima effect."

Semiconductors as photocatalysts

The function of semiconductors such as TiO_2,[1, 2] ZnO,[3, 4]is explained on the basis of the energy band structure which consists of electron-vacant conduction band, electron-filled valence band and forbidden band between them. Semiconductors are excited by an energy larger than that of energy gap between the bottom level of the conduction band and the top level of valence band, where excited electrons in the conduction band and positive holes in valence band are produced. These electrons and positive holes play a role in reduction and oxidation, respectively.

The representative topic is decomposition of water into hydrogen and oxygen over powdered semiconductors loaded with co-catalysts. The excited electrons react with protons, then H_2 are produced, while positive holes produce O_2 by oxidation of OH^-. While semiconductive compounds such as CdS undergo photo-corrosion in an aqueous solution,[5] some of metal oxide semiconductors are available for water photocleavage. Typical catalysts are listed as follows; metal loaded TiO_2,[6-8] RuO_2/TiO_2,[9-11] modified $SrTiO_3$,[12-14] ZrO_2,[15] family of layered materials $K_4Nb_6O_{17}$,[16-18] $Pb_{1-x}K_{2x}Nb_2O_6$,[19] $RuO_x/Na_2Ti_6O_{13}$,[20] $RuO_x/BaTi_4O_9$,[21] *etc*.

Among the photocatalysts, the most important one is TiO_2 which exhibits high oxidizing ability originated from the photoexcited holes and also has high stability. This ability of TiO_2 is practically applied to our daily lives; *e.g*. TiO_2-loaded glass beads for oil decomposition,[22] street and highway walls containing TiO_2 for decomposition of NO_x as air pollutants in a city, self-cleaning tiles and TiO_2 loaded filter for air-cleaner. Degradation of pollutants in the aqueous solution such as CN^-,[23] organo-halogen compounds,[24-26] aromatics,[27]by using TiO_2 is also studied.

It can be said that the photocatalysis by semiconductors has already been established in a view of academic interest; there remains only minor improvement by modification.

Supported transition metal oxide systems as photocatalysts

Other approach to develop the photocatalysis is attempted to find new catalytic system, *e.g*., supported catalysts systems. In some cases, photocatalytically inactive compounds often turn into photoactive materials when they are dispersed on support materials.

One of famous example is vanadium oxide. Although the bulk V_2O_5 is photoinactive, highly dispersed vanadium oxide species on silica[28] or porous Vycor glass[29] are photoactive; they are excited by UV irradiation, emit photoluminescence and function as photocatalysts.[30-37] The supports change the local structure of vanadium oxide to tetrahedral VO_4^{3-} species on their surface[38-40] and let the vanadium species to be photoactive. In the supported vanadium system, silica is superior than other materials.[30, 31] The V_2O_5/SiO_2 system has recently improved by addition of alkali-ion, and become to function under visible light.[37, 41-43]

The local structure of titanium oxide is changed by being dispersed on the support. Also in this case, silica and family of silica materials play an important role as support material. The support in these systems affect not only the dispersion of titanium oxide particle but also the local structure of highly dispersed titanium oxide species, and simultaneously, the photocatalytic activity changes. Especially, silica supports[44-47] are reported to improve the photocatalytic properties.

In these ways, new photocatalytic properties are expected by supporting on the surface of the other oxide. There are many reports concerning supported photocatalysts; Nb/SiO_2,[48, 49] Ta/SiO_2,[50] Mo/SiO_2,[51-53] Ag/ZSM-5,[54, 55] Cu/SiO_2[56], Cu/zeolite,[57-59] *etc*.

Silica is often used as a support for photocatalysts but is usually inactive itself. However, it can function as a catalyst for some reactions; *e.g*. ammoximation of ketones,[60, 61] dehydrogenation of heptane,[62] dehydrogenation of ethanol,[63, 64] selective oxidation of methane,[65-68] oxidative dehydrogenation of propane,[69] oxidation of carbon monoxide,[70, 71] hydrogen-deuterium exchange,[72] and some organic reaction catalyzed by weak acid.[73] Silica is also activated by photoirradiation and promotes some reactions; *e.g*. isomerization of butene,[74] photooxidation of carbon monoxide,[75] olefin photooxidation.[76, 77] Therefore, silica seems to

have a kind of photoactivity and to be a good support material for photocalatysts as mentioned above.

Survey of this thesis

In this thesis, the author presents his studies focused on the "silica and silica-based materials." In part I, preparation chemistry of silica-based catalysts is presented on two systems. At first, the structure of niobium oxalate complexes and the interaction between the complexes and silica surface are discussed. Second, the difference in the local structure of magnesium oxide species in/on silica prepared by the four different methods are discussed. In part II, characterization of silica and silica-based materials by means of phosphorescence spectroscopy is presented. The author found that the silica modified by heteroatoms, Mg or Al, shows the phosphorescence spectrum with fine structure. The phosphorescence spectroscopy would be powerful characterization method for photocatalysts. Part III is the central part in this thesis; comprising studies concerning photocatalysis over silica and silica-based catalysts; photometathesis alkene, photoepoxidation of propene and photooxidation of carbon monoxide.

References

1 A. Fujishima and K. Honda, *Bull. Chem. Soc. Jpn.*, 1971, **44**, 1148.
2 A. Fujishima and K. Honda, *Nature*, 1972, **238**, 37.
3 G. Heiland, E. Mollow and F. Stöckmann, *Solid State Physics* (Academic Press Inc., 1959), vol. 8.
4 E. Baur, *Helv. Chim. Acta*, 1927, **10**, 901.
5 R. Memming, *Electrochim. Acta*, 1980, **25**, 77.
6 A. V. Bulatov and M. L. Khidekel, *Izv. Akad. Nauk. SSSR, Ser. Khim.*, 1976, 1902.
7 S. Sato and J. M. White, *Chem. Phys. Lett.*, 1980, **72**, 83.
8 K. Yamaguti and S. Sato, *J. Chem. Soc., Faraday Trans. 1*, 1985, **81**, 1237.
9 T. Kawai and T. Sakata, *Chem. Phys. Lett.*, 1980, **72**, 87.
10 D. Duonghong, E. Borgarello and M. Graetzel, *J. Am. Chem. Soc.*, 1981, **103**, 4685.
11 E. Borgarello, J. Kiwi, E. Peizzetti, M. Visca and M. Graetzel, *J. Am. Chem. Soc.*, 1981, **103**, 6324.
12 M. S. Wrighton, P. T. Wolczanski and A. B. Ellis, *J. Solid State Chem.*, 1977, **22**, 17.

Supported transition metal oxide systems as photocatalysts

Other approach to develop the photocatalysis is attempted to find new catalytic system, *e.g.*, supported catalysts systems. In some cases, photocatalytically inactive compounds often turn into photoactive materials when they are dispersed on support materials.

One of famous example is vanadium oxide. Although the bulk V_2O_5 is photoinactive, highly dispersed vanadium oxide species on silica[28] or porous Vycor glass[29] are photoactive; they are excited by UV irradiation, emit photoluminescence and function as photocatalysts.[30-37] The supports change the local structure of vanadium oxide to tetrahedral VO_4^{3-} species on their surface[38-40] and let the vanadium species to be photoactive. In the supported vanadium system, silica is superior than other materials.[30, 31] The V_2O_5/SiO_2 system has recently improved by addition of alkali-ion, and become to function under visible light.[37, 41-43]

The local structure of titanium oxide is changed by being dispersed on the support. Also in this case, silica and family of silica materials play an important role as support material. The support in these systems affect not only the dispersion of titanium oxide particle but also the local structure of highly dispersed titanium oxide species, and simultaneously, the photocatalytic activity changes. Especially, silica supports[44-47] are reported to improve the photocatalytic properties.

In these ways, new photocatalytic properties are expected by supporting on the surface of the other oxide. There are many reports concerning supported photocatalysts; Nb/SiO_2,[48, 49] Ta/SiO_2,[50] Mo/SiO_2,[51-53] Ag/ZSM-5,[54, 55] Cu/SiO_2[56], Cu/zeolite,[57-59] *etc.*

Silica is often used as a support for photocatalysts but is usually inactive itself. However, it can function as a catalyst for some reactions; *e.g.* ammoximation of ketones,[60, 61] dehydrogenation of heptane,[62] dehydrogenation of ethanol,[63, 64] selective oxidation of methane,[65-68] oxidative dehydrogenation of propane,[69] oxidation of carbon monoxide,[70, 71] hydrogen-deuterium exchange,[72] and some organic reaction catalyzed by weak acid.[73] Silica is also activated by photoirradiation and promotes some reactions; *e.g.* isomerization of butene,[74] photooxidation of carbon monoxide,[75] olefin photooxidation.[76, 77] Therefore, silica seems to

have a kind of photoactivity and to be a good support material for photocalatysts as mentioned above.

Survey of this thesis

In this thesis, the author presents his studies focused on the "silica and silica-based materials." In part I, preparation chemistry of silica-based catalysts is presented on two systems. At first, the structure of niobium oxalate complexes and the interaction between the complexes and silica surface are discussed. Second, the difference in the local structure of magnesium oxide species in/on silica prepared by the four different methods are discussed. In part II, characterization of silica and silica-based materials by means of phosphorescence spectroscopy is presented. The author found that the silica modified by heteroatoms, Mg or Al, shows the phosphorescence spectrum with fine structure. The phosphorescence spectroscopy would be powerful characterization method for photocatalysts. Part III is the central part in this thesis; comprising studies concerning photocatalysis over silica and silica-based catalysts; photometathesis alkene, photoepoxidation of propene and photooxidation of carbon monoxide.

References

1 A. Fujishima and K. Honda, *Bull. Chem. Soc. Jpn.*, 1971, **44**, 1148.

2 A. Fujishima and K. Honda, *Nature*, 1972, **238**, 37.

3 G. Heiland, E. Mollow and F. Stöckmann, *Solid State Physics* (Academic Press Inc., 1959), vol. 8.

4 E. Baur, *Helv. Chim. Acta*, 1927, **10**, 901.

5 R. Memming, *Electrochim. Acta*, 1980, **25**, 77.

6 A. V. Bulatov and M. L. Khidekel, *Izv. Akad. Nauk. SSSR, Ser. Khim.*, 1976, 1902.

7 S. Sato and J. M. White, *Chem. Phys. Lett.*, 1980, **72**, 83.

8 K. Yamaguti and S. Sato, *J. Chem. Soc., Faraday Trans. 1*, 1985, **81**, 1237.

9 T. Kawai and T. Sakata, *Chem. Phys. Lett.*, 1980, **72**, 87.

10 D. Duonghong, E. Borgarello and M. Graetzel, *J. Am. Chem. Soc.*, 1981, **103**, 4685.

11 E. Borgarello, J. Kiwi, E. Peizzetti, M. Visca and M. Graetzel, *J. Am. Chem. Soc.*, 1981, **103**, 6324.

12 M. S. Wrighton, P. T. Wolczanski and A. B. Ellis, *J. Solid State Chem.*, 1977, **22**, 17.

13 F. T. Wagner and G. A. Somorjai, *J. Am. Chem. Soc.*, 1980, **102**, 5459.

14 K. Domen, S. Naito, S. Soma, M. Ohnishi and K. Tamaru, *J. Chem. Soc., Chem. Commun.*, 1980, 543.

15 K. Sayama and H. Arakawa, *J. Phys. Chem.*, 1993, **97**, 531.

16 K. Domen, A. Kudo, A. Shinozaki, A. Tanaka, K. Maruya and T. Ohnishi, *J. Chem. Soc., Chem. Commun.*, 1986, 356.

17 K. Domen, A. Kudo, M. Shibata, A. Tanaka, K. Maruya and T. Ohnishi, *J. Chem. Soc., Chem. Commun.*, 1986, 1706.

18 K. Sayama, A. Tanaka, K. Domen, K. Maruya and T. Ohnishi, *J. Catal.*, 1990, **124**, 541.

19 Y. Inoue, O. Hayashi and K. Sato, *J. Chem. Soc., Faraday Trans.*, 1990, **86**, 2277.

20 Y. Inoue, T. Kubokawa and K. Sato, *J. Chem. Soc., Chem. Commun.*, 1990, 1298.

21 Y. Inoue, T. Niiyama, Y. Asai and K. Sato, *J. Chem. Soc., Chem. Commun.*, 1992, 579.

22 A. Heller, 1st International Conference on TiO2 Photocatalytic Purification and Treatment of Water and Air London, Ontario, Canada, 1992), pp. 17.

23 S. N. Frank and A. J. Bard, *J. Phys. Chem.*, 1977, **81**, 1487.

24 A. L. Pruden and D. F. Ollis, *J. Catal.*, 1983, **81**, 404.

25 C.-Y. Hsiao, C.-L. Lee and D. F. Ollis, *J. Catal.*, 1983, **82**, 418.

26 D. F. Ollis, C.-Y. Hsiao, L. Budiman and C.-L. Lee, *J. Catal.*, 1984, **88**, 89.

27 R. W. Mathews, *J. Chem. Soc., Faraday Trans. 1*, 1984, **80**, 457.

28 A. M. Gritscov, V. A. Shvets and V. B. Kazansky, *Chem. Phys. Lett.*, 1975, **35**, 511.

29 M. Anpo, I. Tanahashi and Y. Kubokawa, *J. Phys. Chem.*, 1980, **84**, 3440.

30 S. Yoshida, Y. Magatani, S. Noda and T. Funabiki, *J. Chem. Soc., Chem. Commun.*, 1981, 601.

31 S. Yoshida, Y. Matsumura, S. Noda and T. Funabiki, *J.Chem.Soc.,Faraday Trans.I*, 1981, **77**, 2237.

32 S. Yoshida, T. Tanaka, T. Funabiki and T. Yonezawa, in *ROC-Japan Symposium on Fundamental and Applied Catalysis -New Horizon and Approaches* ed. 1982, 59.

33 S. Yoshida, T. Tanaka, M. Okada and T. Funabiki, *J. Chem. Soc., Faraday Trans. 1*, 1984, **80**, 119.

34 T. Tanaka, M. Ooe, T. Funabiki and S. Yoshida, *J. Chem. Soc., Faraday Trans.1*, 1986, **82**, 35.

35 T. Tanaka, Y. Nishimura, S. Kawasaki, M. Ooe, T. Funabiki and S. Yoshida, *J. Catal*, 1989, **118**, 327.

36 S. Yoshida, T. Tanaka, Y. Nishimura, T. Hiraiwa, T. Tanaka and T. Funabiki, 13th Seminar on Science and Technology, Japan-Taiwan Catalysis Seminar 1990, 185.

37 S. Takenaka, T. Kuriyama, T. Tanaka, T. Funabiki and S. Yoshida, *J. Catal*, 1995, **155**, 196.
38 T. Tanaka, Y. Nishimura, S.-i. Kawasaki, T. Funabiki and S. Yoshida, *J. Chem. Soc., Chem. Commun.*, 1987, 506.
39 T. Tanaka, H. Yamashita, R. Tsuchitani, T. Funabiki and S. Yoshida, *J. Chem. Soc., Faraday Trans.1*, 1988, **84**, 2987.
40 S. Yoshida, T. Tanaka, Y. Nishimura, H. Mizutani and T. Funabiki, *Proc. 9th Int. Congr. Catal.*, 1988, **3**, 1473.
41 T. Tanaka, S. Takenaka, T. Funabiki and S. Yoshida, *Chem. Lett.*, 1994, 1585.
42 T. Tanaka, S. Takenaka, T. Funabiki and S. Yoshida, *J. Chem. Soc., Faraday Trans.*, 1996, **92**, 1975.
43 S. Takenaka, T. Tanaka, T. Funabiki and S. Yoshida, *Catal. Lett.*, 1997, **44**, 67.
44 S. Yoshida, S. Takenaka, T. Tanaka and T. Funabiki, *Journal de Physique IV*, 1997, **7**, C2-859.
45 S. Yoshida, S. Takenaka, T. Tanaka, H. Hirano and H. Hayashi, *Stud. Surf. Sci. Catal.*, 1996, **101**, 871.
46 M. Anpo, N. Aikawa and Y. Kubokawa, *J. Chem. Soc., Chem. Commun.*, 1994, 644.
47 M. Anpo, N. Aikawa, Y. Kubokawa, M. Che, C. Louis and E. Giamello, *J. Phys. Chem.*, 1985, **89**, 5017.
48 S. Yoshida, Y. Nishimura, T. Tanaka, H. Kanai and T. Funabiki, *Catalysis Today*, 1990, **8**, 67.
49 T. Tanaka, S. Takenaka, T. Funabiki and S. Yoshida, *Chem. Lett.*, 1994, 809 .
50 T. Tanaka, S. Takenaka, T. Funabiki and S. Yoshida, in *Acid-Base Catalysis II* ed. H. Hattori, M. Misono and Y. Ono, Kodansha, Tokyo, 1994, 485.
51 M. Anpo, I. Tanahashi and Y. Kubokawa, *J. Chem. Soc., Faraday Trans. 1*, 1982, **78**, 2121.
52 T. Ono, M. Anpo and Y. Kubokawa, *J. Phys. Chem.*, 1986, **90**, 4780.
53 M. Anpo, M. Kondo, C. Louis, M. Che and S. Coluccia, *J. Am. Chem. Soc.*, 1989, **111**, 8791.
54 M. Matsuoka, E. Matsuda, K. Tsuji, H. Yamashita and M. Anpo, *Chem. Lett.*, 1995, 375.
55 M. Matsuoka, E. Matsuda, K. Tsuji, H. Yamashita and M. Anpo, *J. Mol. Catal. A: Chem.*, 1996, **107**, 399.
56 M. Anpo, T. Nomura, T. Kitao, E. Giamello, M. Che and M. A. Fox, *Chem. Lett.*, 1991, 889.
57 H. Yamashita, M. Matsuoka, K. Tsuji, Y. Shioya, E. Giamello, M. Che and M. Anpo, *Stud. Surf. Sci. Catal.*, 1995, **92**, 227.

58 H. Yamashita, M. Matsuoka, K. Tsuji, Y. Shioya and M. Anpo, *J. Phys. Chem.*, 1996, **100**, 397.
59 H. Yamashita, Y. Ichikawa, M. Anpo, M. Hashimoto, C. Louis and M. Che, *J. Phys Chem.*, 1996, **100**, 16041.
60 J. N. Armor, *J. Catal.*, 1981, **70**, 72.
61 J. N. Armor and P. M. Zambri, *J. Catal.*, 1982, **73**, 57.
62 M. Lacroix, G. M. Pajonk and S. J. Teichner, *J. Catal.*, 1986, **101**, 314.
63 Y. Matsumura, K. Hashimoto and S. Yoshida, *J. Chem. Soc., Chem. Commun.*, 1987, 1599.
64 Y. Matsumura, K. Hashimoto and S. Yoshida, *J. Catal.*, 1989, **117**, 135.
65 G. N. Kastanas, G. A. Tsigdinos and J. Schwank, *J. Chem. Soc., Chem. Commun.*, 1988, 1298.
66 G. N. Kastanas, G. A. Tsigdinos and J. Schwank, *Appl. Catal.*, 1988, **44**, 33.
67 A. Parmaliana, F. Frusteri, D. Miceli, A. Mezzapica, M. S. Scurrell and N. Giordano, *Appl. Catal.*, 1991, **78**, L7.
68 A. Parmaliana, F. Frusteri, A. Mezzapica, D. Miceli, M. S. Scurrell and N. Giordano, *J. Catal*, 1993, **143**, 262.
69 A. Parmaliana, V. Sokolovskii, F. Arena, F. Frusteri and D. Miceli, *Catal. Lett.*, 1996, **40**, 105.
70 Y. Matsumura, K. Hashimoto and J. B. Moffat, *J. Phys. Chem.*, 1992, **96**, 10448.
71 Y. Matsumura, J. B. Moffat and K. Hashimoto, *J. Chem. Soc. Faraday Trans.*, 1994, **90**, 1177.
72 E. W. Bittner, B. C. Bockrath and J. M. Solar, *J. Catal.*, 1994, **149**, 206.
73 K. Tanabe, M. Misono, Y. Ono and H. Hattori, *Stud. Surf. Sci. Catal.*, 1989, vol. 51.
74 A. Morikawa, M. Hattori, K. Yagi and K. Otsuka, *Z. Phys. Chem., N.F.*, 1977, **104**, 309.
75 A. Ogata, A. Kazusaka and M. Enyo, *J. Phys. Chem.*, 1986, **90**, 5201.
76 M. Anpo, C. Yun and Y. Kubokawa, *J. Catal.*, 1980, **61**, 267.
77 Y. Kubokawa, M. Anpo and C. Yun, in *Proc. 7th Int. Congr. Catal.* ed. T. Seiyama and K. Tanabe, Kodansha, Tokyo, 1981, vol. B, p. 1170.

Part I

Preparation chemistry of silica-based catalysts

Introduction of Part I

Preparation of heterogeneous catalysts is one of the important subjects in science and technology of catalysis chemistry. We, catalysts researchers, often face the difficulty of obtaining reproducible activities; a subtle difference in the preparation conditions often leads to a drastic variation in catalytic performance. Therefore understanding and analysis of the chemical phenomena in the preparation process is very important.

The study of preparation chemistry is anchored in basic science: solid state chemistry, surface and colloid chemistry, advanced analytical chemistry. Since catalysis takes place on the active sites, we must study the local structure of the active site for complete understanding of catalysis. To study the preparation chemistry of solid catalysts, we had better observe directly the states of element which is to function as an active site. It is also important to observe the local structure at each step of preparation. The direct observation has been made possible by the development of physical techniques; one of the most powerful techniques for that purpose is XAFS (X-ray Absorption Fine Structure) by which we can look into the local structures and electronic states of the desired elements.

In the part I of this thesis, the author describes preparation chemistry of heterogenous catalysts in two systems, Nb/SiO_2 and $MgO\text{-}SiO_2$. The author employed XAFS to study the local structures of Nb and Mg. The background of the X-ray absorption spectroscopy is briefly summarized below, followed by the survey of this part.

XAFS (X-ray absorption fine structure)

X-ray absorption spectrum recorded in the transmission mode is defined by

$$\mu(E)t = \ln(I_0 / I) \qquad (1)$$

where E is the photon energy, μ is an X-ray absorption coefficient, t is an effective thickness of the sample, I_0 and I are the incident and transmitted X-ray intensities, respectively.

Absorption decreases monotonously with an increase in X-ray energy at first. It abruptly arises at $E = E_0$; an ionization energy to release a core electron of X-ray absorbing atom. Then, the absorbance again decreases with E.

The X-ray absorption spectrum is conventionally divided into near-edge and extended fine structures; X-ray Absorption Near Edge Structure (XANES) observed in the range of 50 eV around the edge, and Extended X-ray Absorption Fine Structure (EXAFS) observed in the range of 50-1000 eV above the edge.[1]

EXAFS

The theory and application of EXAFS has already been established, and is presented by some reviews[2-4] and books.[1, 5] EXAFS is due to the interference of the outgoing wave of electrons excited by X-ray with the backscattering wave of electrons scattered by surrounding atoms. That is, EXAFS is principally dependent on the configuration of atoms surrounding the X-ray absorbing atom.

The EXAFS oscillation function χ (k) is represented as follows in the single scattering appoximation.

$$\chi(k) = \Sigma\, N_j / (kr_j^2)\, f_j(k) \exp(-2\sigma_j^2 k^2)\, S_j(k) \sin(2kr_j + \delta_j(k)) \qquad (2)$$

where N_j is the coordination number of j th scattering atoms at distance r_j, k the wavenumber of photoelectron, $f_j(k)$ the back scattering amplitude, σ_j the Debye-Waller factor, $\delta_j(k)$ the phase shift and $Sj(k)$ the damping factor for compensation of loss by inelastic scattering. The wavenumber, k, can be obtained according to the equation;

$$k = h^{-1}\, 2\pi\, (2m(E - E_0))^{1/2} \qquad (3)$$

where h is Planck's constant, m is the mass of an electron.

The normalized EXAFS, $\chi(E)$, is obtained as follows;

$$\chi(E) = (\mu(E) - \mu_b(E)) / \mu_0(E) \qquad (4)$$

where $\mu_b(E)$ is a back ground due to the absorption excluding EXAFS oscillation and $\mu_0(E)$ is an absorption of the target atom on the assumption that the atom is isolated in free space. $\mu_0(E)$ is determined in this thesis according to the equation,

$$\mu_0(E) = A / E^{2.75}. \qquad (5)$$

A is a constant to be determined by least-squares fitting, as proposed and applied by Tanaka *et al.*[6]

Thus, the EXAFS oscillation represented in k-space is extracted from experimental data. By performing Fourier filtering[7] and curve-fitting to the extracted EXAFS oscillation, information of the coordination numbers and the interatomic distances can be obtained.

XANES

XANES are usually the easiest part of the absorption spectrum to be measured for complex chemical systems because of its intense change of the relevant spectral features. Since XANES phenomena are more complex than EXAFS phenomena, the analysis of XANES is not as straightforward as that of EXAFS. In other words, however, it may mean that XANES contains much information. The information obtained from XANES are valence state, coordination symmetry, local structure and electronic structure. Indeed, there are a number of works which show the information obtained from the XANES region as follows.

The edge shift often exhibits a change of valence, as in the case of Mn,[8] Fe[9] and Cu compounds,[10] or electronegativity of the nearest-neighbor ligand, as in the case of Si and Al

compounds.[11] Although not common, it can be used as an index whether or not occurs the change in the electronic state of the X-ray absorbing atom.

Pre-edge peak appearing at a low energy side of the edge, is often attributed to 1s → n d transition, which is mainly caused by mixing of p and d orbitals of the X-ray absorbing atom. It has been well known that pre-edge peak becomes more intense as the symmetry around the absorbing atom is distorted from the regular octahedron.[12-14] Therefore, there are plenty of works discussing the symmetry around absorbing atom by the intensity of pre-edge peak.[15-20] For example, Yoshida *et al.*[21] concluded that tetrahedrally coordinated VO_4 species supported on SiO_2 change to octahedrally coordinated VO_6 species by adsorption of H_2O on the basis of the change in pre-edge peak intensity. In addition, the enhancement of the pre-edge peak is sometimes caused by mixing of p orbitals of the ligands with d orbitals of the absorbing atom, which is observed as large pre-edge peaks in XANES of Ti, V and Cr compounds as examples.[22-25]

Resonance peaks, the fine structure observed above edge, give us information of the local site symmetry and the coordination number has been deduced by comparison to that of standard compounds.[26, 27] The local structure of carbonaceous compounds deposited on zeolite[28] and the structural change during synthesis of zeolite from ferrisilicate[29] were discussed by using resonance peaks in XANES as a fingerprint. The configulation of adsorbed molecules[27, 30, 31] were also discussed. However the analyses using this region are still not common.

Recently, a deconvolution method of XANES spectra was developed for the characterization of catalysts by Yoshida *et al.*.[32] This deconvolution method has been applied to some systems.[33, 34] In addition, superposition analysis of XANES spectra was developed and applied to the $Mg(OH)_2$ - MgO phase transformation.[35, 36]

Survey of this part

In the part I of this thesis, the author describes preparation chemistry in two systems. In the chapter 1, niobium oxide species were stabilized on the surface of silica by equilibrium

adsorption method, a kind of impregnation method, using niobium oxalate complexes as precursors. The structure of niobium species at some steps during the preparation process were investigated by the XAFS analysis; the deconvolution of XANES and the curve fitting of EXAFS. The best condition for the preparation of highly dispersed niobium oxide species on silica is shown there. In the chapter 2, four samples in silica-magnesia systems were prepared from two starting materials; $Mg(NO_3)_2$ and $Mg(OCH_3)_2$, and by two preparation method; impregnation and sol-gel method. In this case, only the samples after calcination were investigated because of the limitation in condition of Mg K-edge XAFS measurment.

References

1 B. K. Teo, *EXAFS : Basic Principles and Data Analysis* (Springer-Verlag, Berlin, 1986).
2 P. A. Lee, P. H. Citrin, P. Eisenberger and B. M. Kincaid, *Rev. Mod. Phys.*, 1981, **53**, 769.
3 J. C. Bart, *Adv. catal.*, 1986, **34**, 203.
4 J. C. Bart and G. Vlaic, *Adv. Catal.*, 1987, **35**, 1.
5 Y. Iwasawa, in *X-ray Absorption Fine Structure for Catalysts and Surfaces* ed. Y. Iwasawa, World Scientific, Danvers, 1996, vol. p. 1.
6 T. Tanaka, H. Yamashita, R. Tsuchitani, T. Funabiki and S. Yoshida, *J. Chem. Soc., Faraday Trans. 1*, 1988, **84**, 2987.
7 D. E. Sayers, E. A. Stern and F. W. Lytle, *Phys. Rev. Lett.*, 1971, **27**, 1204.
8 N. M. D. Brown, J. B. McMonagle and G. N. Greaves, *J. Chem. Soc. Faraday Trans. 1*, 1984, **80**, 589.
9 H. Kanai, H. Mizutani, T. Tanaka, T. Funabiki, S. Yoshida and M. Takano, *J. Mater. Chem.*, 1992, **2**, 703.
10 G. Vlaic, J. C. J. Bart, W. Cavigiolo and S. Mobilio, *Chem. Phys. Lett.*, 1980, **76**, 453.
11 J. Wong, Z. U. Rek, M. Rowen, T. Tanaka, F. Schäfers, B. Müller, G. N. George, I. J. Pickering, G. Via, B. DeVries, G. E. J. Brown and M. Fröba, *Physica B*, 1995, **208&209**, 220.
12 G. Michell and W. W. Beeman, *J. Chem. Phys.*, 1952, **20**, 1298.
13 F. A. Cotton and H. P. Hanson, *J. Chem. Phys.*, 1956, **25**, 619.
14 H. P. Hanson and J. R. Knight, *Phys. Rev.*, 1956, **102**, 632.
15 K. I. Asakura, I.Kuroda, H.Kobayashi, T. Shirakawa, H., *Bull. Chem. Soc. Jpn.*, 1985, **58**, 2113.

16 P. E. Best, *J. Chem. Phys.*, 1966, **44**, 3248.
17 G. L. Glen and C. G. Dodd, *J. Appl. Phys.*, 1968, **39**, 5372.
18 W. Seka and H. P. Hanson, *J. Chem. Phys.*, 1969, **50**, 344.
19 R. G. Shulman, Y. Yafet, P. Eisenberger and W. E. Blumberg, *Proc. Natl. Acad. Sci. U.S.A.*, 1976, **73**, 1384.
20 U. C. Srivastava and H. L. Nigam, *Cood. Chem. Rev.*, 1973, **9**, 275.
21 S. Yoshida, T. Tanaka, Y. Nishimura, H. Mizutani and T. Funabiki, *Proc. 9th Inten. Congr. Catal.*, 1988, 1473.
22 A. L. Roe, D. J. Schneider, R. I. Mayer, J. W. Pyrz, J. Widom and L. Que, *J. Am. Chem. Soc.*, 1984, **106**, 1676.
23 T. Tanaka, Y. Nishimura, S. Kawasaki, T. Funabiki and S. Yoshida, *J. Chem. Commun.*, 1987, 506.
24 T. D. Tullius, W. O. Gillum, R. M. K. Carlson and K. O. Hodgson, *J. Am. Chem. Soc.*, 1980, **102**, 5670.
25 M. R. Antonio, R. G. Teller, D. R. Sandstrom, M. Mehicic and J. F. Brazdil, *J. Phys. Chem.*, 1988, **92**, 2939.
26 D. H. Maylotte, J. Wong, R. L. S. Peters, F. W. Lytle and R. B. Greegor, *Science*, 1981, **214**, 554.
27 H. Ishii, K. Asakura, T. Ohta, Y. Kitajima and H. Kuroda, *Jpn. J. Appl. Phys.*, 1992, **32 Suppl. 32-2**, 368.
28 S. M. Davis, Y. Zhou, M. A. Freeman, D. A. Fischer, G. M. Meitzner and J. L. Gland, *J. Catal.*, 1992, **139**, 322.
29 H. Shimada, N. Matsubayashi, M. Imamura, T. Sato, Y. Yoshimura, K. Okabe, K. Asakura and A. Nishijima, *Physica B*, 1995, **208&209**, 593.
30 Y. Teraoka, T. Tai, H. Furukawa, S. Shikagawa, K. Asakura and Y. Iwasawa, *Shokubai*, 1990, **32(6)**, 426.
31 A. Bianconi, *EXAFS for Inorganic Systems*. C. D. Garner and S. S. Hasnain, Eds., (Daresbury Lab. Rep. DL/SCI/R17, Daresbury, 1981).
32 S. Yoshida, T. Tanaka, T. Hanada, T. Hiraiwa, H. Kanai and T. Funabiki, *Catal. Lett.*, 1992, **12**, 277.
33 T. Tanaka, T. Hanada, S. Yoshida, T. Baba and Y. Ono, *Jpn. J. Appl. Phys.*, 1993, **32 Suppl. 32-2**, 481.
34 T. Tanaka, T. Yoshida, S. Yoshida, T. Baba and Y. Ono, *Physica B*, 1995, **208&209**, 687.
35 T. Yoshida, T. Tanaka, H. Yoshida, S. Takenaka, T. Funabiki, S. Yoshida and T. Murata, *Physica B*, 1995, **208&209**, 581.
36 T. Yoshida, T. Tanaka, H. Yoshida, T. Funabiki, S. Yoshida and T. Murata, *J. Phys. Chem.*, 1995, **99**, 10890.

Chapter 1

Preparation chemistry of niobium oxide on silica-support

Abstract

The loading amount and dispersion of tetrahedral species of niobium oxide in the NbO_x/SiO_2 catalysts could be controlled by adjusting the niobium and ammonia concentrations of impregnating oxalic acid solutions in the preparation by the equilibrium adsorption method. The structures in the solution and the adsorption state of the niobium oxalate complexes were the most important to control the structures of niobium oxide species on the silica surface. The addition of ammonia to the preparation solution affected not only the pH of the solution but also the states of the liquid-solid interface. The former influences the structure and adsorption equilibrium of niobium oxalate complex, while the latter changes the state of adsorption.

Introduction

Supported metal oxide often shows different catalytic activity from its bulk oxide, in this case niobium oxide. Therefore, recently, many studies on the nature of supported niobium species have been done.

Our previous studies have shown that niobium oxides supported on silica catalyze the photooxidation of propene to produce propanal or propene oxide and the selectivity is influenced by the local structure of niobium oxide species.[1-3] In this system, propene oxide was selectively produced over the highly dispersed monomeric NbO_4 species prepared by the equilibrium adsorption method, while propanal was formed over the oligomeric NbO_4 species. Polymeric NbO_6 octahedra directly produced ethanal, whereas oligomeric NbO_4 indirectly produced it via a propene oxide intermediate. This example makes it clear that the control of the local structure of niobium species is important and it is a key technique to obtain the desired performance of supported catalysts. From this view point, many investigations have been done to control the surface species by selecting suitable support materials (PVG,[4] silica, alumina, magnesia, titania and zirconia[5-8]), niobium precursors (niobium oxalate, niobium ethoxide and niobium complexes with hydrocarbon ligands[9-15]) and preparation methods.[16-19] Among them, the equilibrium adsorption of metal complexes in aqueous solution is a simple and possible procedure for preparation of uniform species dispersed on supports.[3, 20] Local structure and/or dispersion of metal oxide species prepared in this method was often controlled by the pH of solution. In the case of vanadium oxide catalysts supported on silica,[20] the dispersion of vanadium oxide species on silica depended on the pH of impregnating solution; some aggregates of octahedral species are formed from a low pH (3.3) solution, while tetrahedral species are dominant in the preparation from solutions of pH higher than 6.6, since the structure of vanadate species in a solution were varied with the pH. In the case of the niobium oxalate solution, the niobium complexes were varied with the pH: monomer oxalate complexes existed in a low pH solution and a dimer complex existed in a high pH solution.[21]

The catalytic activity of niobium oxide on silica was affected by the pH of impregnating solution.[3] Therefore, it has been concluded that there were some types of local structure showing specific activity. There remain the following questions. Is there a correlation between the structure of the complexes in the impregnation solution and the structure of active species in the prepared catalysts and what is the important factor controlling the dispersion and local structure in this method?

In this study, we focus our attention on the structures of niobium species formed during the preparation procedure by the equilibrium adsorption method under several conditions to clarify the key factors controlling the structures of the niobium oxide species supported on silica. We measured the X-ray absorption fine structure (XAFS) for the structural analysis of niobium species in preparation.[22]

Experimental

NbO_x/SiO_2 samples were prepared by the equilibrium adsorption method as follows. Niobic acid (CBMM) was dissolved in a 0.5 M oxalic acid solution ranging in niobium concentration from 8.4 to 134.4 mM. The pH of the solutions at this stage were ca. 0.8. The pH was controlled ranging in pH from 1 to 5 by addition of aqueous ammonia. A sample solution of the pH 1 was readjusted to pH 0.8 by addition of oxalic acid (referred to as " 0.8* "). Silica (1 g; BET surface area: 568 $m^2\ g^{-1}$) was impregnated with the solutions (50 cm^3) in a stoppered flask and magnetically stirred for 24 h at room temperature, followed by filtration with suction. The silica adsorbing Nb ions was dried at 343 K for 24 h and calcined in a dry air stream at 773 K for 5 h. These were evacuated at 673 K for 2 h and sealed in polyethylene packs for the measurements of X-ray absorption spectra. Silica was prepared by a sol-gel method as described elsewhere.[23] Niobium oxalate complex in solid state as a reference sample was donated by Prof. Wachs. Niobium pentoxide was prepared from niobic acid by calcination at 773 K for 5 h.

The loading amount of niobium oxide as Nb_2O_5 in the samples were determined by X-ray fluorescence intensities. Nb K-edge XAFS were recorded at room temperature at BL-6B, 7C, 10B stations in KEK-PF (proposal No. 93G005) with a Si(311) or Si(111) two crystal monochromator (ring energy 2.5-3.0 GeV and stored current 140-370 mA). XAFS measurements were carried out to the following samples: (1) niobium oxalic acid solutions, (2) niobium complexes adsorbed on the silica, which were filtered after achieving the adsorption equilibrium followed by drying at 343 K, (3) calcined niobium oxides on silica under ambient condition, (4) evacuated ones in situ and (5) reference compounds such as niobium pentoxide, niobium oxalate and so on. Low loading samples were measured in the fluorescence mode and others including reference samples were measured in the transmission mode.

XANES (X-ray absorption near edge structure) analyses were carried out as described elsewhere.[2] The normalized XANES spectrum was deconvoluted to a set of one pre-edge peak (A) and two post-edge peaks (B, C) with a continuum absorption curve (Fig. 1). The peaks at higher energy than the three peaks were not considerate because the assignment is very difficult due to the influence by multiple scattering of photo-electrons.

Curve-fitting analysis of Fourier-filtered EXAFS was performed by using empirical parameters extracted from EXAFS of reference compounds. As there were no suitable niobium compounds to extract the parameters for Nb-O, Nb-Nb and Nb-C (of carboxyl group) shells, we adopted the parameters for a Mo-O shell extracted from K_2MoO_4, for a Zr-Zr shell from ZrC, for a Rh-C (of carboxyl group) shell from Rh(I) Vasca complex[24] to fit the Nb-O, Nb-Nb and Nb-C (carbonyl) shells, respectively. As there were also no suitable compounds for the Nb-Si shell, the phase shift function for a Mo-Mg shell was calculated from Mo-O, Ni-O and Ni-Mg shells in K_2MoO_4, NiO and Ni-Mg-O solid solution,[25] to fit the Nb-Si shell. The amplitude function for a Ni-Mg shell extracted from a Ni-Mg-O solid solution[25] was adopted to fit the function for the Nb-Si shell.

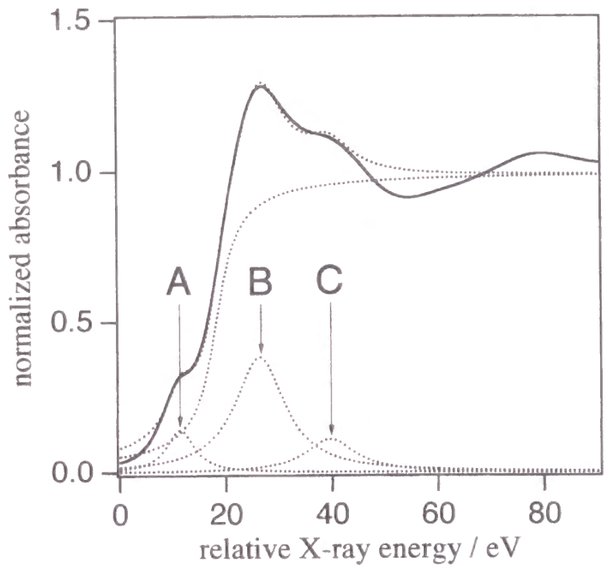

Fig. 1 The normalized Nb K-edge XANES and its deconvoluted spectra of niobium oxalate in solid state. A, B, C: see text.

Results and Discussion

Loading amount of niobium oxide on silica

When niobium acid was dissolved in an oxalic acid aqueous solution, it would exist as a niobium oxalate complex in the solution.[21] It precipitated in a solution of low niobium concentration at a pH above 5, while precipitation was observed in a lower pH value for a solution of high niobium concentration. The preparation of the samples was carried out under such conditions that the precipitation did not occur.

The adsorption equilibrium would control the loading amount; we can obtain the information of the equilibrium state from the loading amount of niobium oxide in the prepared samples. Fig. 2 shows a relationship between the loading amount of niobium oxide supported on silica and the niobium concentration of the prepared oxalic acid solution. The plots were divided into two groups: (*a*) pH 0.8 to 4 and (*b*) of pH 5. Both groups showed a good relationship in which the loading amount was proportional to the concentration of niobium, although only one point was out of line. This indicates that the loading amount could be controlled by the niobium concentrations at each pH. Fig. 3 shows the effect of pH of the impregnating solution on the loading amount. It was clear that the loading amounts were constant in the range of pH 0.8 to 4 for the solution of low niobium concentrations although the constant range was reduced in the case of high niobium concentration. The loading amounts in this range corresponded to 3%-4% of the dissolved niobium ions. In the case of the solution of pH 5, the adsorbed amount was 8%-13%. This difference of the loading amount indicates that the chemistry of adsorption depends on the pH. It is expected that the structures of niobium complexes or the surface condition of silica were affected by the pH of the solutions. It has been reported that a monomeric niobium oxalate complex changed to a dimeric niobium oxalate complex before precipitation.[21] Therefore, the niobium complex would be a dimeric one in the solution of pH 5, and it would be a monomeric one in the solution of pH 1-4 and the adsorption equilibrium of these complexes could be different from each other.

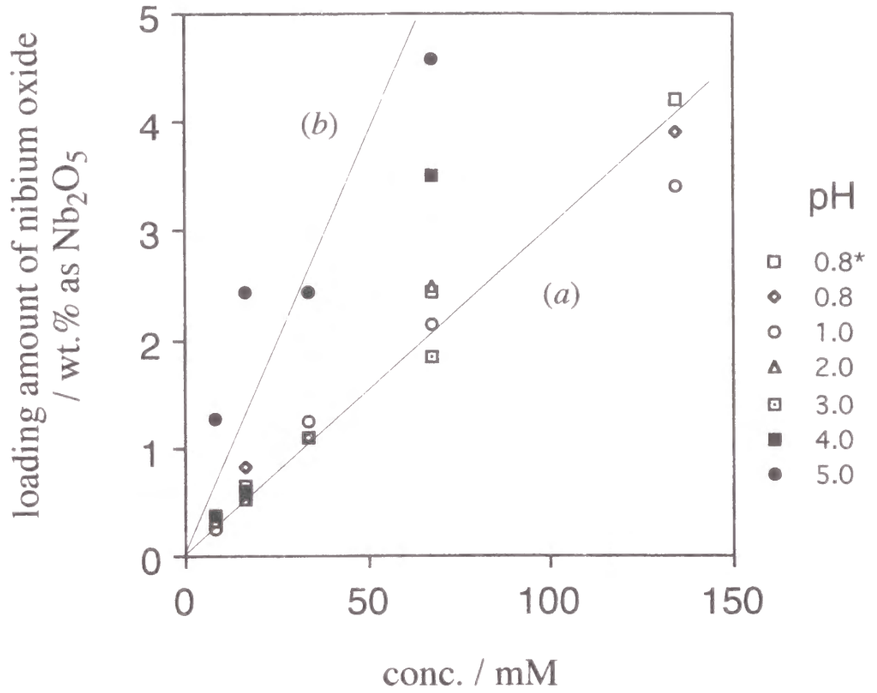

Fig. 2 Loading amount of niobium oxide as Nb_2O_5 vs. concentration of niobium ion in the impregnating solutions. The points along line (*a*) are those for samples prepared with pH 0.8-4 solutions and the points along line (*b*) are those with pH 5 solutions.

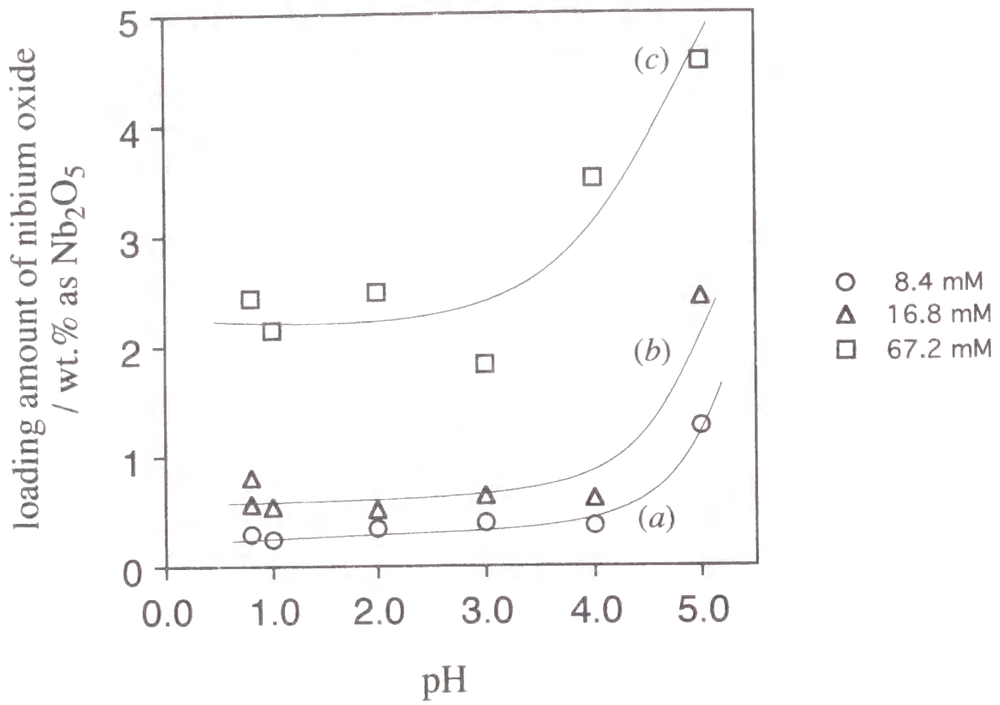

Fig. 3 Effect of pH and niobium concentration of the impregnating solutions on the loading amount of niobium oxides on silica. The niobium concentration of the solutions were (*a*) 8.4, (*b*) 16.8 and (*c*) 67.2 mM, respectively.

Assuming that all of the species in the solution of pH 5 exist as the dimer complex, the concentration of niobium complex should be a half in comparison with the case of all species being the monomer under the constant niobium concentration as shown in eq.(1).

$$C_1 = 2 \cdot C_2, \tag{1}$$

where, C_1: concentration of the monomer complex in the solution,

C_2: that of the dimer complex.

The concentrations of adsorbed complexes and loading amount of niobium oxide were as follows:

$$C_{a1} = K_1 \cdot C_1, \quad C_{a2} = K_2 \cdot C_2, \tag{2}$$

$$A_1 = a \cdot C_{a1}, \quad A_2 = 2 \cdot a \cdot C_{a2}, \tag{3}$$

where, C_{a1}: concentration of the adsorbed monomer complex,

C_{a2}: that of the dimer complex,

K_1: equilibrium constant of the monomer complex,

K_2: that of the dimer complex,

A_1 : loading amount of niobium oxide prepared from the monomer,

A_2: loading amount of niobium oxide prepared from the dimer,

a : constant for conversion the concentration to the loading amount.

Therefore,

$$A_2 = (K_2 / K_1) \cdot A_1. \tag{4}$$

If the equilibrium constant of monomer complex K_2 is equal to K_1, the loading amount A_2 should be equal to A_1, as well. However, the slope of the line (b) of the solution of pH 5 in Fig. 2 was more than two times greater than that of line (a), indicating that the value of K_2 was

more than two times greater than that of K_1. The equilibrium in the solution of pH 5 was obviously shifted to the adsorption side in comparison with the equilibrium of the solution of pH 0.8-4.

Niobium complexes in the solution

The structure of the niobium complex in the oxalic acid solution was studied by X-ray absorption spectroscopy. XANES spectra of niobium complexes in the solution and niobium oxalate in solid state are shown in Fig. 4*a*, Fig.4*e* and Fig.4*i*. The line shape of each spectrum resembles each other as a whole: broad and small pre-edge and two peaks in post-edge, indicating that the local structures of niobium complexes in the oxalic acid solution resemble that of the octahedral niobium oxalate complex $[NbO(C_2O_4)_2H_2O]^-$ in solid state.[21]

To discuss in detail, a deconvolution analysis was carried out,[2, 22] as shown in Fig. 1 as an example. The areas and positions of the three peaks are given in Table 1. Those of the sample in the solution of pH 0.8 were similar to those of solid niobium oxalate, although the area of peak A of solid niobium oxalate was slightly larger than that of the sample in the solution. The agreement of these values indicates that the complex at pH 0.8 has the same structure as the niobium oxalate complex $[NbO(C_2O_4)_2H_2O]^-$.

The peak positions of pre-edge peak (A) and the post-edge peak (B or C) for the species in the solutions were also the same regardless of pH values, suggesting that the excited electrons from 1s orbital in niobium were captured by the same empty bound states; the bonds of ligands-niobium ions in each pH solution are the same. On the other hand, the peak areas varied with pH in the range from 0.8 to 5. With an increase in the pH, the peak area of B decreased and that of C increased; the ratio of areas (B/C) was reduced, indicating that the local structure was slightly changed by the pH. In the study of XANES of vanadium compounds, the B peak was concluded to be a characteristic peak of octahedra.[2] The reduction of B peak area suggested that the symmetry was a little distorted. While the area and position of peak A was constant, therefore, the coordination structure around a niobium atom in the solution of pH 5 is described to be distorted octahedral.

The solution of pH 0.8* contained more oxalic acid than the solution of pH 1; more oxalic acid and ammonia than the solution of pH 0.8. The A peak area of the complex in the solution of pH 0.8* was larger than that in the solution of pH 1 and 0.8; the B peak area was smaller, suggesting that the symmetry of complex was distorted. This would be caused by an increase in the concentration of oxalic anions which were further coordinated to the niobium atom.

EXAFS spectra (Fig. 5) also showed the structural variation of the niobium oxalate complexes. In the higher wavenumber region, 10-16 $Å^{-1}$, the oscillation was drastically varied with the pH of solution. This region of EXAFS oscillation was affected by the atoms which have a maximum of back scattering amplitude in this region, usually heavy atoms such as niobium atom in this case, and/or affected by "focusing effects",[26-28] which was caused by a collinear arrangement of three (and more) atoms including a target atom; a carboxyl group is typical and the oxalic anion also shows the effect.

The peaks at 2-4 Å in Fourier-transform of EXAFS (Fig. 6) indicates the contribution from oxalate anions. The curve-fitting analysis of Fourier-filtered EXAFS revealed that the niobium complexes in the solution have five Nb-O bonds (2.11 Å) and one Nb=O bond (1.70 Å). A fairly strong scattering by the second (2.8, 3.2 Å) and third (3.8, 4.25 Å) neighboring oxygen and/or carbon was observed by the focusing effect, indicating that oxalate ions are coordinated to the niobium atom. Two coordination distances observed at each second and third shells would mean that each oxalate anion binds to the niobium atom asymmetrically.

Jehng and Wachs had studied niobium complexes in the solutions by Raman spectroscopy.[21] On the basis of their conclusion and our results, the major complexes in the solution is suggested as follows (Scheme 1): $[NbO(C_2O_4)_2H_2O]^-$ in the range of pH 0.8-4, a dimeric complex such as $[Nb_2O_4(C_2O_4)_2(H_2O)_2]^{2-}$ at pH 5 before precipitation, and $[NbO(C_2O_4)_3]^{3-}$ at pH 0.8*. The feature of EXAFS at pH 1 (Fig. 5d) was slightly different from other samples. This may result from the existence of other complexes such as $[NbO(C_2O_4)(OH)_2H_2O]^-$ or $[NbO(C_2O_4)_2(OH)_2]^{3-}$ as proposed by Jehng and Wachs.[21]

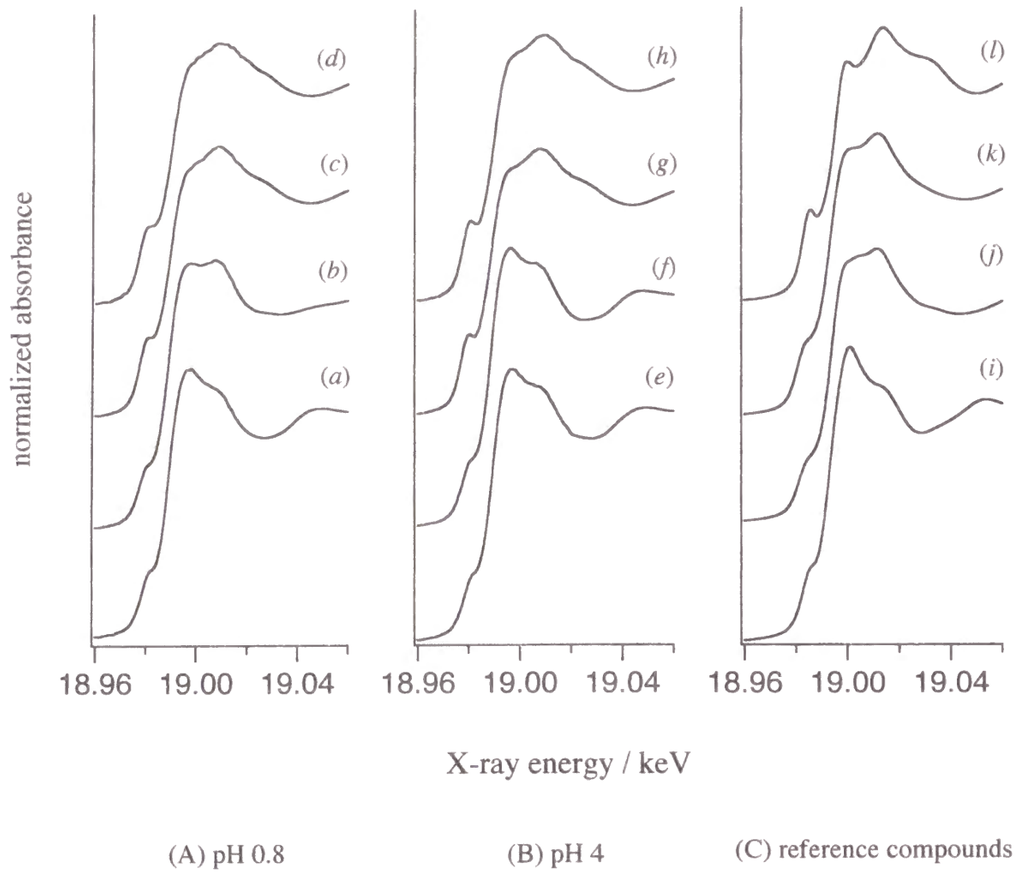

Fig. 4 Nb K-edge XANES spectra of samples during the preparation from the solution of pH 0.8 (A), 4 (B) and the spectra of reference compounds (C). (*a*), (*e*) solution samples, (*b*), (*f*) dried samples, (*c*), (*g*) calcined samples (ambient), (*d*), (*h*) calcined sample (evacuated). (*i*) niobium oxalate in solid state, (*j*) niobium pentoxide, (*k*) niobic acid and (*l*) $YbNbO_4$. The niobium concentration of the impregnating solutions in (A) and (B) were 16.8 mM.

Table 1 Areas and relative peak positions of pre-edge in Nb K-edge XANES spectra of niobium complexes in aqueous solution (67.2 mM) and niobium oxalate(solid).

pH	Peak position / eV [a]			Area / eV			
	A [b]	B	C	A	B	C	B/C
0.8	-7.0	7.8	18.5	1.0	6.8	1.9	3.6
1.0	-6.8	7.9	19.0	0.94	6.4	2.5	2.6
3.0	-6.9	7.5	18.5	0.94	6.5	2.5	2.6
5.0	-6.8	7.7	18.9	0.97	5.2	2.7	1.9
0.8*	-6.9	7.9	19.1	1.3	6.0	2.2	2.7
oxalate	-6.9	8.2	20.2	1.4	6.7	1.9	3.5

[a] Relative energy to the ionization threshold determined as the position of the inflection point of the continuum curve. [b] Consult Fig.1 for the peak assignment.

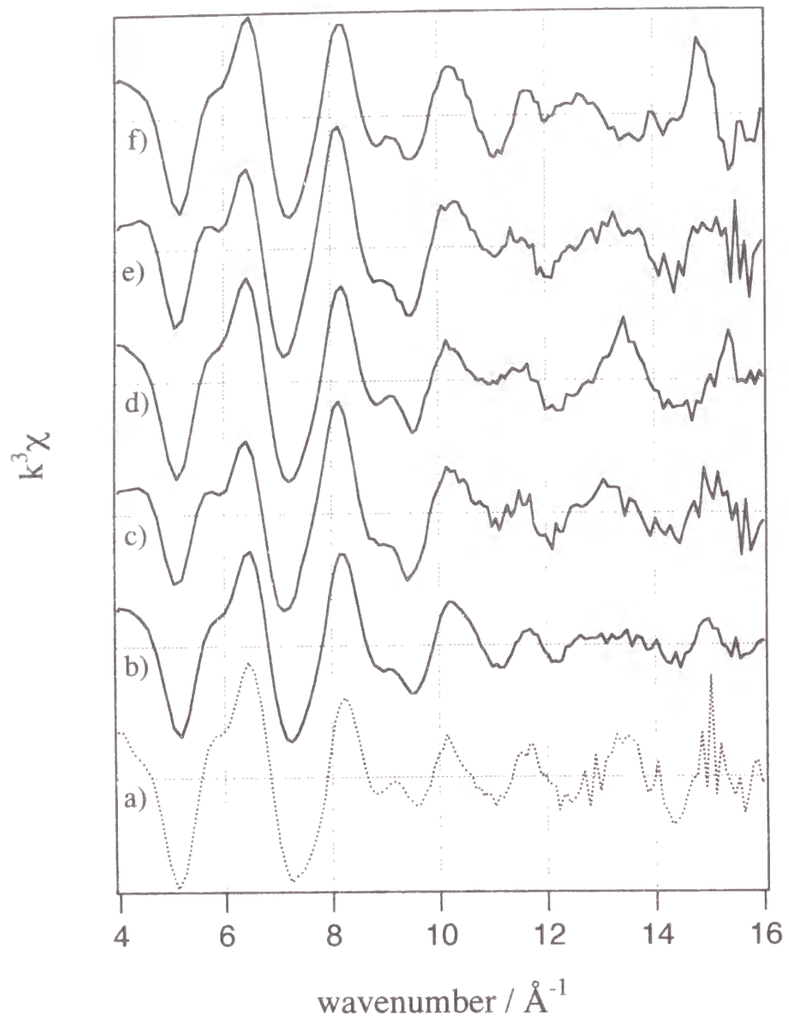

Fig. 5 The k^3 weighted EXAFS spectra of (*a*) the niobium oxalate in solid state and (*b*)-(*f*) the solution samples (67.2 mM) of various pH (*b*) 0.8, (*c*) 0.8*, (*d*) 1, (*e*) 3 and (*f*) 5.

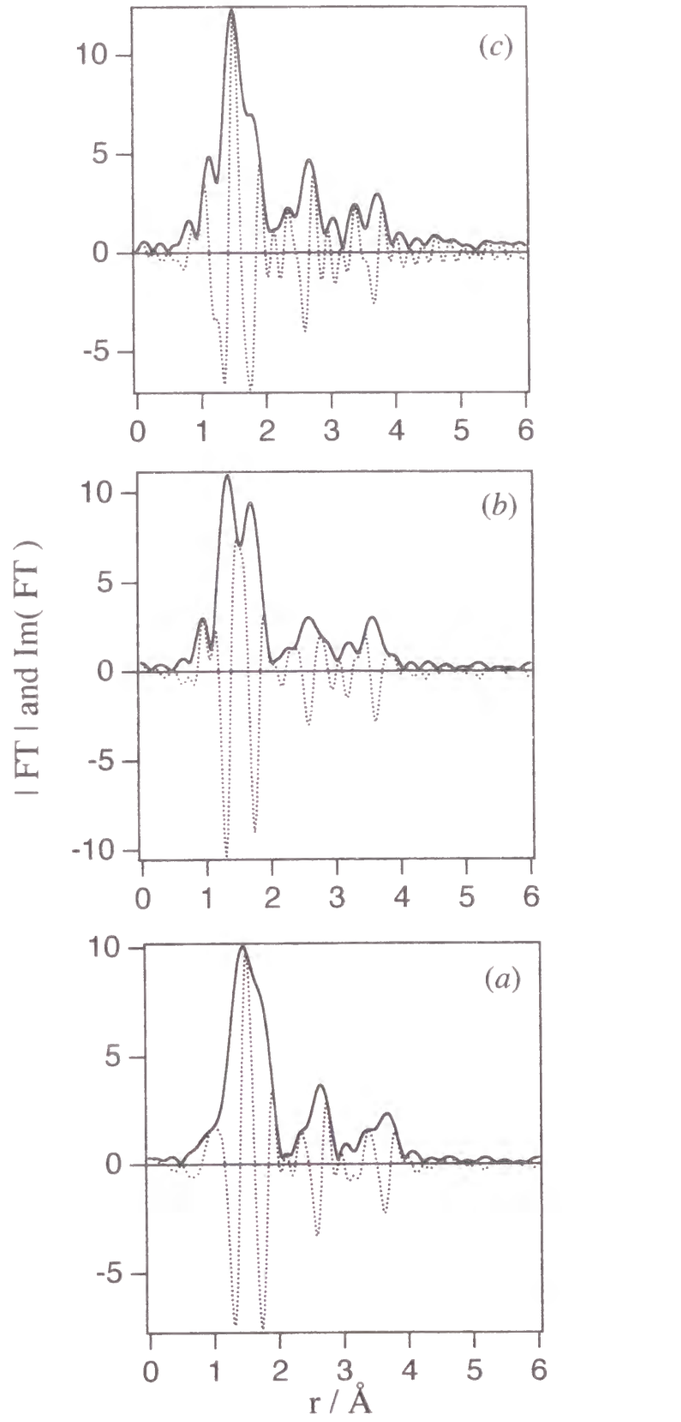

Fig. 6 Absolute of FT(|FT|) and imaginary part of FT(Im(FT)) of the EXAFS of the solution samples of (*a*) pH 0.8, (*b*) pH 1 and (*c*) pH 5. The niobium concentration was 67.2 mM.

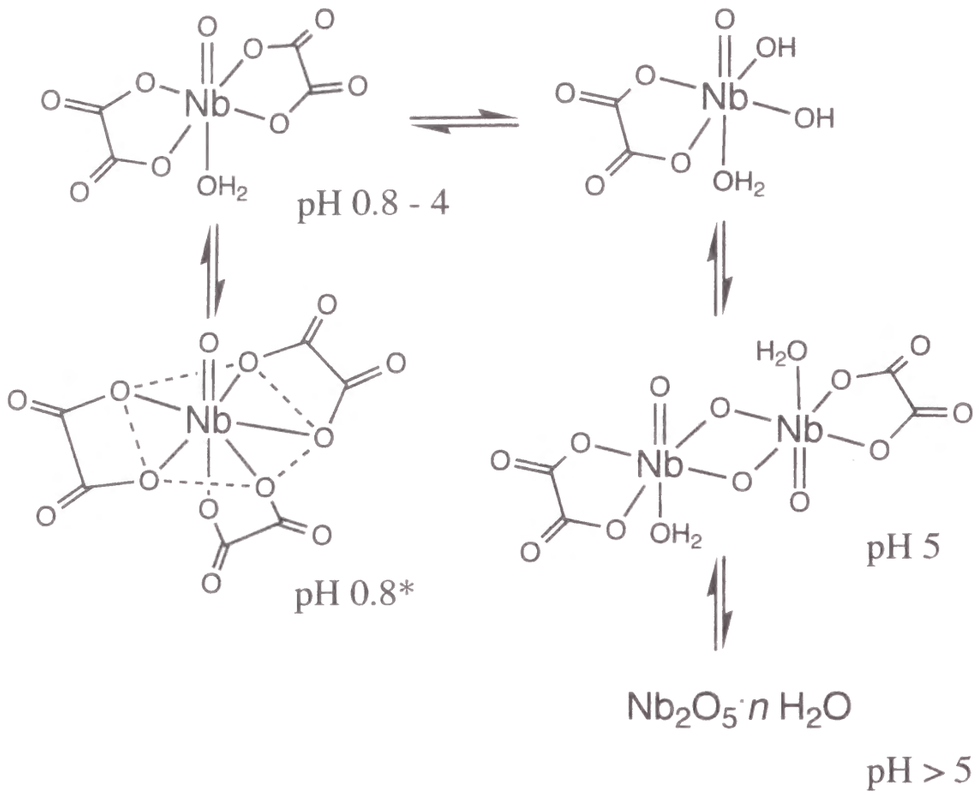

Scheme 1 Proposed structures of niobium complexes in oxalic acid solutions.

Dried samples (before calcination)

The adsorbed niobium species on silica which were obtained by filtration followed by drying at 343 K are discussed in this section. XANES spectra of adsorbed niobium species on silica clearly showed the structural difference caused by different pH of impregnating solutions (Fig. 4*b*, Fig. 4*f*). The adsorbed species prepared from the solution of pH 4 exhibited the same XANES spectrum (Fig. 4*f*) as that of the complex in the solution (Fig. 4*e*). The samples prepared from the solutions of pH 1-4 and 0.8* also exhibited the same spectra. In these cases, ammonia existed in the solutions. On the other hand, the spectrum of adsorbed species prepared from the pH 0.8 solution (Fig. 4*b*), which was free from ammonia, was different from that in the solution, or rather, resembled that of niobium pentoxide (Fig. 4*j*) or niobic acid (fig. 4*k*).

The difference was clearly demonstrated in the position and area of pre-edge listed in Table 2. Although the peak position and peak area did not change by adsorption on silica in the case of the pH 0.8* and 4, those values changed in the case of pH 0.8. These results suggest that the complex in the pH 0.8 solution, which did not contain ammonia, reacted with the silica surface and the coordination geometry around the niobium atom was changed from that in the solution. On the contrary, the coordination states of the complexes in the solution containing ammonia did not change in contact with the silica surface.

The EXAFS oscillations (Fig. 7) of the dried samples became unclear above 10 Å region. This could be caused by the interactions of complexes with silica surface. The structural parameters obtained by the curve-fitting analyses of Fourier-filtered EXAFS of the adsorbed species were the same as those of the complexes in the solution for all samples, except the sample of pH 0.8. On the other hand, the adsorbed species from the pH 0.8 solution exhibited a weak EXAFS oscillation and the results of curve-fitting analysis showed that the species had four Nb-O (2.07 Å), one Nb=O (1.71 Å) and another Nb-O bond (1.86 Å) whose distance was similar to a Nb-O (1.91 Å) bond found for the niobium oxide dispersed on silica, and also the contribution of the second and third oxygen or carbon was observed. This

suggests that the niobium oxalate complex in the solution of pH 0.8 reacted with the silica surface and formed a Nb-O-Si bond, releasing the oxalate ligand(s) in part.

The effect of ammonia on the adsorption of complexes could result from the modification of the silica surface. As the silica surface is weekly acidic, ammonia is adsorbed on the surface preferentially to prevent direct fixation of the niobium complexes on the silica surface. Eventually, the complexes are in a physical adsorption state on the surface. While, on the surface free from ammonia, the complex can be fixed by reacting with the surface Si-OHs.

The dimer complex adsorbed from the solution of pH 5 exhibited a little smaller amplitude in EXAFS (Fig. 7*e*), although the feature of EXAFS oscillation is similar to that of the complex in the solution. The smaller amplitude would indicate that the adsorbed state of the dimer complex was not uniform because the dimer would have two or more coordination sites.

Table 2 Areas and relative peak positions of pre-edge peaks in Nb K-edge XANES of samples.

Sample [a]	Peak position / eV [b]			Area / eV		
	pH 0.8	0.8*	4	pH 0.8	0.8*	4
solution	-6.7	-6.7	-6.6	1.04	1.11	1.04
dried	-7.2	-6.7	-6.7	1.12	1.12	1.04
calcined(ambient)	-7.4		-7.4	2.21		2.15
calcined(evac.)	-8.0		-7.9	2.83		2.51
Nb_2O_5		-7.3			1.88	
oxalate		-7.1			1.43	

[a] The concentration of the impregnating niobium solution was 16.8 mM. [b] Relative energy to the ionization threshold determined as the position of the inflection point of the continuum curve.

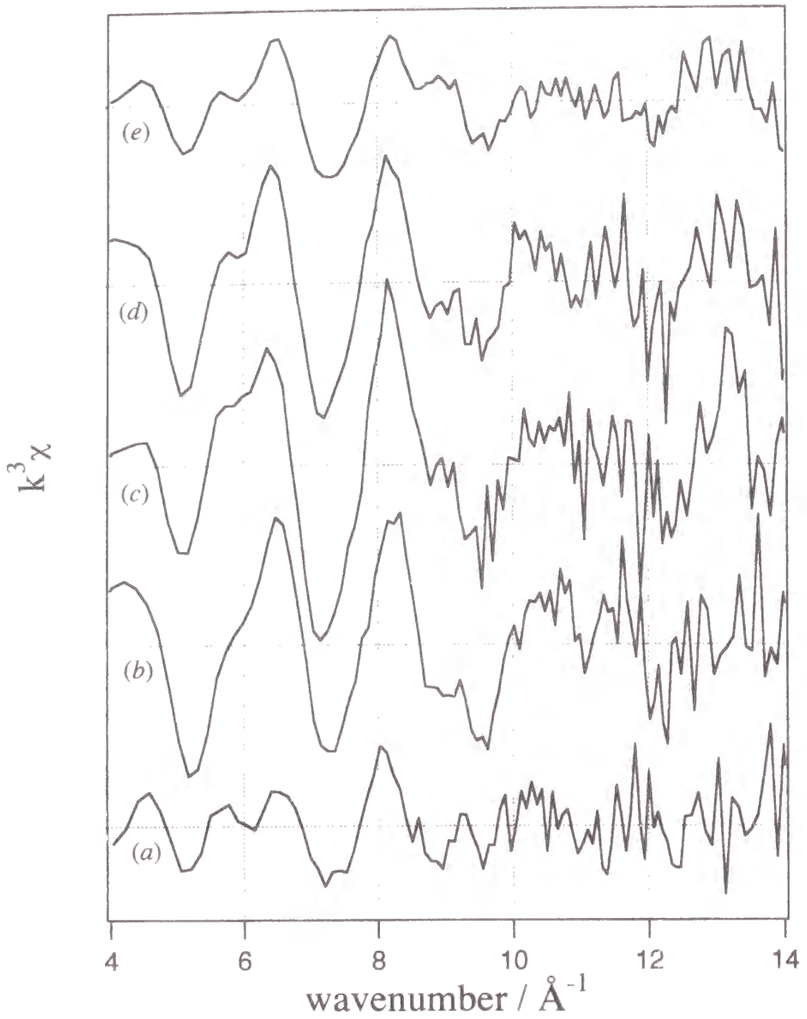

Fig. 7 The EXAFS spectra of the dried samples prepared from the solutions of pH (*a*) 0.8, (*b*) 0.8*, (*c*) 1, (*d*) 4 and (*e*) 5. The niobium concentration of the impregnating solution was 16.8 mM.

Calcined niobium oxide on silica

The adsorbed niobium species on silica were converted to niobium oxide species by calcination at 773 K. The obtained NbO_x/SiO_2 catalysts were evacuated at 673 K and the XAFS spectra were recorded. XANES spectra of the evacuated samples are shown in Fig. 8 (also Fig. 4*d* and Fig. 4*h*). Regardless of the loading amount of niobium oxide and pH of the impregnating solution, the shapes of spectra are identical. The pre-edge peak is clearly observed in each spectra of the NbO_x/SiO_2 samples. The positions are lower and the areas are larger than those of the octahedra (Table 2), indicating that the niobium oxides on silica surface prepared in this method were tetrahedral species.[1, 2, 29] The pre-edge peak of the spectra of the 4.6 wt.-% NbO_x/SiO_2 catalysts prepared in the equilibrium adsorption method was obviously clearer than that of the 4.6 wt.-% NbO_x/SiO_2 catalysts prepared in a conventional evaporation to dryness method.[1] This shows the advantage of the equilibrium adsorption method for the preparation of silica supported niobium oxide catalysts comprised of tetrahedral niobium oxide species even in the high loading, such as 4.6 wt.-%.

EXAFS spectra of the evacuated NbO_x/SiO_2 samples are shown in Fig. 9. The spectra (Fig. 9*a*, and Fig. 9*b*) are also clearly different from those of niobium pentoxide. Asakura and Iwasawa[18] proposed that the shoulder at around 5.5 Å^{-1} was resulted from the scattering by neighboring Si atom. In our result, the same shoulder was also observed, indicating that niobium oxide species were fixed on silica surface and did not aggregated so much.

In the Fourier-transforms of the EXAFS (Fig. 10), the twin peaks observed at 2.9-3.4 Å can be assigned to the secondary neighboring Si and/or Nb, and this is confirmed by the curve-fitting analysis of Fourier-filtered EXAFS. The peaks for the sample prepared from pH 0.8 solution were smaller than that from pH 4 solution. The structural parameters were evaluated by the curve-fitting analysis and the results are given in Table 3. The amplitude and phase shift functions are empirical ones estimated by extraction of a combination of reference compounds, as described in the experimental section. Therefore, the absolute values of the results are not highly reliable, especially in the numbers of coordination at secondary neighboring atoms. Thus, we discuss the results qualitatively.

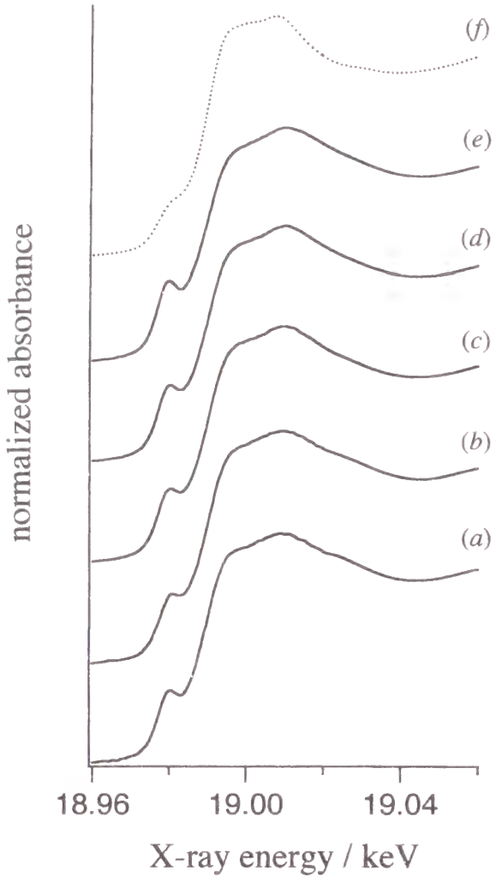

Fig. 8 Nb K-edge XANES spectra of the evacuated niobium oxide on silica (*a*)-(*e*) and niobium pentoxide (*f*). The loading amounts (wt.% as Nb_2O_5) and the pH of impregnating solutions for the samples are (*a*) 0.29, 0.8, (*b*) 0.37, 4, (*c*) 3.9, 0.8, (*d*) 4.2, 0.8* and (*e*) 4.6, 5, respectively.

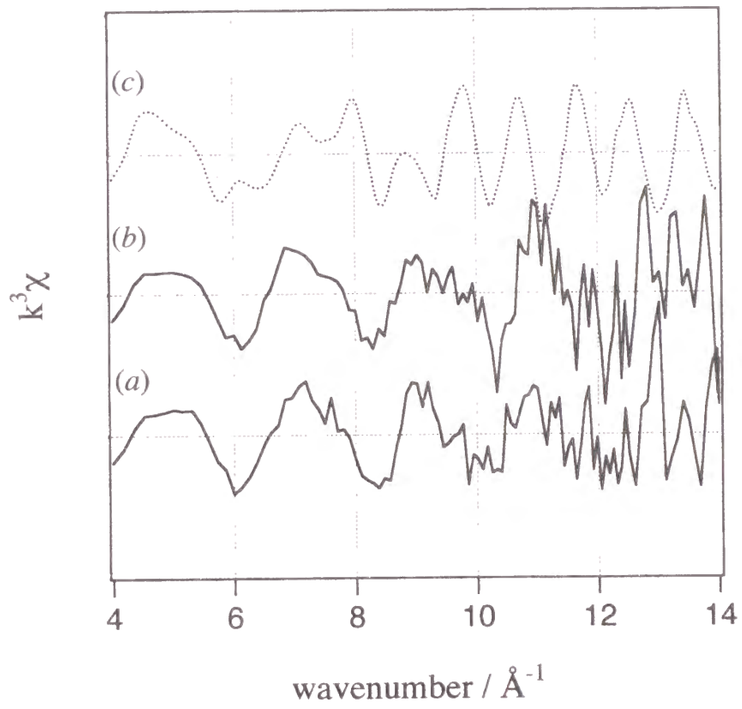

Fig. 9 The k^3 weighted EXAFS spectra of the evacuated niobium oxide on silica prepared from the solution (16.8 mM) of (*a*) pH 0.8, (*b*) pH 4, and that of (*c*) niobium pentoxide.

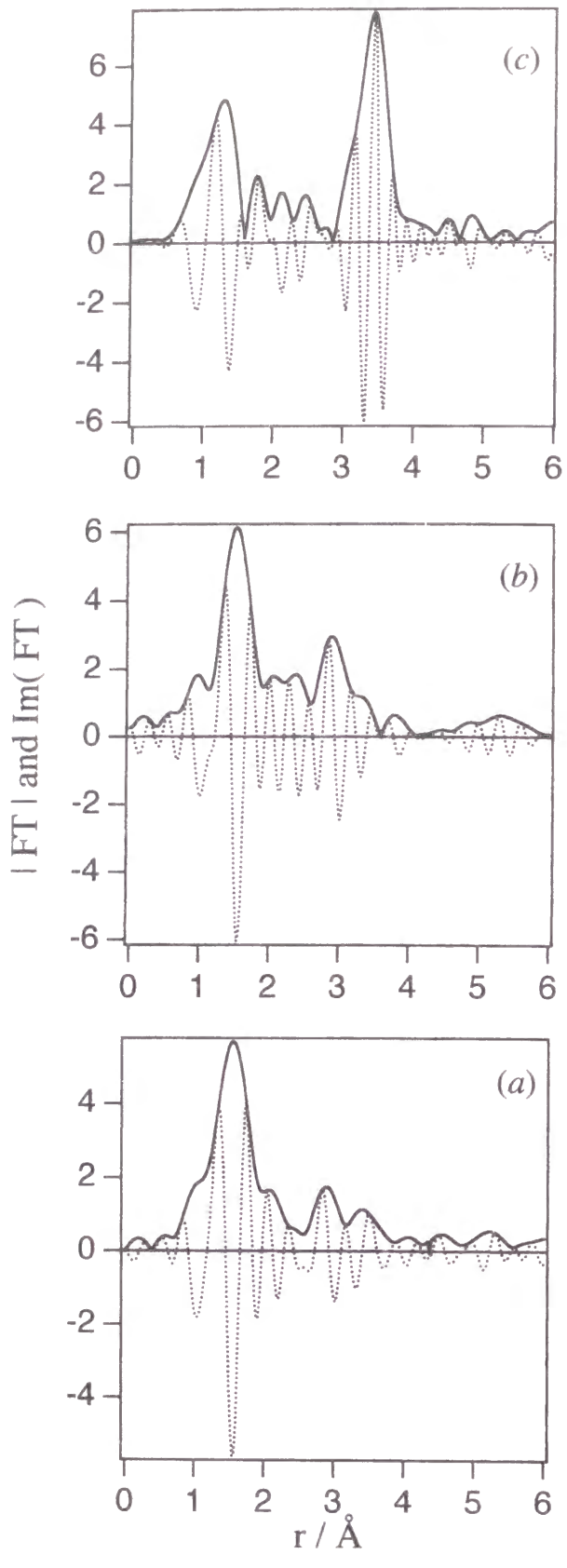

Fig. 10 Absolute of FT(|FT|) and imaginary part of FT(Im(FT)) of the EXAFS of the evacuated niobium oxide on silica prepared from the solutions (16.8 mM) of (*a*) pH 0.8 and (*b*) pH 4, and that of (*c*) niobium pentoxide.

Table 3 Curve-fitting results of the evacuated niobium oxides on silica[a] and niobium pentoxide.

pH	Nb-O			Nb=O			Nb-Si			Nb-Nb		
	N	r / Å	$\Delta\sigma^2$	N	r / Å	$\Delta\sigma^2$	N	r / Å	$\Delta\sigma^2$	N	r / Å	$\Delta\sigma^2$
0.8	2.4	1.93	-0.001	1.2	1.69	0.003	0.9	3.23	-0.005	0.2	3.35	-0.006
0.8*	3.0	1.90	0.003	0.9	1.64	0.001	0.9	3.24	-0.005	0.5	3.34	-0.001
1	2.6	1.91	0.001	1.0	1.67	0.001	1.0	3.26	-0.004	0.6	3.35	0.005
4	2.6	1.91	0.000	0.8	1.65	-0.003	0.9	3.24	-0.002	0.7	3.33	-0.002
5	2.8	1.89	0.002	1.1	1.66	-0.004	1.0	3.23	0.005	0.4	3.30	-0.003
Nb_2O_5	3.7	2.02	0.007	1.3	1.76	0.006				1.1	3.33	0.009
(X-ray)[b]	(4)	(2.06)		(1)	(1.78)					(1.6)	(3.32)	
										2.5	3.70	0.002
										(3)	(3.86)	

[a] The concentration of the impregnating niobium solution was 16.8 mM.

[b] Ref. 18.

The parameters associated with the first neighboring oxygen atoms and of the secondary neighboring silicon atom were not affected by the pH of impregnating solutions. The number of coordination of the Nb-Nb shell varied apparently with the pH; the lowest coordination of the Nb-Nb shell was exhibited by the sample prepared from the pH 0.8 solution. It indicates that the niobium oxide species on the sample prepared from the pH 0.8 solution was the most highly dispersed. In this case, the niobium complex under the adsorption equilibrium is supposed to be fixed on the silica surface, as mentioned above. Since, the complex is fixed by a Nb-O-Si bond, the complex could not migrate easily on the surface by calcination in the air. On the other hand, the complexes physically adsorbed from the ammoniacal solution could migrate easily and aggregate under calcination.

Although the present results did not clarify the state of aggregation, we could propose that niobium pentoxide was not produced and only the tetrahedral niobium oxide species were obtained on silica surface. We propose the local structure of the species fixed on the silica tetrahedral network, shown in Fig. 11.

The calcined samples before evacuation could be regarded as hydrated samples in ambient condition. The samples exhibited the same XAFS spectra regardless of the condition of the impregnating solutions. As shown in Table 2, the areas of the pre-edge peak of the samples were larger than that of the complexes in the solution and smaller than that of the following evacuated samples. The positions of the pre-edge were in a lower energy side than that of complexes in the solution and in a higher energy side than that of evacuated samples. The results indicate that the niobium oxide species has lower symmetry than the oxalate complexes and higher symmetry than the evacuated oxide species. Although the evacuated niobium oxide species were tetrahedral as described above, the species on the calcined samples under ambient condition would be a distorted octahedral, because of the adsorption of water molecules.[2, 30]

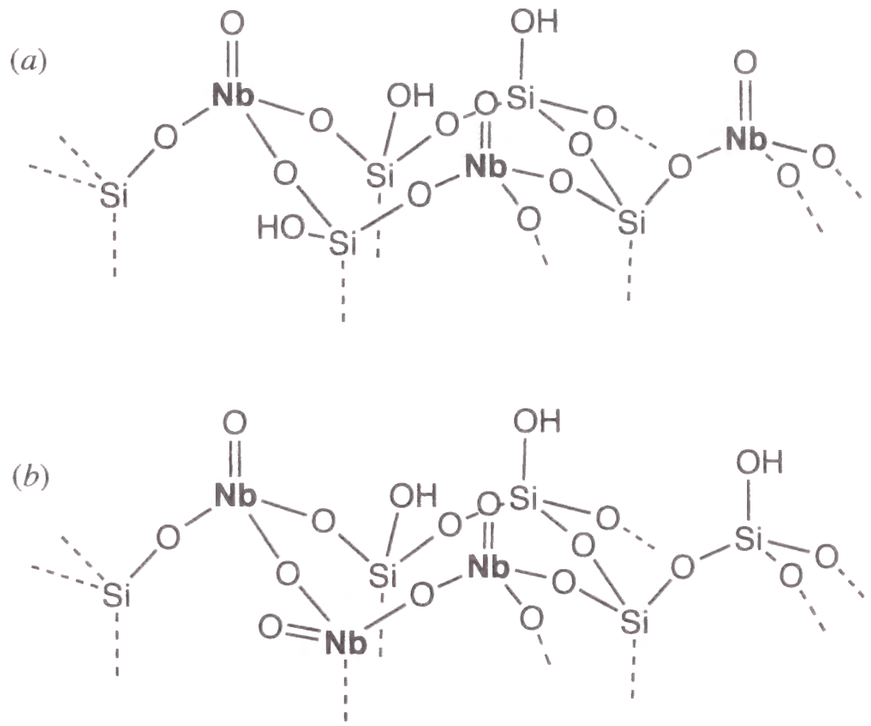

Fig. 11 Proposed models for the surface structure of (*a*) niobium monomer species and (*b*) niobium oligomer species attached on silica.

Conclusion

The present study reveals that the dispersion of tetrahedral niobium oxide species supported on the silica surface can be controlled by changing the conditions of the equilibrium adsorption method as follows: (1) the loading amount of niobium oxide species on silica is proportionally controlled by adjusting the niobium concentration of the impregnating solution, (2) when the solution is adjusted at pH 5 by the addition of ammonia, the loading amount increases more than two times on keeping a highly dispersion, where the tetrahedral species exist as small oligomers without much aggregation, (3) the most dispersed monomeric tetrahedron of niobium oxide is obtained from the solution of pH 0.8 which does not contain ammonia, while a small oligomer comprised of the tetrahedral species on silica is prepared from the solution of pH 0.8-4 in the presence of ammonia.

References

1 S. Yoshida, Y. Nishimura, T. Tanaka, H. Kanai and T. Funabiki, *Catalysis Today*, 1990, **8**, 67.

2 S. Yoshida, T. Tanaka, T. Hanada, T. Hiraiwa, H. Kanai and T. Funabiki, *Catal.Lett.*, 1992, **12**, 277.

3 T. Tanaka, H. Nojima, H. Yoshida, H. Nakagawa, T. Funabiki and S. Yoshida, *Catal.Today*, 1993, **16**, 297.

4 A. Morikawa, T. NAkajima, I. Nishiyama and K. Otsuka, *Nihonnkagakukaisi*, 1984, 239.

5 J.-M. Jehng and I. E. Wachs, *Catal. Today*, 1990, **8**, 37.

6 J.-M. Jehng and I. E. Wachs, *J. Mol. Catal.*, 1991, **67**, 369.

7 J.-M. Jehng and I. E. Wachs, *J. Phys. Chem.*, 1991, **95**, 7373.

8 J.-M. Jehng and I. E. Wachs, *Catal. Today*, 1993, **16**, 417.

9 M. Nishimura, K. Asakura and Y. Iwasawa, *Chem. Lett.*, 1986, 1457.

10 M. Nishimura, K. Asakura and Y. Iwasawa, *J. Chem. Soc., Chem. Commun.*, 1986, 1660.

11 M. Nishimura, K. Asakura and Y. Iwasawa, *Chem. Lett.*, 1987, 573.

12 M. Nishimura, K. Asakura and Y. Iwasawa, Proc. 9th Int. Congr. Catal., 1988, 1842.

13 N. Ichikuni, K. Asakura and Y. Iwasawa, *J. Chem. Soc., Chem. Commun.*, 1991, 112.

14 N. Ichikuni and Y. Iwasawa, *Catal Today*, 1993, **16**, 427.

15 N. Ichikuni and Y. Iwasawa, Proc. 10th Int. Congr. Catal., 1993, 477.

16 K. Asakura and Y. Iwasawa, *Chem. Lett.*, 1986, 859.

17 M. Shirai, N. Ichikuni, K. Asakura and Y. Iwasawa, *Catal. Today*, 1990, **8**, 57.

18 K. Asakura and Y. Iwasawa, *J. Phys. Chem.*, 1991, **95**, 1711.

19 M. Shirai, K. Asakura and Y. Iwasawa, *J. Phys. Chem.*, 1991, **95**, 9999.

20 S. Yoshida, T. Tanaka, Y. Nishimura, T. Hiraiwa, T. Tanaka and T. Funabiki, Proc. 13th Seminar Sci. Technol, Japan-Taiwan Catal. Seminar, 1990, 185.

21 J.-M. Jehng and I. E. Wachs, *J. Raman Spectroscopy*, 1991, **22**, 83.

22 H. Yoshida, T. Tanaka, T. Yoshida, T. Funabiki and S. Yoshida, *Physica B*, 1995, **208**, 681.

23 S. Yoshida, T. Matsuzaki, T. Kashiwazaki, K. Mori and K. Tarama, *Bull. Chem. Soc. Jpn.*, 1974, **47**, 1564.

24 K. Ebitani, A. Jitosyo, H. Yoshida, T. Tanaka, S. Yoshida and A. Morikawa, *Photon Factory Activity Report*, 1993, **11**, 136.

25 T. Yoshida, T. Tanaka, H. Yoshida, S. Takenaka, T. Funabiki, S. Yoshida and T. Murata, *J. Phys. Chem.*, 1995, 10890.

26 J. J. Boland, S. E. Crane and J. D. Baldeschwieler, *J. Chem. Phys.*, 1982, **77**, 142.

27 T. Ishii, *Prog. Theor. Phys.*, 1984, **72**, 412.

28 B. K. Teo, *EXAFS, Principles and Data Analysis*, Springer-Verlag, Berlin, 1986.

29 J. A. Horsley, I. E. Wachs, J. M. Brown, G. H. Via and F. D. Hardcastle, *J. Phys. Chem.*, 1987, **91**, 4014.

30 S. Yoshida, T. Tanaka, Y. Nishimura, H. Mizutani and T. Funabiki, *Proc. 9th International Congress on Catalysis*, 1988, **3**, 1473.

Chapter 2

Preparation chemistry of silica-magnesia catalysts

Abstract.

Mg K-edge XAFS study was carried out to clarify the local structure of silica-magnesia systems prepared in four ways; by impregnation of silica with an aqueous solution of magnesium nitrate or with a methanol solution of magnesium methoxide, and by sol-gel method with tetraethyl orthosilicate and magnesium solutions mentioned above. It is clarified that the preparation method decides the structure of Mg species respectively; (i) MgO particle on silica, (ii) dispersed Mg species on silica surface, (iii) dispersed Mg tetrahedral species in silica bulk.

Introduction

Silica-magnesia system is known as an acid-base bifunctional catalyst which promotes dehydration and dehydrogenation of alcohols and so on.[1-3] However, the function of the catalysts was not controlled completely, since the acid-base properties are affected by various factors, *e.g.* preparation method, composition and treatment.[4-6] In order to control the function sophisticatedly, it is important to know the status of component ion, especially the local structure of Mg ion; *e.g.* Mg ion in magnesium oxides is octahedrally coordinated, while it is believed that Mg ion located in silica matrix is tetrahedral coordinated.[4, 5, 7, 8] In this study Mg K-edge XAFS was employed to obtain information of the local structure of the Mg ions in silica-magnesia samples.

Experimental

Silica-magnesia samples were prepared in following four ways. MgO content of each sample was 15 mass% as standard. (I) Supported sample MgO/SiO_2(W) was prepared by impregnation of silica with an aqueous solution of $Mg(NO_3)_2$ followed by evaporation to dryness and calcination in air at 773 K. Silica support was prepared from $Si(OC_2H_5)_4$, ethanol and water by sol-gel method.[9] (II) Another supported sample MgO/SiO_2(M) was prepared in the same manner with a methanol solution of $Mg(OCH_3)_2$ instead of the aqueous solution. The solution was prepared by reaction of magnesium metal with refluxed methanol.[10] (III) Binary oxide sample MgO-SiO_2(W) was synthesized from $Si(OC_2H_5)_4$, ethanol and an aqueous solution of $Mg(NO_3)_2$ by sol-gel method followed by drying and calcination. (IV) Another binary oxide sample MgO-SiO_2(M) was synthesized in the same way with a methanol solution of $Mg(OCH_3)_2$ instead of the aqueous solution. In addition to these four samples, a reference catalyst[11] JRC-SM-1 (MgO contents was 29 mass%, the Catalysis Society of Japan) was also employed, which was synthesized hydrothermally from MgO and SiO_2. X-ray absorption

experiments were carried out on the BL-7A at UVSOR, Institute for Molecular Science, Okazaki, Japan,[12] with a ring energy 750 MeV and stored current of 80-200 mA. Spectra were recorded at room temperature, using a beryl two-crystal monochromator in a total electron yield mode. The sample was mixed with active carbon in dry hexane and was put on the first photocathode made of Cu-Be of the electron multiplier.

Results and discussion

Figure 1 shows XANES spectra of the silica-magnesia samples (*a*)-(*e*) and reference compounds (*f*)-(*k*). Reference spectra (*f*)-(*k*) seem to be dominantly composed of three peaks, though the energy position, intensity and sharpness are different from each other. The spectra of the prepared silica-magnesia samples (*a*)-(*d*) are classified into three types, indicating that the local structures around Mg atom are obviously distinguishable.

The XANES of MgO/SiO_2(M) (*b*) was obviously identical with that of MgO (*f*) of typical rock salt structure, indicating Mg ion exists as MgO particle, *i.e.* the Mg ion is octahedrally surrounded by 6-oxygen atoms. It has been also reported that MgO small particles on silica[13] and zeolite[14] were produced in this method. $Mg(OCH_3)_2$ easily reacts with water. In methanol solution, $Mg(OCH_3)_2$ react with surface hydroxyl groups on silica and/or react with H_2O and $Mg(OCH_3)_2$ molecules in methanol. Each reactions leads to dispersed Mg species or MgO particle, respectively. Since MgO particle was produced in this sample, the latter reaction would be dominant;

$$2\ Mg(OCH_3)_2 + H_2O \rightarrow Mg(OCH_3)\text{-}O\text{-}Mg(OCH_3) + 2\ CH_3OH. \qquad (1)$$

The XANES of MgO-SiO_2(M) (*d*) is essentially identical to that of JRC-SM-1 (*e*) and a magnesium silicate, $Mg_2Si_3O_8$ (*i*). Sol-gel method and hydrothermal synthesis are known to be suitable for preparing binary oxide whose components were well mixed at an atomic level, *i.e.*, Mg ions would be completely in the silica tetrahedral matrix. Therefore this spectra would be assigned to the tetrahedrally coordinated Mg ion. Through hydrolysis and condensation

between $Mg(OCH_3)_2$ and $Si(OC_2H_5)_4$, Mg-O-Si network would be constructed, and high dispersion of Mg ion in silica matrix would be achieved;

$$Mg(OR)_2 + Si(OR)_4 + H_2O \rightarrow Mg(OR)\text{-}O\text{-}Si(OR)_3 + 2\ ROH\ (R = H, CH_3, C_2H_5). \quad (2)$$

$MgO/SiO_2(W)$ (*a*) shows another type of XANES which have twin broad peaks at 1310 and 1315 eV. There are no identical spectrum of the references. Generally in the supported catalysts, metal oxide loaded is classified into alternative structures; particle or dispersed species on the surface. The XANES of $MgO/SiO_2(W)$ is clearly different from that of the former, therefore this is assigned to the latter species. Since the species on the silica surface would be affected by silica matrix structurally or electronically, we tentatively propose that it is surface tetrahedral species. The difference between the spectra (*a*) and (*d*) would be explained by the location of Mg species; on the surface or in the bulk.

This sample $MgO/SiO_2(W)$ (*c*) was prepared by using aqueous solution of $Mg(NO_3)_2$. A similar spectrum has reported for Mg/zeolite prepared in the same manner.[14] Under the preparation, it is suggested that Mg ion in aqueous solution adsorbed on the negative charge points of silica surface so that Mg oxide species produced are dispersed and strongly affected by silica surface.

The sample $MgO\text{-}SiO_2(W)$ were also prepared by using aqueous solution of $Mg(NO_3)_2$. The spectrum is identical to that of $MgO/SiO_2(W)$, suggesting that the magnesium species are mainly located on the surface of silica. While Mg ion exists as a hydrate cation in aqueous solution, silica-gel network was constructed through the hydrolysis and condensation,

$$2\ Si(OR)_4 + H_2O \rightarrow Si(OR)_3\text{-}O\text{-}Si(OR)_3 + 2\ ROH \qquad (R = H, C_2H_5). \quad (3)$$

Mg ion would not react with $Si(OC_2H_5)_4$ but only adsorb on silica gel, resulting in the dispersed Mg oxide species like that of $MgO/SiO_2(W)$.

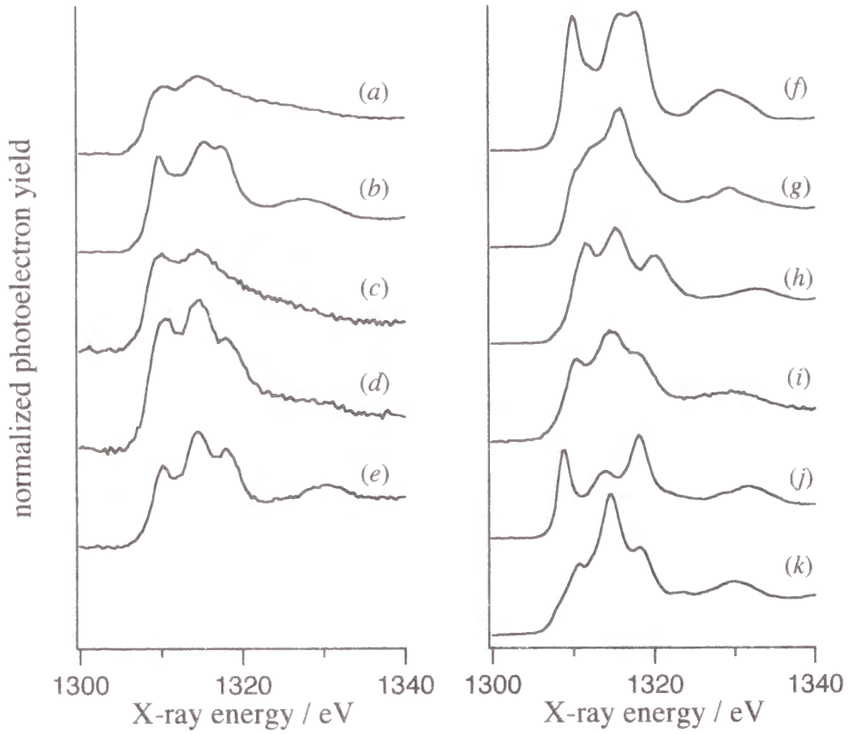

Fig. 1 XANES spectra of the silica-magnesia samples and reference compounds. (*a*) $MgO/SiO_2(W)$, (*b*) $MgO/SiO_2(M)$, (*c*) $MgO\text{-}SiO_2(W)$, (*d*) $MgO\text{-}SiO_2(M)$, (*e*) JRC-SM-1, (*f*) MgO, (*g*) Mg_2SiO_4 ,[13] (*h*) $MgSiO_3$,[13] (*i*) $Mg_2Si_3O_8$, (*j*) $MgAl_2O_4$, (*k*) $Mg(OH)_2$.

Conclusion

In conclusion, it is clarified that three type of magnesium oxide species in silica-magnesia system are respectively prepared by each suitable method; (i) MgO particle on silica, where Mg ion is located octahedral site, (ii) dispersed magnesium oxide species on the silica surface, which is interacted with surface silica matrix, (iii) dispersed Mg species in the silica matrix, which is tetrahedral.

References

1 H. Niiyama and E. Echigoya, *Bull. Chem. Soc. Jpn.*, 1971, **44**, 1739.
2 H. Niiyama, S. Morii and E. Echigoya, *Bull. Chem. Soc. Jpn.*, 1972, **45**, 655.
3 H. Niiyama and E. Echigoya, *Bull. Chem. Soc. Jpn.*, 1972, **45**, 938.
4 M. Briend-Fraure, M. Kermarec and D. Delafosse, *Bull. Soc. Chim. France*, 1974, **11**, 2393.
5 M. Kermarec, M. Briend-Faure and D. Delafosse, *J. Chem. Soc. Faraday Trans. 1*, 1974, **70**, 2180.
6 K. Tanabe , M. Misono, Y. Ono and H. Hattori, in *New Solid Acids and Bases*, Elsevier, Amsterdam, 1989, p. 108.
7 V. A. Dzis'ko, M. S. Borisova, L. G. Karachiev, A. D. Makarov, KN. C. otsapenko, R. I. Zusman and L. A. Chrupin, *Kinetika i Kataliz*, 1965, **6**, 1033.
8 H. Yoshida, T. Tanaka, A. Satauma, T. Hattori, T. Funabiki and S. Yoshida, *Chem. Commun.*, 1996, 1153.
9 S. Yoshida, T. Matsuzaki, T. Kashiwazaki, K. Mori and K. Tarama, *Bull. Chem. Soc. Jpn.*, 1974, **47**, 1564.
10 T. Tanaka, H. Yoshida, K. Nakatsuka, T. Funabiki and S. Yoshida, *J.Chem.Soc.Faraday Trans.*, 1992, **88**, 2297.
11 T. Uchijima, *Catalytic Science and Technology*, ed. S. Yoshida, N. Takezawa and T. Ono, Kodansha, Tokyo, 1991, p. 393.
12 T. Murata, T. Matsukawa, S. Naoe, T. Horigome, O. Matsudo and M. Watanabe, *Rev. Sci. Instrum.*, 1992, **63**, 1309.
13 H. Yoshida, T. Tanaka, K. Nakatsuka, T. Funabiki and S. Yoshida, *Stud. Surf. Sci. Catal.*, 1994, **90**, 473.
14 H. Tsuji, F. Yagi , H. Hattori and H. Kita, *Proc.10th Intern. Congr. Catal.*, ed. L. Guczi, F. Solymosi and P. Tetenyi , Akademiai Kiado, Budapest, 1993, p. 1171.

Part II

Characterization of silica and silica-based materials by means of phosphorescence spectroscopy

Introduction of Part II

To understand catalysis, we should know the details of the reaction mechanism and the structure of the active species. In particular, the structural information of the active species in a working state is quite important. In the case of photocatalysis, *in situ* instrumental investigation of the active species is more difficult than in the case of the catalysis driven thermally because only a few parts of the total sites are excited and one can not obtain the information of the excited species selectively by usual spectroscopic techniques. However, among the available physicochemical techniques, photoluminescence spectroscopy is a suitable one for characterization of photoactive sites. Since photoluminescence is emitted from the photoexcited site, it gives us information on the structure of photoactive sites and photoexcitation-deactivation process. Here, the author briefly summarizes the principle of photoluminescence and the examples of application to the characterization of catalysts, followed by the survey of this part.

Principle of photoluminescence

When the site absorbs photon, an electron is excited from the ground state (singlet state, S_0, Fig. 1) to the upper state (S_1) following to Franck-Condon principle.

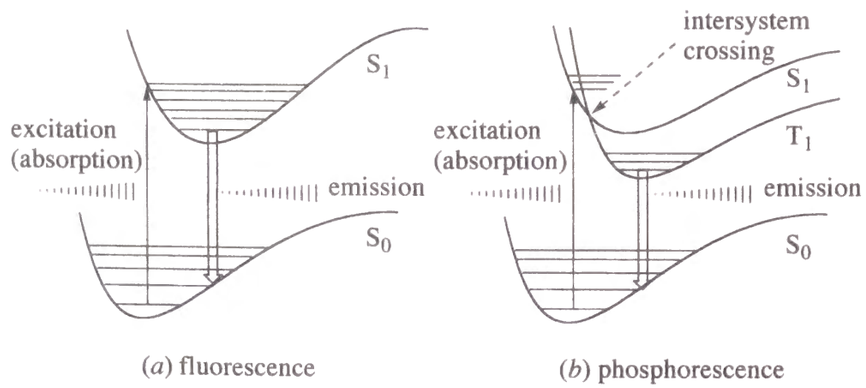

(*a*) fluorescence (*b*) phosphorescence

Fig. 1 Scheme on photoexcitation and luminescence.

There are two kinds of deactivation processes, radiative and/or radiationless deactivation. Moreover, radiative deactivation is classified into two emission process, fluorescence (Fig.1*a*) and phosphorescence (Fig.1*b*).

When the electron in S_1 is directly transferred to S_0, fluorescence is emitted. Since this deactivation is the allowed transition (the selection rule, $\Delta S=0$), the lifetime of excitation state is very short. A typical lifetime of an excited singlet electronic state is 10^{-8} s in the absence of collisions.[1]

The electron in S_1 is often transferred radiationlessly to another excitation state (triplet state, T_1) by way of intersystem crossing (Fig. 1*b*). The electron in the excited state, T_1, can be gradually deactivated to the singlet ground state S_0 accompanied by emitting photons, so called phosphorescence. Since phosphorescence is out of the selection rules $\Delta S=0$ and has a very low probability of occurring, decay time of phosphorescence is longer than that of fluorescence; typically 10^{-3} to 1 s in the absence of collisions.[1]

In the presence of gases, the luminescence is usually quenched by collision or adsorption of the molecules. The quenching of the luminescent intensity shows that the luminescence sites exist on the surface of the sample, and that the excited energy is transferred to the molecules. Photocatalysis is initiated by the adsorption of the molecules on the photoexcited sites, or by the photoexcitation of the site adsorbing molecules. In the former case, it would be easily accepted that the longer lifetime of T_1 states is advantageous for the starting of photocatalysis. The author employed the phosphorescence spectroscopy rather than fluorescence spectroscopy for the characterization of the photoactive sites in this thesis.

Figure 2 shows the system for measurement of phosphorescence employed in this study. To record the phosphorescence free from fluorescence, a simple method is cutting off the excitation light by chopper and monitoring the emission intensity after a time lag. We can obtain three types of phosphorescence spectra by this apparatus.

The first is an excitation spectrum, which is obtained by scanning excitation wavelength (monochromator-1) under recording emission intensity at a fixed wavelength (monochromator-2). The excitation spectrum shows demanded excitation wavelength for the photoluminescence

at the monitored wavelength. Although the spectrum seems to be similar to the absorption spectrum, that is not identical since the excitation spectrum is recorded only by monitoring phosphorescent emission (when radiationless deactivation does not occur, the excitation spectrum is equal to absorption spectrum). The spectrum mainly reflects the excitation state S_1; if a fine structure on spectrum is observed, information of vibration energy level in an excitation state S_1 is given.

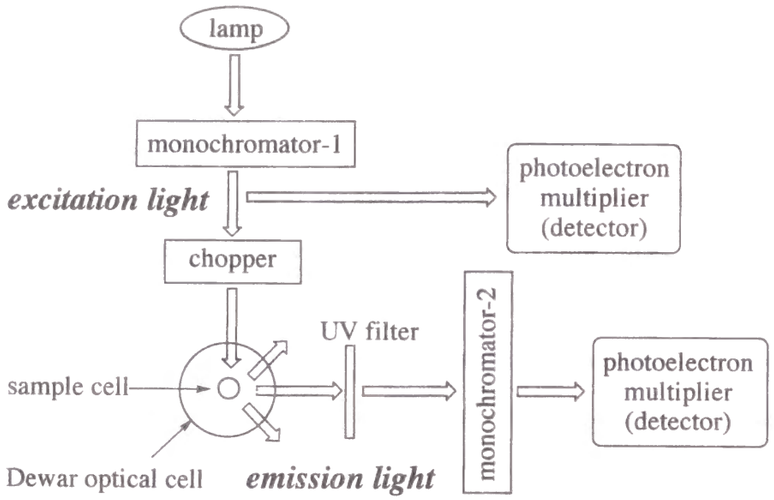

Fig. 2 Schematic drawing of spectrometer for the photoluminescence

The second type is a phosphorescent emission spectrum, so called phosphorescence spectrum, which is obtained by scanning emission light wavelength (monochromator-2) with a fixed excitation wavelength under recording emission light intensity. When the fine structure is observed on spectrum, we can obtain information about vibronic structure of the ground state (S_0) of a luminescent site.

The third is a decay curve of phosphorescence. To obtain it, the emission intensities at appropriate time interval are recorded at a fixed excitation and emission wavelength. Analysis of this decay curve by a curve fitting procedure gives us information about the fraction of the

luminescence sites and the lifetime of excited state T_1 of each luminescent site. In other words, it is clarified whether the luminescent sites on the sample are uniform or not.

Application to the characterization of the catalysts

1) bulk oxide surface

The photoluminescent spectroscopy has been applied to the characterization of catalysts. For example, the structure of MgO surface has been studied using photoluminescence. Mg ions in bulk MgO have six oxygen ions as the nearest neighbors. However, the coordination number of the surface ions is lower, such as 5, 4 or 3. Although a MgO single crystal absorbs a higher energy (9 - 8 eV), MgO powder with high surface area evacuated at high temperatures absorbs UV light (5 - 4 eV), and shows broad photoluminescence around at 3 eV.[2] The luminescence is quenched in the presence of oxygen, indicating that the luminescent sites exist on surface.[2] The values of the absorption energy are in a good agreement with that of the surface band gaps calculated by taking the surface electrostatic potentials into consideration.[2, 3] It is commonly accepted that the photoexcitation and luminescence are due to charge transfer at coordinately unsaturated Mg-O pair,[3-7]

$$Mg^{2+} - O^{2-} \underset{h\nu'}{\overset{h\nu}{\rightleftharpoons}} Mg^{+} - O^{-} \text{ (excited state)} \qquad (1)$$

although a long-lived emission is a radiative recombination process of photo-produced electrons and holes via defects such as F^+ centers.[7, 8]

In photoisomerization of 2-butene on MgO, it was reported that there are good correlation between the catalytic activity and intensity of luminescence assigned to 4-coordinated ion pair, indicating that the 4-coordinated sites are catalytic active sites.[9, 10]

The luminescence spectra are also observed in the powder of other oxides such as SrO,[11, 12] CaO, BaO,[3] ZnO[13, 14], ZrO_2,[15-17] porous Vycor glass,[18-21] and so on. On these oxides, the broad spectra were observed and the luminescence is explained on the basis of charge

transfer in coordinatively unsaturated metal-oxygen pairs. However, surface or inner hydroxy groups also exhibit broad photoluminescence.[7, 22] This luminescence is assigned to OH radicals[23] or triplet state of OH groups.[24]

Since transition metal ions such as Cr^{3+}, Mn^{2+}, Fe^{3+} emit photoluminescence, studies employing these ions as a tracer has been applied to investigations of the structural change of solid materials.[25]

2) supported catalysts and ion-exchanged zeolites

Bulk oxide usually shows a broad band in the photoluminescent spectrum since the states of the luminescent sites are not uniform. No fine structures in the spectra are expected in that case. On the other hand, highly dispersed metal oxide species supported on other oxide sometimes show the fine structure. Silica supported vanadium oxide is such an example. Although unsupported bulk V_2O_5 has no photoactivity, vanadium oxide highly dispersed on silica surface, whose structure is a VO_4 tetrahedron,[26-30] exhibits photoluminescence with a fine structure.[31-33] The vibration energy estimated from the progression of the fine structure of photoluminescence was assigned to that of terminal oxygen-vanadium double bond, V=O,[31-33] in comparison with the value estimated from IR spectroscopy.[34] In the case of vanadium species in a xerogel matrix, it was recently claimed that the fine structure was associated with a basal V-O bond.[35] In the case of photocatalytic isomerization of trans-2-butene, a good relationship between the relative intensity of the photoluminescence and photocatalytic activity was reported,[36] indicating that the luminescent site is photocatalytic active site.

Several supported transition metal catalysts have been characterized by using photoluminescence. However, V/MgO, V/Al_2O_3, V/TiO_2,[33] Cu/SiO2,[37] Mo/SiO_2,[38] Mo/PVG,[39] and Nb/SiO_2,[40, 41] showed no clear fine structure mentioned above.

Photoluminescence spectroscopy has also been applied to characterization of ion-exchanged zeolites such as Cu/ZSM-5,[42-46] Ag/ZSM-5.[47, 48] For example, Anpo *et al.* claimed that copper ions are dispersed as monomeric species in a zeolite, ZSM-5, although copper ions exist on silica or PVG as dimmeric species.[43] In this case, no fine structure was

observed. Rare earth metal ions, such as Eu^{3+}, Gd^{3+}, also show clear photoluminescence spectra of inner electron-transition and charge-transition. Therefore, rare earth metal ion exchanged zeolites have been characterized.[49-51]

Survey of Part II

In this thesis, the author applies photoluminescence spectroscopy to non-transition metal oxide species on silica matrix, *i.e.* Mg/SiO_2 (chapter 3 and 4) and SiO_2-Al_2O_3 (chapter 5). In chapter 3, the author presents the first finding that highly dispersed magnesium species on silica support evacuated at a high temperature (dehydrated) show a fine structure in a phosphorescence spectrum. On the other hand, in chapter 4, phosphorescence spectrum resulting from surface hydroxyl groups on hydrated Mg/SiO_2 was shown. In chapter 5, it was indicated that SiO_2-Al_2O_3 also exhibits the fine structure which is similar to that of Mg/SiO_2, indicating that the phenomenon in the case of Mg/SiO_2 is not exceptional. It suggests that the essential factor for observing the fine structure is existance of heteroatoms in silica matrix. These spectroscopic approaches predict that "silica and silica-based catalysts" work as photocatalysts and the phosphorescence spectroscopy is available for characterization of these silica-based catalysts.

References

1 I. N. Levine, *Physical Chemistry* (McGraw-Hill, New York, 1995), Chapter 21, section 16.

2 A. J. Tench and G. T. Pott, *Chem. Phys. Lett.*, 1974, **26**, 590.

3 S. Coluccia, A. M. Deane and A. J. Tench, *J. Chem. Soc. Faraday Trans. 1*, 1978, **74**, 2913.

4 S. Coluccia, A. J. Tench and R. L. Segall, *J. Chem. Soc., Faraday Trans. 1*, 1979, **75**, 1769.

5 S. Coluccia, A. Barton and A. J. Tench, *J. Chem. Soc., Faraday Trans. 1*, 1981, **77**, 2203.

6 S. Coluccia and A. J. Tench, in *7th Intr. Congr. Catal* ed. T. Seiyama and K. Tanabe, Kodansha, Tokyo, 1981, vol. B, p. 1154.

7 M. Anpo, Y. Yamada, Y. Kubokawa, S. Coluccia, A. Zecchina and M. Che, *J. Chem. Soc., Faraday Trans. 1*, 1988, **84**, 751.
8 V. A. Shvets, A. V. Kuznetsov, V. A. Fenin and V. B. Kazansky, *J. Chem. Soc., Faraday Trans. 1*, 1985, **81**, 2913.
9 M. Anpo, Y. Yamada and Y. Kubokawa, *J. Che. Soc., Chem, Commun.*, 1986, 714.
10 M. Anpo, Y. Yamada, S. Coluccia, A. Zecchina and M. Che, *J. Chem. Soc., Faraday Trans. 1*, 1989, **85**, 609.
11 S. Coluccia, J. F. Hemidy and A. J. Tench, *J. Chem. Soc. Faraday Trans. 1*, 1978, **74**, 2763.
12 S. Coluccia and A. J. Tench, *J. Chem. Soc., Faraday Trans. 1*, 1983, **79**, 1881.
13 M. Anpo and Y. Kubokawa, *J. Phys. Chem.*, 1984, **88**, 5556.
14 S. Komada, M. Yabuta, M. Anpo and Y. Kubokawa, *Bull. Chem. Soc. Jpn.*, 1985, **58**, 2307.
15 S.-C. Moon, T. Hieida, H. Yamashita and M. Anpo, *Chem. Lett.*, 1995, 447.
16 S.-C. Moon, H. Yamashita and M. Anpo, *Stud. Surf. Sci. Catal.*, 1994, **90**, 479.
17 S.-C. Moon, K. Tsuji, T. Nomura and M. Anpo, *Chem. Lett.*, 1994, 2241.
18 C. Yun, M. Anpo and Y. Kubokawa, *J. Chem. Soc., Chem. Commum.*, 1977, 665.
19 M. Anpo, C. Yun and Y. Kubokawa, *J. Catal.*, 1980, **61**, 267.
20 M. Anpo, C. Yun and Y. Kubokawa, *J. Chem. Soc., Faraday Trans.I*, 1980, **76**, 1014.
21 Y. Kubokawa, M. Anpo and C. Yun, in *Proc. 7th Int. Congr. Catal.* ed. T. Seiyama and K. Tanabe, Kodansha, Tokyo, 1981, vol. B, p. 1170.
22 W. W. Duley, *J. Chem. Soc., Faraday Trans. I*, 1984, **80**, 1173.
23 H. J. Maria and S. P. McGlynn, *J. Chem. Phys.*, 1970, **52**, 3402.
24 P. B. Merkel and W. H. Hamill, *J. Chem. Phys.*, 1971, **55**, 2174.
25 G. T. Pott and W. H. J. Stork, *Catal. Rev.*, 1975, **12**, 163.
26 T. Tanaka, Y. Nishimura, S.-i. Kawasaki, T. Funabiki and S. Yoshida, *J. Chem. Soc., Chem. Commun.*, 1987, 506.
27 S. Yoshida, T. Tanaka, Y. Nishimura, H. Mizutani and T. Funabiki, *Proc. 9th Int. Congr. Catal.*, 1988, **3**, 1473.
28 H. Kobayashi, M. Yamaguchi, T. Tanaka, Y. Nishimura, H. Kawakami and S. Yoshida, *J. Phys. Chem.*, 1988, **92**, 2516.
29 T. Tanaka, H. Yamashita, R. Tsuchitani, T. Funabiki and S. Yoshida, *J. Chem. Soc., Faraday Trans.1*, 1988, **84**, 2987.
30 S. Yoshida, T. Tanaka, T. Hanada, T. Hiraiwa, H. Kanai and T. Funabiki, *Catal. Lett.*, 1992, **12**, 277.
31 A. M. Gritscov, V. A. Shvets and V. B. Kazansky, *Chem. Phys. Lett.*, 1975, **35**, 511.
32 M. Anpo, I. Tanahashi and Y. Kubokawa, *J. Phys. Chem.*, 1980, **84**, 3440.

33 M. Iwamoto, H. Furukawa, K. Matsukami, T. Takenaka and S. Kagawa, *J. Am. Chem. Soc.*, 1983, **105**, 3719.
34 K. Tarama, S. Teranishi, S. Yoshida and N. Tamura, in *Proc. 3rd Intern. Congr. Catal.* ed. W. M. H. Sachtler, G. C. A. Schuit and P. Zwietering, North-Holland Publishing Company, Amsterdam, 1965, vol. I, p. 282.
35 K. Tran, M. A. Hanning-Lee, A. Biswas, A. E. Stiegman and G. W. Scott, *J. Am. Chem. Soc.*, 1995, **117**, 2618.
36 M. Anpo, M. Sunamoto and M. Che, *J. Phys. Chem.*, 1989, **93**, 1187.
37 M. Anpo, T. Nomura, T. Kitao, E. Giamello, M. Che and M. A. Fox, *Chem. Lett.*, 1991, 889.
38 Y. Iwasawa and S. Ogasawara, *Bull. Chem. Soc. Jpn.*, 1980, **53**, 3709.
39 M. Anpo, T. Suzuki, Y. Kubokawa, F. Tanaka and S. Yamashita, *J. Phys. Chem.*, 1984, **88**, 5778.
40 S. Yoshida, Y. Nishimura, T. Tanaka, H. Kanai and T. Funabiki, *Catalysis Today*, 1990, **8**, 67.
41 T. Tanaka, H. Nojima, H. Yoshida, H. Nakagawa, T. Funabiki and S. Yoshida, *Catal.Today*, 1993, **16**, 297.
42 M. Iwamoto, N. Mizuno and H. Yahiro, *Sekiyu Gakkaishi*, 1991, **34**, 375.
43 M. Anpo, T. Nomura, Y. Shioya, M. Che, D. Murphy and E. Giamello, *Stud. Surf. Sci. Catal.*, 1993, **75**, 2155.
44 M. Anpo, M. Matsuoka, Y. Shioya, H. Yamashita, E. Giamello, C. Morterra, M. Che, H. H. Patterson, S. Webber, S. Ouellette and M. A. Fox, *J. Phys. Chem.*, 1994, **98**, 5744.
45 H. Yamashita, M. Matsuoka, K. Tsuji, Y. Shioya, E. Giamello, M. Che and M. Anpo, *Stdu. Surf. Sci. Catal.*, 1995, **92**, 227.
46 H. Yamashita, M. Matsuoka, K. Tsuji, Y. Shioya and M. Anpo, *J. Phys. Chem.*, 1996, **100**, 397.
47 M. Matsuoka, E. Matsuda, K. Tsuji, H. Yamashita and M. Anpo, *Chem. Lett.*, 1995, 375.
48 M. Matsuoka, E. Matsuda, K. Tsuji, H. Yamashita and M. Anpo, *J. Mol. Catal. A: Chem.*, 1996, **107**, 399.
49 B. D. McNicol, G. T. Pott, K. R. Loos and N. Mulder, *Advan. Chem. Ser.*, 1973, **121**, 152.
50 M. F. Hazenkamp, A. M. H. van der Veen and G. Blasse, *J. Chem. Soc., Faraday Trans.*, 1992, **88**, 133.
51 M. F. Hazenkamp, A. M. H. van der Veen, N. Feiken and G. Blasse, *J. Chem. Soc., Faraday Trans.*, 1992, **88**, 141.

Chapter 3

Phosphorescence spectra of dehydrated Mg-loaded silica

Abstract

Highly dispersed magnesium oxide on silica exhibits photoluminescent emission. Evacuation of the sample at 1073 K promotes a solid-solid reaction, resulting in formation of a magnesium oxide species interacting with silica, which is the emission site of a new type of photoluminescence.

Introduction

Phosphorescent emission from UV-excited MgO is often used as a probe for the surface structure of MgO1-5, which varies with the temperature of the treatment. Excitation and emission wavelengths are thought to be closely related to the coordination of surface Mg and O ions2-4 because the process of excitation and emission involves charge transfer between coordinatively unsaturated surface Mg and O ions. It is widely admitted that these ions play an important role in heterogeneous catalysis. To increase the concentration of such ions, we have prepared magnesium oxide finely dispersed on a silica support and have been studying its character. Here, we report that new phosphorescent species are formed on the silica surface.

Experimental

Samples (MgO/SiO_2) were prepared by impregnation of silica powder (568 $m^2\ g^{-1}$) with a solution in methanol of $Mg(OCH_3)_2$, followed by filtration , evaporation of methanol and calcination at 773 K in a stream of dry air for 5 h. Silica was prepared by hydrolysis of $Si(OC_2H_5)_4$ as described elsewhere[6]. The solution of $Mg(OCH_3)_2$ in methanol was prepared by the reaction between magnesium metal and dry methanol (338 K for 4 h). Two kinds of sample with different Mg^{2+} loading were prepared; MS1 (1 wt.% as MgO) and MS20 (20 wt.% as MgO). Prior to each measurement and reaction, the samples were evacuated at 773 K or 1073 K for 2 h. The photoluminescence spectra were recorded at 77 K with a Hitachi 850 fluorescence spectrometer using a UV filter (permitted wavelength l> 300 nm) to remove scattered light from the UV source.

Results and discussion

Owing to the low loading in the case of MS1, no appreciable peaks were observed in the X-ray diffraction (XRD) pattern, while in the case of MS20, a broad diffraction peak of the MgO (200) plane was observed. In the case of MS20, the (200) diffraction peak became clearer and sharpened by evacuation at 1073 K. The estimated particle sizes and other physicochemical data of the samples are given in Table 1.

As shown in Fig. 1(*a*) and (*b*), the samples evacuated at 773 K exhibited the same emission spectra centred at 430 nm . These emission spectra are quenched effectively by CO and oxygen. The emission sites are supposed to be related to those for oxidation of CO. The difference of the reaction rates for MS1 and MS20 might be due to the difference in the particle size. Tench and co-workers proposed that such phosphorescence proves the existence of three-coordinated Mg^{2+} in MgO, like the Mg-O pair located at corners of crystallite.[4] Anpo *et al.* found[5] the similar emission spectra for MgO and observed that the peak position shifts to lower wavelength after evacuation at higher temperatures due to a sintering and dehydration effect. In our case, evacuation of MS20 at 1073 K caused the emission band, seen as the tailing part in the region of longer wavelength as shown in Fig. 1(*c*). No shift of the main peak position was observed. The XRD and XPS results in Table 1 show that evacuation at 1073 K causes aggregation of particles on the SiO_2 surface and promotes crystalline growth rather than dehydration. This is in accordance with the decrease in CO photo-oxidation rate, although the rate is higher than that expected from the decrease in the active surface area estimated by MgO particle size.

On the other hand, the spectrum of MS1 changed drastically after the sample was evacuated at 1073 K, when a new emission spectrum appeared. The emission has fine structure which disappeared at room temperature. This indicates that the emission is associated with excitation of specific bonds in the MgO diatomic moiety with low coordination to the silica. The fine structure reveals vibrational energy levels of the ground state and the highest

peak was found to be at 520 nm corresponding to the 0-6 bond transition. This shows that the bond, an emission site, is elongated in the excited state by the Frank- Condon principle. The spacings of energy levels, estimated from the difference between adjacent maxima, are 900 - 1000 cm^{-1}. These vibration energies are assignable to that of a metal-oxygen bond. Since silica did not exhibit photoluminescence and bulk MgO itself did not exhibit the emission centred at such long-wavelength region, this emission site should be an Mg-O bond, which may be interacting with the SiO_2 surface. Sintering and/or segregation is not brought about by evacuation at high temperature. Rather, it is likely that new surface compounds of Mg and Si are formed like Mg_2SiO_4. The emission is also quenched by contact with oxygen and CO. In contrast to the case of MS20, CO photo-oxidation became faster than on the sample evacuated at 773 K, suggesting that the new surface species is also photoactive, like the V=O bond in V_2O_5/SiO_2 photocatalyst[7]. As shown in Table 1, surface concentration of Mg decreased after evacuation of the sample at 1073 K. This result implies that Mg ions penetrate into silica to form new compounds. The same kind of species would be formed in the case of MS20 when it is evacuated at 1073 K and these species can compensate for the decrease in the photooxidation activity by crystal growth to some extent.

Table 1 Physicochemical properties of the samples

sample[a]	evacuation temp./K	area[b]/m^2g^{-1}	surface MgO[c](mol%)	rate[d]/μmol min^{-1} (g MgO)	d(MgO)[e]/Å
MS1	673	517	5.0	6.20	-
MS1	1073	496	3.5	10.8	-
MS20	673	396	59	2.45	90
MS20	1073	352	61	1.43	268
MgO	673	50.1	-	3.77	356
SiO_2	673	568	-	0.0	-

[a] Loading amount of MgO for MS1 and MS20 is 1.0 wt.%(1.4 mol%) and 21 wt.%(29 mol%), determined by X-ray fluorescent. [b] Specific surface area by BET method using nitrogen physisorption at 77 K. [c] Surface concentration of MgO (MgO/MgO + SiO_2) estimated by XPS. [d] Rate of photooxidation of CO. The reaction was carried out as described ref. 8. The volume of reaction vessel is 250 cm^3. Sample was spread over the catalyst bed made of quartz. The irradiated area was 12 cm^2 and a 250 W Hg lamp was used as a light source. [e] Particle size of MgO, estimated by Scherrer's method using the width of the diffraction line by the MgO (200) plane.

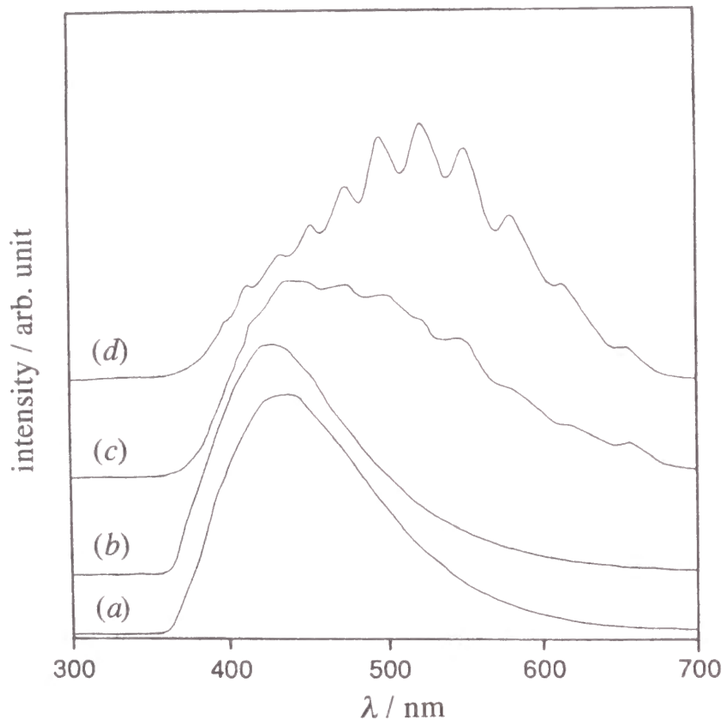

Fig. 1 Photoluminescent emission spectra at 77 K of the MgO/SiO2 samples excited by 240 nm light. (*a*) MS20 evacuated at 773 K, (*b*) MS1 evacuated at 773 K, (*c*) MS20 evacuated at 1073 K and (*d*) MS1 evacuated at 1073 K

References

1 A. J. Tench and G. T. Pott, *Chem. Phys. Lett.*, 1974, **26**, 590.

2 A. Zecchina, M. G. Lofthouse and F. S. Stone, *J. Chem. Soc., Faraday Trans. 1*, 1975, **71**, 1476.

3 S. Coluccia, J. F. Hemidy and A. J. Tench, *J. Chem. Soc., Faraday Trans. 1*, 1978, **74**, 2763.

4 S. Coluccia, M. Deane and A. J. Tench, *J. Chem. Soc., Faraday Trans. 1*, 1978, **74**, 2913.

5 M. Anpo, Y. Yamada, Y. Kubokawa, S. Coluccia, A. Zecchina and M. Che, *J. Chem. Soc. Faraday Trans. 1*, 1988, **84**, 751.

6 S. Yoshida, T. Matsuzaki, T. Kashiwazaki, M. Mori and K. Tarama, *Bull. Chem. Soc. Jpn.*, 1974, **47**, 1564.

7 A. M. Gritzkov, V. A. Shvets and V. B. Kazansky, *Chem. Phys. Lett.*, 1975, **35**, 511; M. Anpo, I. Tanahashi and Y. kubokawa, *J. Phys. Chem.*, 1980, **84**, 3440; S. Yoshida, T. Tanaka, M. Okada and T. Funabiki, *J. Chem. Soc., Faraday Trans. 1*, 1984, **80**, 119.

8 S. Yoshida, Y. Matsumura, S. Noda and T. Funabiki, *J. Chem. Faraday, Trans. 1*, 1981, **77**, 2237.

Chapter 4

Phosphorescence spectra of hydrated Mg-loaded silica

Abstract

Photoluminescent excitation and emission spectra resulting from hydroxy groups on magnesium oxide have been investigated using highly dispersed magnesium oxide species supported on silica. Since this sample has almost only one kind of Mg-O species, reaction of the Mg-O species with H_2O produces hydroxy groups uniformly coordinated to Mg ions. Therefore, clear photoluminescent excitation spectra were obtained. Coordination states of hydroxy groups were elucidated from excitation spectra. The hydroxy group attached to the surface Mg ion is excited by 255 nm light. The other hydroxy groups which are coordinated to Mg ions within the silica matrix are excited by 265 nm light. Hydroxy groups on the sample exhibit almost the same broad emission spectra centred at 440 nm regardless of their coordination.

Introduction

The excited triplet states of photoactive sites on solid catalysts often play an important role in photocatalysis, and phosphorescence emitted from triplet states allows the photoactive sites to be studied. Consequently, photoluminescence[1-5] and the photocatalytic activity[6] of MgO have been studied extensively.

We can not disregard hydroxy groups on MgO when we examine the photoluminescence of MgO. These hydroxy groups are directly related to photoluminescent emission, and interfere or mask the emission from Mg-O ion pairs on the surface.[1,2] Investigations into the properties of MgO bulk have been of particular interest[1-7] and have revealed that hydroxy groups were removed by evacuation at high temperatures; however, the assignment of luminescence by hydroxy groups remained unclear.

Several coordination states of surface ions exist in the MgO bulk. The type of coordination affects the surface properties, for example, the basicity[8] or surface band-gap.[3] The properties of hydroxy groups on the surface may also be influenced by the coordination state. There have been some studies on photoluminescence of dehydrated magnesium hydroxide[7] and also of the hydrated surface of MgO.[1,2] However, in these studies, coordination of the hydroxy groups, especially the surface ones, were not well defined, with the exception of the intrinsic hydroxy groups in $Mg(OH)_2$ because of the variety of states involved.[7] In order to clarify the coordination, it is necessary to prepare a sample which contains the uniform luminescent sites.

Recently, we have found that highly dispersed magnesium oxide on silica exhibits a new type of photoluminescence[9] and concluded that new Mg-O bonds are the emission sites. The fine structure on the photoluminescence emission spectrum reveals that the emission site, an Mg-O, is distributed uniformly. When hydroxy groups coordinated to these Mg ions are produced, or the O ions in Mg-O bonds convert to hydroxy groups, the hydroxy group is expected to be highly uniform. In this paper, we describe the change of photoluminescence

caused by adding water to this sample, and discuss the coordination states of the hydroxy groups produced.

Experimental

In this study, we used MgO supported on silica of 1 wt.% loading, MgO / SiO_2 (MS), because it gives a clear photoluminescence spectrum due to the Mg-O bond.[9] Silica (568 m^2 g^{-1}), used as a support material, was prepared by the sol-gel method as described elsewhere.[10] The sample was prepared as described in ref. 9. Prior to measurements, the sample was treated with 50 Torr O_2 for 1 h at 1073 K, followed by 1 h evacuation at 1073 K.

Deionized H_2O was distilled, and purified by several freeze-pump-thaw cycles in a vacuum line before adsorption experiments.

Photoluminescence spectra were recorded at 77 K with a Hitachi 850 fluorescence spectrometer using a UV filter (permitted wavelength > 300 nm) to remove scattered light from the UV source. An *in situ* sample cell made of quartz (0.5 × 10 × 44 mm) was used. The amount of the sample in the cell was 200 mg, therefore the total amount of magnesium ions contained in the MS sample was 50 μmol. H_2O was introduced to the sample cell at room temperature.

Results

The photoluminescent emission spectra of the sample vary with the wavelength of the excitation light. The characteristic spectra of the MS sample can be classified in two sets: A, emission spectra produced by excitation of the sample with light of 240 nm and the excitation spectra monitored at 520 nm emission; B, emission spectra of the sample excited by 265 nm light and excitation spectra monitored at 430 nm emission.

Photoluminescence of SiO_2

Photoluminescence spectra of the silica support were recorded as a blank test. The pretreatment was the same as that for the MS sample.

Fig. 1 shows the photoluminescent emission spectra of SiO_2 excited by light at 240 nm (Fig. 1A) and 265 nm (Fig. 1B). In Fig. 1A, a broad band centred at 480 nm was observed after evacuation at 1073 K. Upon adsorption of H_2O, a component at *ca.* 440 nm was detected. Its intensity increased with further addition of H_2O. (Note that the scales are different.) The emission at 440 nm was quenched by contact with 100 Torr He, indicating that the luminescent sites are on the silica surface. Therefore, it should be assigned to hydroxy groups produced on the silica surface.

In Fig. 1B, a band centred at 440 nm was already observed after evacuation at 1073 K. The peak position suggests that the band results from residual hydroxy groups on silica.

Fig. 2 shows photoluminescent excitation spectra monitored at 520 nm (Fig. 2A) and 430 nm (Fig. 2B) emission. After evacuation at 1073 K, a peak was observed at 250 nm. After adsorption of H_2O, a peak at 240 nm appeared instead.

These results show that the luminescence, which was observed after the addition of H_2O, is clearly attributed to the hydroxy groups on the SiO_2 surface. Therefore, we conclude that the hydroxy groups on silica are excited by 240 nm light and that luminescence is emitted at 440 nm.

The luminescent site exhibiting a component of emission band at around 500 nm after evacuation at 1073 K, and the site exhibiting the excitation peak at 250 nm, are identical. The luminescence was not quenched by the presence of 100 Torr He, indicating that the luminescent site exists in the silica matrix and not on the surface. This site presumably results from internal residual hydroxy groups or a radical species such as an oxygen dangling bond.

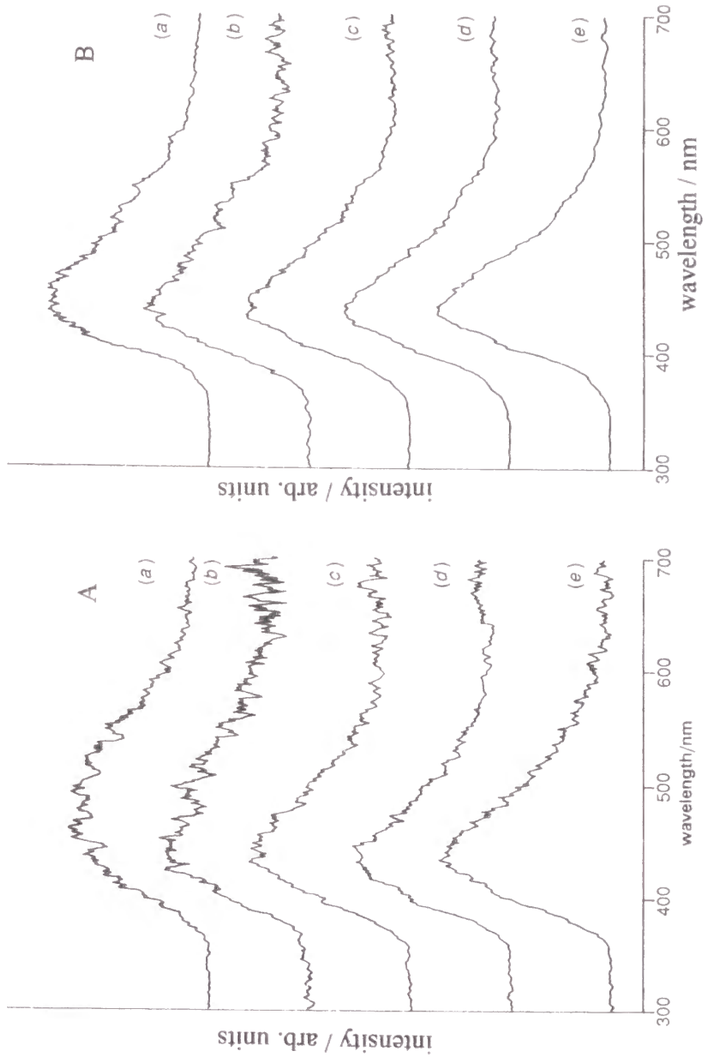

Fig. 1 Photoluminescent emission spectra of SiO_2 excited by A, 240 nm and B, 265 nm light; (*a*) after evacuation at 1073 K, (*b*) in the presence of 20 μmol H_2O, (*c*) in the presence of 50 μmol H_2O, (*d*) exposed to excess H_2O, (*e*) followed by evacuation at room temperature. Intensities of recorded spectra are: A, (*a*) ×1.0, (*b*) ×1.0, (*c*) ×0.47, (*d*) ×0.40, (*e*) ×0.40; B, (*a*) ×1.4, (*b*) ×2.7, (*c*) ×1.2, (*d*) ×1.2 and (*e*) ×0.78.

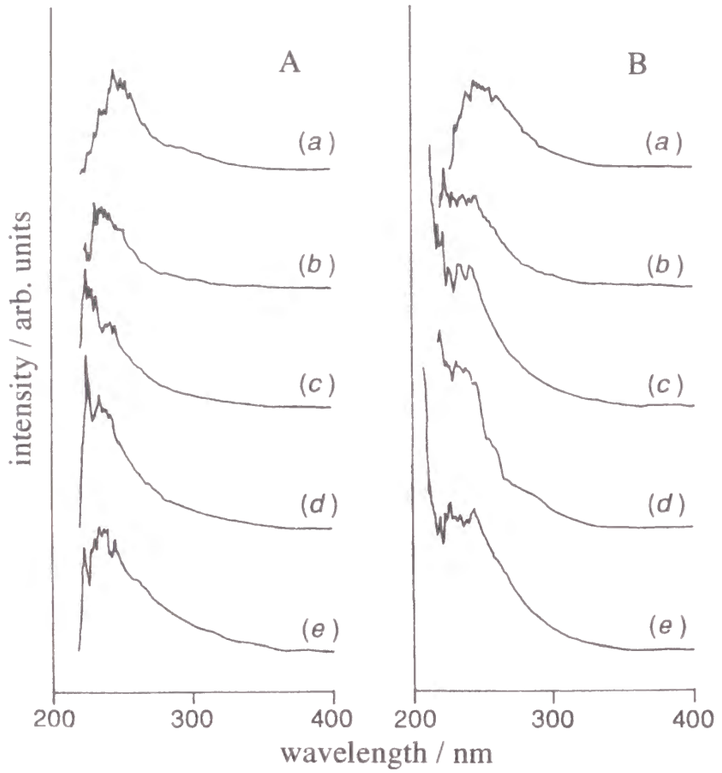

Fig. 2 Photoluminescent excitation spectra of SiO_2 recorded by monitoring the emission at A, 520 nm and B, 430 nm; (*a*)-(*e*): see caption to Fig. 1. Intensities of recorded spectra are: A, (*a*) ×1.0, (*b*) ×1.3, (*c*) ×0.80, (*d*) ×1.2, (*e*) ×1.1; B, (*a*) ×1.4, (*b*) ×1.0, (*c*) ×0.60, (*d*) ×0.58 and (*e*) ×0.48.

Photoluminescence of the MS sample: Set A

In this section, the emission spectra of the MS sample excited by 240 nm light (Fig. 3) and the excitation spectra monitored at 520 nm emission (Fig. 4) are discussed.

Fig. 3(*a*) shows the emission spectrum recorded after evacuation of the sample at 1073 K. It exhibits a band centred at 520 nm with the fine structure due to vibrational levels of Mg-O bond.[9] The excitation spectrum in Fig. 4(*a*) reveals a shoulder peak at 240 nm, suggesting that this photoactive Mg-O bond was excited by 240 nm light and emitted lights at 520 nm.

Immediately after 20.3 μmol H_2O was added at room temperature, the emission spectrum of the MS sample excited by 240 nm light changed; a broad band was observed with a maximum at 440 nm [Fig. 3(*b*)] and its intensity was reduced to one third. Furthermore, the fine structure disappeared. These results suggest that H_2O molecules interact with the Mg-O bonds and new photoluminescent sites are produced giving rise to a broad peak. Subsequently, the sample was annealed at room temperature and left for 30 min. The emission spectrum was recorded again at 77 K [Fig. 3(*c*)], and exhibits a broad band at 440 nm whose tail extends to the original band at *ca.* 520 nm. When a further 29.7 μmol H_2O was added [Fig. 3(*d*)], the 440 nm band was not quenched but grew larger, whereas the intensity of the band at *ca.* 520 nm decreased. The sample was exposed to saturated H_2O vapour at room temperature for 10 min. and then evacuated. The spectrum in Fig. 3(*e*) changed to that comprising a single broad band centred at 440 nm, and the original band at 520 nm completely disappeared.

These results indicate that the photoluminescent peak at 440 nm relates to hydroxy groups. The hydroxy groups would exist not only on the surface of magnesium oxide, but also on the surface of silica support, and both would exhibit such photoluminescent emission spectra. It is quite probable that the Mg-O species, which exhibits the emission spectrum centred at 520 nm, reacts to give hydroxy groups.

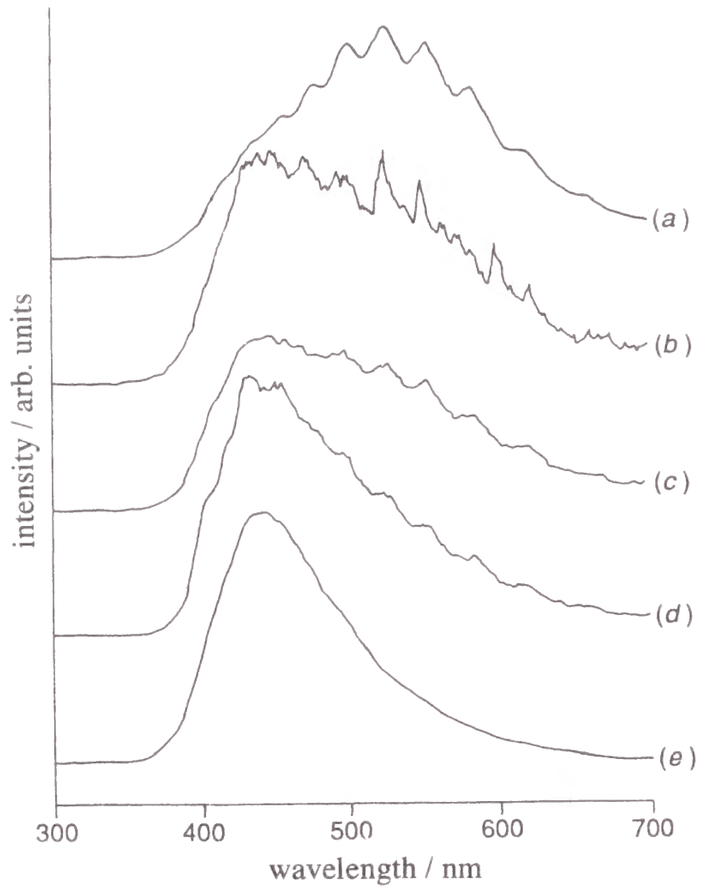

Fig. 3 Photoluminescent emission spectra of the MS sample excited by 240 nm light; (*a*) after evacuation at 1073 K, (*b*) immediately after addition of 20 μmol H_2O, (*c*) 30 min. later, (*d*) in the presence of 50 μmol H_2O, (*e*) exposed to excess H_2O vapor followed by evacuation at room temperature. Intensities of recorded spectra are: (*a*) ×1.0, (*b*) ×2.9, (*c*) ×0.86, (*d*) ×1.3 and (*e*) × *ca.* 0.4.

Fig. 4 shows the photoexcitation spectra. The spectrum after the pretreatment [Fig. 4(*a*)] exhibits a shoulder peak at 240 nm. On addition of a small amount of H_2O (20 or 50 μmol: less than or comparable to the amount of Mg ions), the spectrum did not change as shown in Fig. 4(*b*) and (*c*). After an excess H_2O was added, followed by evacuation at room temperature, the shoulder shifted to 260 nm, as shown in Fig. 4(*d*). Since silica does not exhibit such a peak at 260 nm, this excitation peak is assignable to hydroxy groups coordinated to Mg ions.

On addition of a small amount of H_2O, the excitation spectra did not change although the emission spectra changed as mentioned above. On the other hand, when excess H_2O was added, a new excitation peak appeared. From these results, we suppose that at least two kinds of OH groups are formed; one is formed initially by the adsorption of water molecules comparable to the number of Mg ions, and the other is subsequently formed by adsorption of an excess of water molecules. The spectral change clearly shows that they are distinguishable.

Since magnesium ions in this sample exist as isolated monoatomic or raft-like crystallite species interacting at the silica surface,[11] it is likely that at least two types hydroxy groups coordinated to Mg ions are present on the surface; one is coordinated to only one magnesium ion and the other is bridged to Mg and Si. In this sample, it is probable that the isolated Mg-O bonds exist and that their oxygen is more reactive than the oxygen coordinated to both Mg and Si, so we suggest that the H_2O molecule first react with this isolated Mg-O bond and produce new Mg-(OH) species. The result that the luminescence of the hydroxy groups replaces the luminescence of Mg-O supports this assumption.

It is likely that excess H_2O molecules react with the oxygen bridging Mg and Si, or with MgO microcrystallites. Thus, we speculate that hydroxy groups produced by the addition of an excess of H_2O are coordinated to Mg and Si, or that $Mg(OH)_2$ micro crystallite are formed. The excitation wavelength of these hydroxy groups is 260 nm.

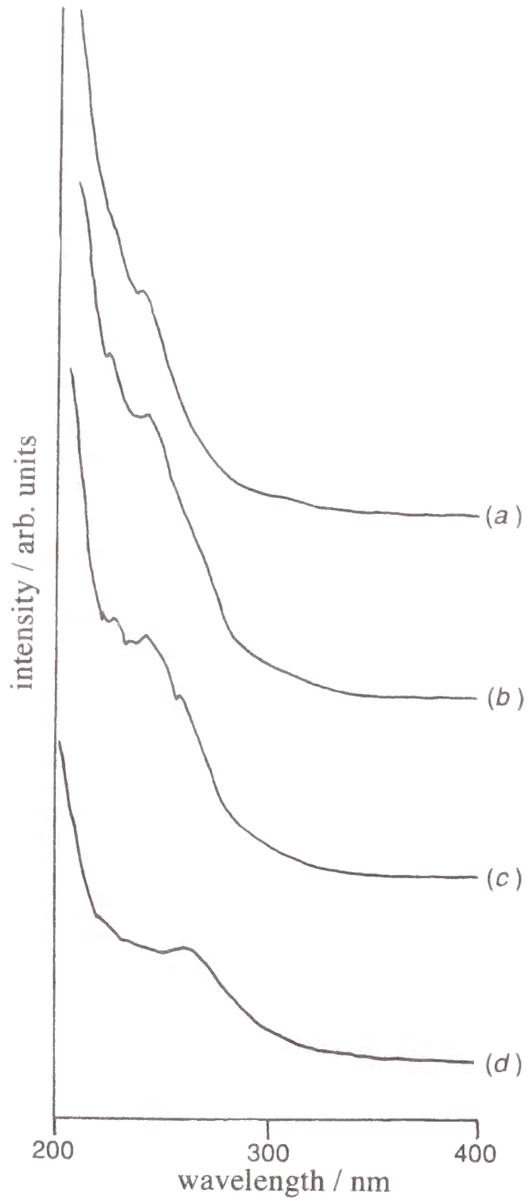

Fig. 4 Photoluminescent excitation spectra of the MS sample recorded by monitoring the emission at 520 nm: (*a*) after evacuation at 1073 K, (*b*) in the presence of 20 μmol H_2O, (c) in the presence of 50 μmol H_2O, (d) exposed to excess H_2O followed by evacuation at room temperature. Intensities of recorded spectra are (*a*) ×1.0, (*b*) ×1.5, (*c*) ×2.3 and (*d*) × *ca.* 0.4.

Photoluminescence of the MS sample: Set B

In this section, the emission spectra of the MS sample excited by 265 nm light (Fig. 5) and the excitation spectra monitored at 430 nm emission (Fig. 6) are discussed.

After pretreatment of the MS sample at 1073 K [Fig. 5(*a*)], the emission peak at 440 nm and the excitation peak at 265 nm [Fig. 6(a)] were observed. Such a peak in the excitation spectra is not reported for evacuated magnesium oxide at a high temperature, and is not observed for silica (Fig. 2). The emission peak at 440 nm is assigned to hydroxy groups as described in a previous section in the case of silica. Therefore, this luminescence which is produced by excited at 265 nm, and which emits at 440 nm is presumably due to hydroxy groups coordinated to Mg ions remaining even after evacuation at 1073 K for 1 h.

Duley[7] reported that the excitations of the OH^- in $Mg(OH)_2$ are promoted by 267-276 nm light, and the emission peaks are seen in the range 435-443 nm, and that OH^- ions remain when Mg(OH)2 was evacuated for 1 h at 1000 K. These values are in good agreement with our observation. We found that luminescence was not quenched by contact with 100 Torr He, indicating that the luminescent species are not present on the surface. Therefore, the luminescence observed in the present work could be due either to hydroxy groups in the magnesium hydroxide crystallite which has been encapsulated in the SiO_2 matrix, or to hydroxy groups located on the inner interface of magnesium oxide species and silica. Hence, both hydroxide species attached to an Mg ion and the new Mg-O species coexist in MS sample evacuated for 1 h at 1073 K.

Addition of a small amount of H_2O, less than, or comparable to the Mg content caused the excitation peak to shift to 255 nm as shown in Fig. 6(*b*) and (*c*). However, addition of an excess of H_2O caused the peak to shift to 260 nm [Fig. 6(*d*)].

As described above, the Mg-O species, which exhibits the fine structure in the photoluminescence excited at 240 nm, reacted with H_2O molecules to produce a new Mg-(OH) species. Hence, we conclude that this new Mg-(OH) species is specifically excited by 255 nm light.

On addition of an excess of H_2O molecules, the peak in the excitation spectrum was replaced by a small broad maximum at 260 nm. It is likely that the excess of H_2O molecules

interferes with the localization of photoexcitation of the new Mg-(OH) species, and hence, the peak at 255 nm in the excitation spectrum vanished. This suggests that all Mg species may react with excess H_2O molecules to form $Mg(OH)_2$-like species.

Although the peak in the excitation spectrum changed, the emission spectra in Fig. 5 did not change on addition of H_2O. As the concentration of Mg ions in the MS sample is only 1 wt.%, one may conjecture that the emission bands centred at 440 nm mainly due to the hydroxy groups coordinated to silica surface. However, the presence of such obvious peaks in the excitation spectra indicates a certain amount of emission from hydroxy groups coordinated to Mg ions. Therefore, regardless of whether hydroxy groups are coordinated to Mg ions or Si ions, we can conclude that all hydroxy groups show the same photoemission spectra at 440 nm.

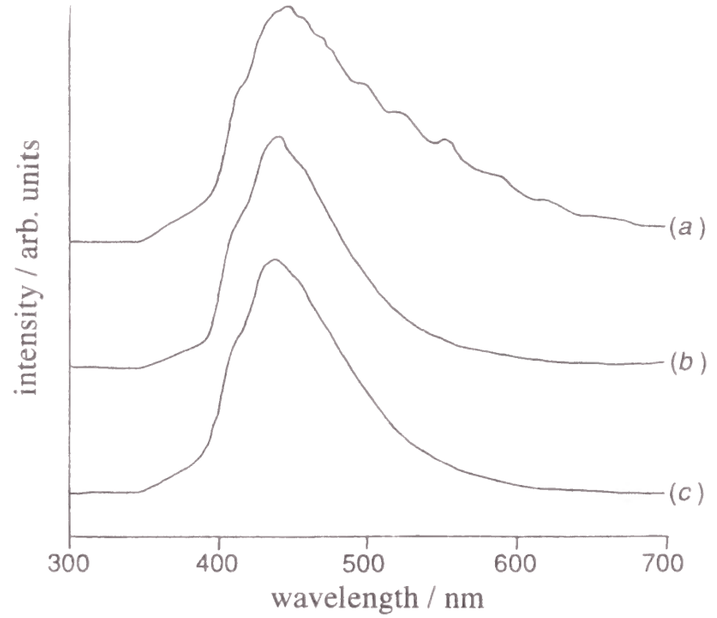

Fig. 5 Photoluminescent emission spectra of the MS sample excited by 265 nm light: (*a*) after evacuation at 1073 K, (*b*) exposed to 50 μmol H_2O vapor followed by evacuation at room temperature, (*c*) exposed to excess H_2O followed by evacuation at room temperature. Intensities of recorded spectra are (*a*) ×1.0, (*b*) ×0.85 and (*c*) × ca. 0.1.

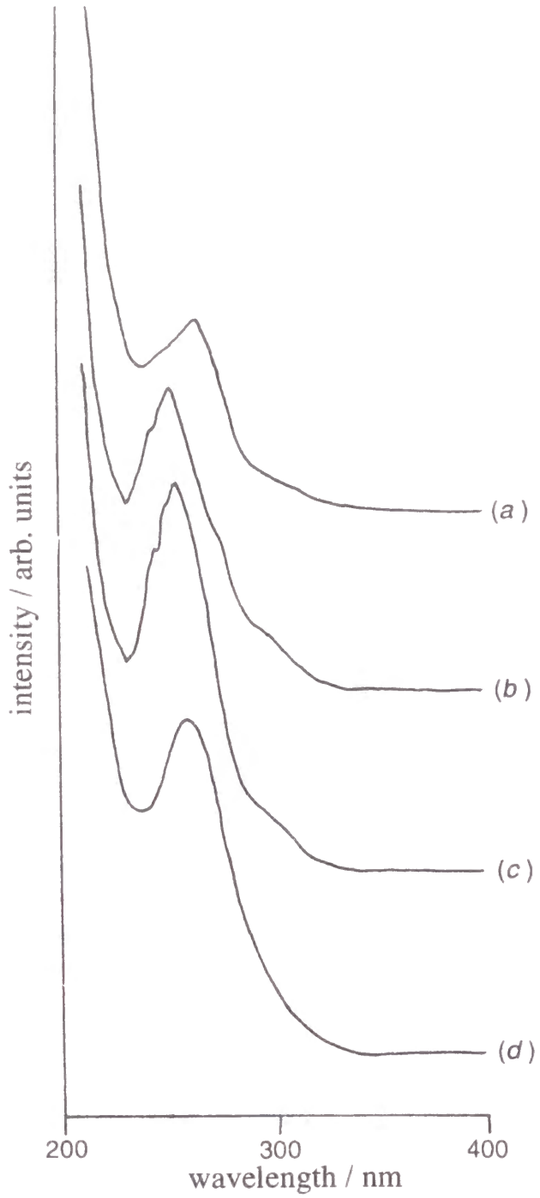

Fig. 6 Photoluminescent excitation spectra of the MS sample recorded by monitoring emission at 430 nm: (*a*) after evacuation at 1073 K, (*b*) in the presence of 20 μmol H_2O, (*c*) in the presence of 50 μmol H_2O, (*d*) exposed to excess H_2O followed by evacuation at room temperature. Intensities of recorded spectra are (*a*) ×1.0, (*b*) ×0.68, (*c*) ×1.0 and (*d*) × *ca.* 0.2.

Discussion

After evacuation at 1073 K, the component of the emission band centred at 440 nm, excited by 240 nm light, resulting from hydroxy groups on the silica support was observed in a blank test, although it was scarcely observed on the MS sample, as shown in Fig. 3(*a*). The loading of MgO in the MS sample was 1 wt.% which corresponds to 0.25 mmol g^{-1}. The population of residual hydroxy groups on silica calcined at 773 K was evaluated at 0.211 mmol g^{-1}.[12] The photoluminescence results in this work suggest that luminescence-active silanols are not present on the surface of the MS sample. These silanols have presumably been lost by the reaction of OH with $Mg(OCH_3)_2$ in methanol during MS sample preparation.

$$Si\text{-}OH + Mg(OCH_3)_2 \rightarrow Si\text{-}O\text{-}MgOCH_3 + CH_3OH$$

The photoluminescent emission spectra of other MS samples evacuated at 773 and 1073 K, which contain 20 and 1 wt.% MgO, respectively, were reported in ref. 9 The spectra of the sample evacuated at 773 K and excited by 240 nm light are the same as those of hydroxy groups reported in the present paper. We mentioned in the previous paper[9] that the spectra result from three-coordinated Mg-O ion pairs at the corners in MgO crystallites. Therefore, we concluded that crystallites of MgO are present on the silica surface in the sample evacuated at 773 K. Since the spectrum of the sample evacuated at 1073 K was assigned to the new Mg-O bond, we reported that the MgO crystallites reacts with silica under the evacuation at 1073 K, to result in the formation of new Mg-O bonds which interact with the silica.

From the results described in the preceding sections, hydroxy groups excited by 240 nm light emit a broad band centred at 440 nm. Taking this into account, there are two possible considerations for the change of the photoluminescent site due to evacuation at 1073 K. One is that the sample, after evacuated at 773 K, contained crystallites of MgO with surface hydroxy groups, and both of dehydration and solid-solid reaction occurred during the evacuation at 1073 K to produce the new Mg-O species. The other is that Mg ions were already dispersed on silica

surface and the new Mg-O bonds, or the precursor, were formed after the evacuation at 773 K. In the latter case, the strong emission form the hydroxy groups on silica masked the emission from the Mg-O bonds, and the dehydration at 1073 K promoted the removal of hydroxy groups to result in the spectrum exhibiting the fine structure.

Duley[7] reported that hydroxide ions in a specific low-coordination site on $Mg(OH)_2$ evacuated for 1h at 1200 K exhibited 472 nm (2.63 eV) emission when it was excited by 270 nm light, and that this emission can be excited by the trapping of excitons created by absorption at a variety of O_{LC}^{2-} and OH_{LC}^{-} sites. The basis of his assignment was the change of the spectrum by subsequent evacuation of the sample for 6 h at 1200 K. The appearing emission excited by the 268 nm (4.63 eV) light with the emission spectrum centred at 386 nm (3.21 eV). He suggested that the excitation peak could be attributed to absorption by three-coordinated O^{2-} ions[3,4] on the MgO surface, and the emission band was assigned to the characteristic blue-violet emission of MgO. Almost all excitation spectra in his paper show a single peak at *ca.* 270 nm, regardless of the evacuation temperature. Duley argued that the emission site was excited by the trapping of excitons created at different absorption sites. However, the explanation is not clear because of discrepancies the emission sites with the excitation sites.

In the preceding sections, we have clearly assigned the peak at 255 nm in the excitation spectra and the band at 440 nm in the emission spectra to surface hydroxy group attached to an Mg ion. In our sample, hydroxy groups function as both excitation sites and emission sites.

Ordinarily MgO crystallite has several kinds of hydroxy groups on the surface, and therefore the photoluminescence of hydroxy groups had not previously been assigned in detail because of complexity and low resolution of photoluminescent spectroscopy. We should make it clear that in the present paper, the sample MgO/SiO_2 has essentially only one kind of Mg-O species.

Conclusion

Hydroxy groups coordinated to Mg or Si in the MgO/SiO_2 are distinguishable from their photoluminescent excitation spectra. We conclude that for the new Mg-OH species, hydroxy group attached to the surface Mg ion is excited by 255 nm light, and that hydroxy groups coordinated to Mg ions which are within the silica matrix are excited by 265 nm light. Surface hydroxy groups coordinated to Mg and Si, or that of $Mg(OH)_2$ microcrystallites, produced by addition of an excess H_2O are excited by 260 nm light. The emission spectra relating to hydroxy groups show a broad band centred at 440 nm regardless of their coordination states.

During sample preparation, the luminescence-active silanols are lost by the reaction with $Mg(OCH_3)_2$. The Mg-O bond species are changed to hydroxy groups by adding H_2O molecules.

References and note

1 S. Coluccia, M. Deane and A. J. Tench, in *Proceedings of the 6th International Congress on Catalysis*. ed. G. C. Bond, P. B. Wells and F. C. Tompkins, the Chemical Society, London, 1977, p.171.

2 M. Anpo, Y. Yamada, Y. Kubokawa, S. Coluccia, A. Zecchina and M. Che, *J. Chem. Soc., Faraday Trans. 1*, 1988, **84**, 751.

3 S. Coluccia, A. M. Deane and A. J. Tench, *J. Chem. Soc., Faraday Trans. 1*, 1978, **74**, 2913.

4 S. Coluccia, A. J. Tench and R. L. Segall, *J. Chem. Soc., Faraday Trans. 1*, 1979, **75**, 1769; S. Coluccia, A. Barton and A. J. Tench, *J. Chem. Soc., Faraday Trans. 1*, 1981, **77**, 2203; S. Coluccia and A. J. Tench, *Proceedings of the 7th International Congress on Catalysis*, ed. T. Seiyama and K. Tanabe, Kodansha, Tokyo, 1981, p.1154.

5 A. J. Tench and G. T. Pott, *Chem. Phys. Lett.*, 1974, **26**, 590; V. A. Shvets, A. V. Kuznetsov, V. A. Fenin and V. B. Kazansky, *J. Chem. Soc., Faraday Trans. 1*, 1985, **81**, 2913.

6 M. Anpo, Y. Yamada and Y. Kubokawa, *J. Chem. Soc., Chem. Commun.*, 1986, 714; M. Anpo, Y. Yamada, S. Coluccia, A. Zecchina and M. Che, *J. Chem. Soc., Faraday Trans. 1*, 1989, **85**, 609.

7 W. W. Duley, *J. Chem.Soc., Faraday Trans. 1*, 1984, **80**, 1173.

8 H. Kawakami and S. Yoshida, *J. Chem. Soc., Faraday Trans. 2*, 1984, **80**, 921.

9 T. Tanaka, H. Yoshida, K. Nakatsuka, T. Funabiki and S. Yoshida, *J. Chem. Soc., Faraday Trans.*, 1992, **88**, 2297.

10 S. Yoshida, T. Matsuzaki, T. Kashiwazaki, K. Mori and K. Tarama, *Bull. Chem. Soc. Jpn.*, 1974, **47**, 1564.

11 H. Yoshida, T. Tanaka, K. Nakatsuka, T. Funabiki and S. Yoshida, in *Acid-Base Catalalysis II*, ed. H. Hattori, M. Misono and Y. Ono, Kodansha, Tokyo, 1994, p. 473..

12 The population of surface hydroxy groups was estimated as follows. Silica was soaked in hexane. Hexane solution of *n*-butyl lithium was introduced into the mixture under an N_2 atmosphere. Evolved butane was estimated volumetrically. Si-OH + C_4H_9Li → Si-OLi + C_4H_{10} ↑.

Chapter 5

Phosphorescence spectra of dehydrated silica-alumina

Abstract

Fine structure is clearly observed in the phosphorescent emission spectra of silica-alumina binary oxides evacuated at high temperature (1073 K) and excited by 300 nm light, although it is not observed in silica or alumina alone.

Introduction

Photoluminescent spectroscopy directly reflects the characteristics of photoexcited species, and has been applied to structural analysis of surfaces of metal oxides. Most metal oxides exhibit only a broad band,[1-4] since there are many photoexcited sites and/or deactivation pathways. Fine structure in photoluminescence spectra are clearly observed only in a few cases of highly dispersed metal (V,[5-10] Mg[11, 12]) oxide on silica.

The fine structure reveals vibrational levels of the ground state and provide some important information for the luminescent site. For vanadium oxide species, the fine structure in the emission spectrum was proposed to be due to the terminal V=O bond in the pseudotetrahedral oxovanadium group.[5-8] However, recently this fine structure was claimed to be from V-O bonds involving basal plane oxygen ions and not from the V=O bond.[10] On the other hand, the luminescent site magnesium oxide species dispersed on silica[11, 12] is not fully understood, this being the first example of observation of fine structure in a non-transition metal oxide system, which is believed to possess no doubly bonded terminal oxygens.

In the present study, we found that silica-alumina binary oxide evacuated at high temperature is also luminescent and exhibits similar fine structure in its phosphorescent emission spectra as do the vanadium and magnesium species despite the fact that silica-alumina is not a supported system and contains no doubly bonded oxygen.

Experimental

The silica-alumina samples employed were Japan Reference Catalysts[13, 14] (JRC-SAH-1 and JRC-SAL-2) which were supplied by the committee on Reference Catalyst, Catalysis Society of Japan. The alumina contents were 28.6 and 13.8 mass% and the specific surface areas were 511 and 560 $m^2\ g^{-1}$, respectively. Silica and alumina were also JRC samples, JRC-SIO-4 and JRC-ALO-4 (surface areas, 347 and 177 $m^2\ g^{-1}$). The samples were

recalcined in air at 773 K for 5 h. Before recording spectra, the samples were treated with 60 Torr oxygen for 1 h at 1073 K, followed by 1 h evacuation at 1073 K to clean the surface, and then transferred *in situ* to the optical cell (quartz tube, 5 mm diameter). The amount of the sample in the cell was *ca.* 150 mg. Photoluminescence spectra were recorded at 77 K with a Hitachi F-3010 fluorescence spectrophotometer using a UV filter ($\lambda_{transmittance} > 300$ nm) to remove scattered light from the UV source (Xe lamp), where the fluorescence emission was cut off mechanically to record phosphorescence spectra.

Results and discussion

Fig. 1 shows the phosphorescent emission spectra of silica, alumina, and silica-alumina samples evacuated at 1073 K and excited by 300 nm light. Silica exhibits a broad band centred at 450 - 480 nm, and alumina shows a broad band centred at 520 nm accompanied by a shoulder at 450 nm; for both silica and alumina the band intensities were very weak. By contrast, silica-alumina samples exhibit the fine structure spectra centred at 520 nm. Although this characteristic feature of the emission spectrum does not change upon varying the aluminium content, the band intensity of the SAL-2 sample is higher than that of the SAH-1 sample. This vibronically structured emission spectrum was reversibly varied upon water adsorption to give a broad spectrum which had been assigned to hydroxy groups on the surface.[12] High temperatures such as 1073 K were required for the silica-alumina samples to exhibit the fine structure. The same treatment was also required in the case of Mg.[11, 12]

The fine structure spectra of silica-alumina samples evacuated at 1073 K are most clearly observed under excitation by 300 - 330 nm light. While neither silica nor alumina alone show a band at *ca.* 300 nm in the excitation spectra (Fig. 2), the silica-alumina samples exhibit a band at *ca.* 300 nm. This band is more prominent in SAL-2 (lower Al content) than in SAH-1 (higher Al content).

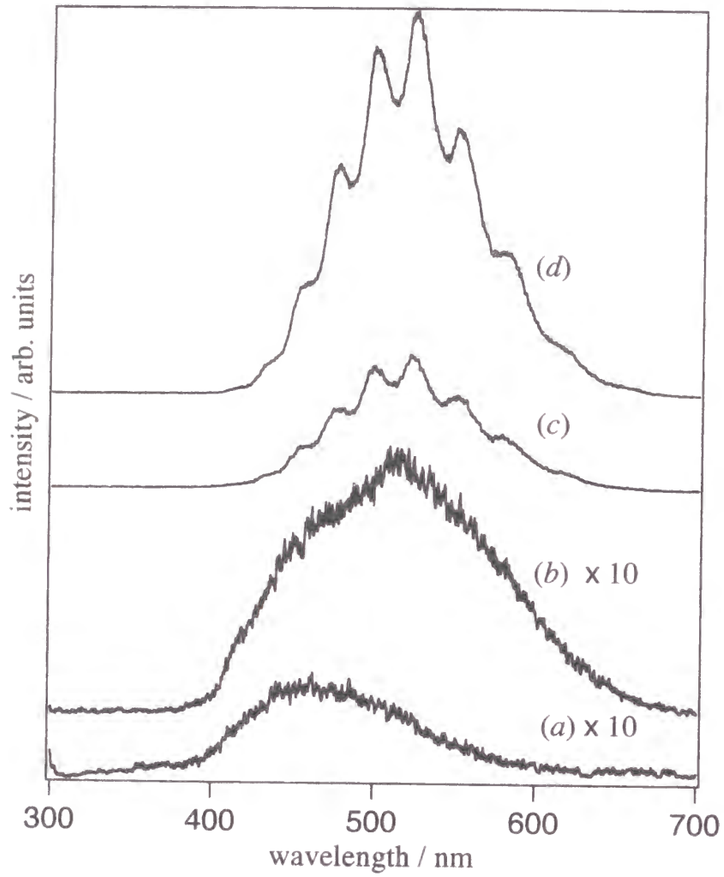

Fig. 1 Phosphorescent emission spectra of samples excited at λ = 300 nm; (*a*) SIO-4, (*b*) ALO-4, (*c*) SAH-1 and (*d*) SAL-2.

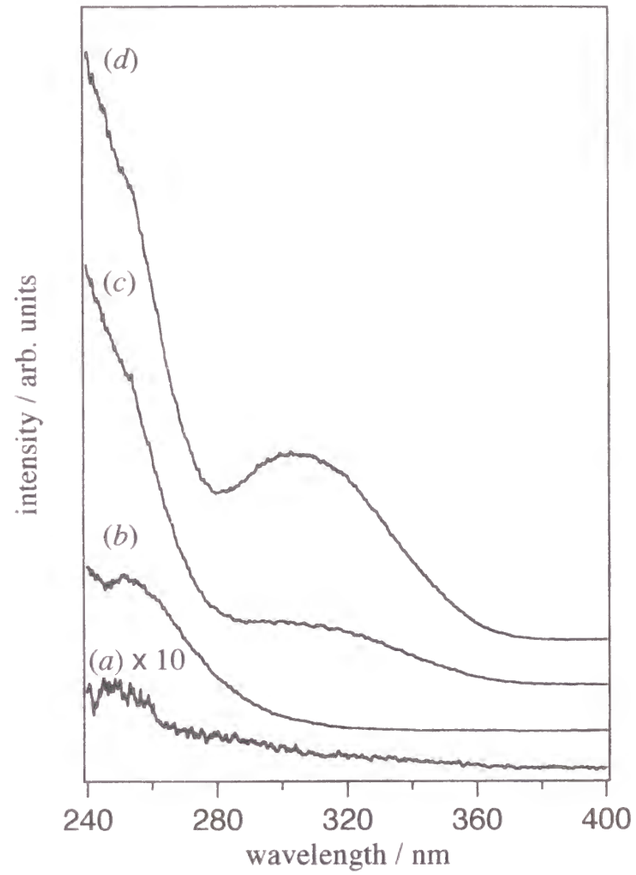

Fig. 2 Phosphorescent excitation spectra of samples recorded by monitoring emission at 520 nm; (*a*) SIO-4, (*b*) ALO-4, (*c*) SAH-1 and (*d*) SAL-2.

The vibrational energy which is estimated from the fine structure in the emission spectra (Fig. 1) is 900 - 1000 cm^{-1}. In IR spectroscopy, such a wavenumber is typical of a metal-oxygen-metal linkage, *e.g.* ν(Si-O-Al) in zeolites.[15, 16] Since silica-alumina samples exhibit characteristic emission spectra in contrast to silica or alumina, the emission site is due to the Al-O-Si linkage.

The larger band intensities in Figs. 1 and 2 of the SAL-2 sample with lower Al content suggest that a high dispersion of Al is required to obtain fine structure. The reactivity to water molecules, which results in the disappearance of the fine structure, establishes that the luminescent sites exist on the surface. Such sites are also coordinatively unsaturated, since evacuation at high temperature is needed for the recovery of the fine structure. Therefore, the luminescent site which exhibits this spectrum is a coordinatively unsaturated site belonging to the heterobond linkage Al-(O-Si)3 on the surface.

It is commonly accepted that the coordinatively unsaturated Al ion on the surface of silica-alumina evacuated at high temperature is positively charged, a so-called Lewis acid site.[17] Therefore, the electrons of oxygens bound to the Al ion might transfer to the Al ion under photoexcitation. When the excited electron is retransferred to oxygen during the deactivation process, the vibration of Al-O-Si linkage would be observed as fine structure in the phosphorescent emission spectrum. This suggestion for the photoexcitation and deactivation mechanism could also be applied to the Mg-O-Si linkage in the highly dispersed magnesium on silica.[11, 12]

Conclusion

We conclude that coordinatively unsaturated sites belonging to the heterobond linkage metal-(O-Si)3 on the silica surface is the active species producing fine structure in phosphorescence spectra for Mg or Al on silica. It is also suggested that other heterolinkages on silica have a potential ability for photoexciting and exhibiting luminescence spectra containing fine structure.

References

1 A. J. Tench and G. T. Pott, *Chem. Phys. Lett.*, 1974, **26**, 590.

2 S. Coluccia, A. M. Deane and A. J. Tench, *J. Chem. Soc. Faraday Trans. 1*, 1978, **74**, 2913.

3 V. A. Shvets, A. V. Kuznetsov, V. A. Fenin and V. B. Kazansky, *J. Chem. Soc., Faraday Trans. 1*, 1985, **81**, 2913.

4 M. Anpo, Y. Yamada, Y. Kubokawa, S. Coluccia, A. Zecchina and M. Che, *J. Chem. Soc., Faraday Trans. 1*, 1988, **84**, 751.

5 A. M. Gritscov, V. A. Shvets and V. B. Kazansky, *Chem. Phys. Lett.*, 1975, **35**, 511.

6 M. Anpo, I. Tanahashi and Y. Kubokawa, *J. Phys. Chem.*, 1980, **84**, 3440.

7 M. Iwamoto, H. Furukawa, K. Matsukami, T. Takenaka and S. Kagawa, *J. Am. Chem. Soc.*, 1983, **105**, 3719.

8 M. F. Hazenkamp and G. Blasse, *J. Phys. Chem.*, 1992, **96**, 3442.

9 S. Takenaka, T. Kuriyama, T. Tanaka, T. Funabiki and S. Yoshida, *J. Catal*, 1995, **155**, 196.

10 K. Tran, M. A. Hanning-Lee, A. Biswas, A. E. Stiegman and G. W. Scott, *J. Am. Chem. Soc.*, 1995, **117**, 2618.

11 T. Tanaka, H. Yoshida, K. Nakatsuka, T. Funabiki and S. Yoshida, *J.Chem.Soc.Faraday Trans.*, 1992, **88**, 2297.

12 H. Yoshida, T. Tanaka, T. Funabiki and S. Yoshida, *J. Chem. Soc. Faraday Trans.*, 1994, **90**, 2107.

13 Y. Murakami, *Stud. Suf. Sci. Catal.*, 1983, **16**, 775.

14 T. Uchijima, *Catalytic Science and Technology*, ed. S. Yoshida, N. Takezawa and T. Onos, Eds., Kodansha, VCH, Tokyo, 1991, vol. 1, p. 393.

15 E. M. Flanigen, in *Zeolite Chemistry and Catalysis* ed. J. A. Rabo, American Chemical Society, Washinton D.C., 1976, p. 80.

16 A. C. Wright, J. P. Rupert and W. T. Granquist, *Am. Mineral.*, 1968, **53**, 1293.

17 K. Tanabe, M. Misono, Y. Ono and H. Hattori, *Stud. Surf. Sci. Catal.*, 1989, **51**, 108.

Part III

Photocatalysis over silica and silica-based catalysts

Introduction of Part III

In part III of this thesis, new catalytic systems are presented: photometathesis of alkenes over amorphous silica and mesoporous silica, and photoepoxidation of propene over Nb-, Mg-loaded silica and bare silica. Here the author describes the backgrounds of the studies on the metathesis reaction and the propene epoxidation, respectively.

Metathesis of alkenes

By the metathesis reaction, two molecules of alkenes are converted selectively into two molecules of another alkenes, according to scheme 1.

Scheme 1 Metathesis reaction of alkenes.

This reaction is applied to not only many kinds of olefin syntheses but also synthesis of polymers. Although many reviews for the metathesis reactions have already been published, the latest book[1] has summarized the olefin metathesis and the metathesis polymerization.

The first report on olefine metathesis[2] was published in 1960, in which ring-opening metathesis polymerization was described. The heterogeneously catalyzed metathesis of alkenes was reported by Banks and Bailey[3] and the homogeneously one by Calderon *et al.*[4] The first heterogeneous catalysts presented by Banks[3] were Mo/Al_2O_3 catalysts' families such as CoO-MoO_3/Al_2O_3 and $Mo(CO)_6/Al_2O_3$. Other heterogeneous systems followed the discovery; *e.g.*, WO_3/SiO_2[5, 6] that exhibited stable activity at a high temperature and Re_2O_7/Al_2O_3[7] that showed high activity and selectivity at a low temperature. The first homogeneous catalytic system was $WCl_6/EtOH/AlEtCl_2$.[4, 8] The homogeneous catalytic systems have been applied to

synthesis of high molecular weight polymers in the ring-opening polymerization by the same reaction mechanism as metathesis.

The nature of the olefin metathesis reaction is that the double bond is apparently cleaved and the pieces put back together again. Yet not only is it possible but in some cases it can proceed to equilibrium within seconds.[1] The first several years after the discovery, the reaction scheme of metathesis was discussed. The reaction scheme of olefin metathesis (scheme 1) was clarified using labeled compounds by Calderon[4, 8, 9] and Mol,[10] independently.

The next basic question concerns the role of the catalyst and especially the transition metal in the olefin metathesis. The idea that a metal carbene species might be involved in olefin metathesis was first proposed by Hérisson and Chauvin[11] on the basis of the initial products of cross-metathesis of cyclic and acyclic olefins. The observation that metal carbene complexes such as $W(=CPh_2)(CO)_5$ functioned as initiators of olefin metathesis provided a good evidence of the metal carbene mechanism.[12] Metallacyclobutanes, the intermediates, were detected by ^1H and ^{13}C NMR spectroscopy at least for certain types of catalyst system.[13-18] The reaction mechanism is summarized in scheme 2 in the case of propene metathesis producing ethene and butene.

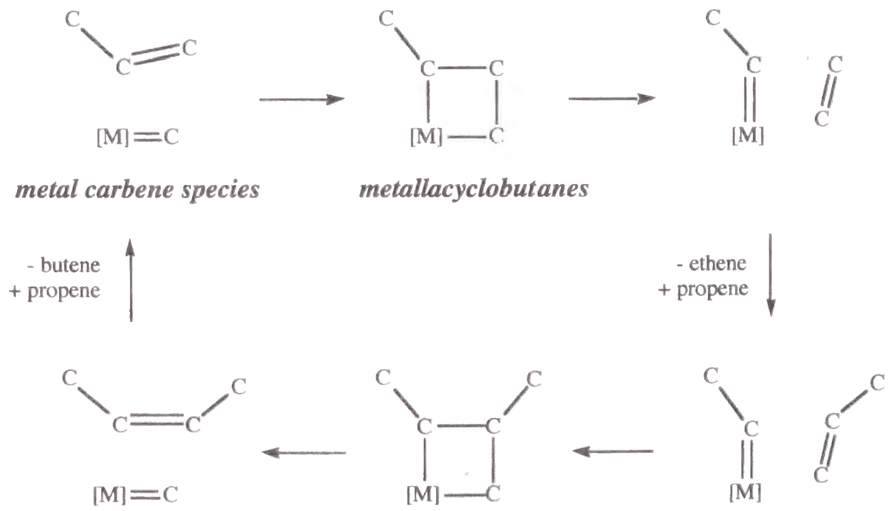

Scheme 2 A proposed mechanism of propene metathesis on transition metals.

Today, a large number of catalyst systems promoting olefin metathesis have been reported. The most important catalyst systems are derived from compounds of the nine transition elements shown in the table 1 (underlined); those shown in bold type are generally the most effective. Catalysis by compounds of non-transition elements is very much the exception.[1] Rare examples appear to be $EtAlCl_2$[19], Me_4Sn/Al_2O_3[20] and $MgCl_2$.[21]

Table 1 The active elements for metathesis reactions.[1]

IVA	VA	VIA	VIIA	VIII	
Ti	*V*	*Cr*			*Co*
Zr	Nb	**Mo**	*Tc*	Ru	*Rh*
	Ta	**W**	**Re**	Os	Ir

Supported molybdenum oxide catalysts have received much attention since they are widely used in industrial petrochemical processes, including metathesis. Many investigations were done, and how to handle the system has been well known. The preparation method and precursor, support materials, the activation mechanism and the active site were widely studied.[1] Using photoirradiation, metathesis reactions were promoted in some systems. The first photocatalytic system for metathesis reaction was WCl_6/*i*-Bu_3Al by Günther.[22] $Mo(CO)_6$ and $W(CO)_6$ adsorbed on porous Vycor glass (PVG) or NaY zeolite become active when they are irradiated with a mercury lamp (>290 nm) at room temperature in the presence of propene.[23] MoO_3 supported on PVG was found to catalyze the metathesis of propene under UV irradiation (>280 nm).[24, 25] Anchored catalyst MoO_3/SiO_2 that obtained by reaction of gaseous $MoCl_5$ with surface silanols exhibited higher activity than that obtained by impregnation.[26, 27] The higher active species are highly dispersed species in low loading samples. Similar results have been obtained for WO_3 and CrO_3 on PVG, although the initial reaction rates are much lower.[28]

In the history of investigation of metathesis reactions, there are no report that metathesis proceeded on silica alone. However, we found the reaction over bare silica under photoirradiation as presented in this thesis (chapter 6 and 7). This finding about

photometathesis over silica seems to be just a special case. Ivin and Mol referred to the phenomena in the newest review[1] as follows: "A curiosity is that silica alone, activated by evacuation at high temperatures, is reported to catalyze metathesis of (deuterated) ethene and propene under photoirradiation."

Epoxidation of propene

The important products in propene oxidation in chemical industries are acrolein (CH_2=CHCHO), acrylic acid (CH_2=CHCOOH), propylene oxide($CH_3CH(O)CH_2$) and acrylonitrile (CH_2=CHCN). Among them, acrolein and acrylonitrile are directly produced by heterogeneous catalytic oxidation/ammoxidation processes. Although a direct oxidation of propene to acrylic acid had been examined, acrylic acid is produced by oxidation of acrolein at present.

Propylene oxide is produced by indirect oxidation *via* chlorohydrin or by oxidation using hydroperoxide as an oxidant in a liquid-phase. In these processes, however, some chemicals were consumed and unnecessary chemicals are produced wastefully. Since epoxides are one of the most important intermediate for many chemicals, new heterogeneous catalytic systems producing epoxides directly from alkenes, if possible with gaseous oxygen, are strongly desirable. Since the epoxidation of ethene with gaseous oxygen over Ag catalysts was found many years ago by Lefort,[29] the application to propene had seemed to be easy.

Since epoxidation over Ag metal is important in industry and science, many studies have done for this system.[30-32] Usually the Ag, supported by alumina, exists as metal particles; the turn over frequencies on surface Ag is the same as that of single crystal. There have been many studies by the techniques of surface characterizations such as XPS, AES, ISS, LEED,[33] HREELS,[32] STM.[34] There were some discussion what is the active oxygen species; molecular oxygen, atomic oxygen[32] or subsurface oxygen atom.[35] It is probable that atomic oxygen adsorbed on Ag is active and reacts with ethene.[30, 32, 36, 37] Although the reaction mechanism over Ag catalyst surface has been deeply clarified, the application to propene epoxidation has

not yet succeeded. To break through the present situation, the other systems have attracted considerable attention.

Catalytic systems that consume organic hydroperoxides (HPO) as oxidants have developed industrially. In Acro-Oxirane method,[38, 39] homogeneous catalysts such as $Mo(CO)_6$ are used in organic solvents such as CH_2Cl_2 or benzene, with HPO such as PhCH(Me)OOH or *t*-BuOOH.[40] The most active catalysts would be Mo complexes.[41, 42] In the system, the reaction starts after substitution of HPO for the ligands of Mo complex in the solution.[43] The reaction mechanism has been studied.[44-48]

Heterogeneous system has also developed. In the Shell method,[49, 50] TiO_2/SiO_2 catalysts were employed. Ti-containing zeolites[51-53] have recently attracted interest as catalysts for epoxidation, although they must consume hydrogen peroxide as an oxidant. It is needless to say that gaseous oxygen is the more desirable oxidant than hydrogen peroxide industrially. Epoxidation of alkenes by gaseous oxygen over heterogeneous catalysts has rarely succeeded except for ethylene. The epoxidation of propene by molecular oxygen is one of the important and difficult subject, so-called "a dream reaction."

Recently, a spectroscopic study was reported on the production of adsorbed propylene oxide from propene and O_2 over Ba Y-zeolite irradiated with visible light.[54] Tanaka *et al.* had already pointed out that the formation of an epoxide intermediate in the photooxidation of alkenes over silica-supported vanadium oxide.[55] Note that all these heterogeneous catalysts are related to silica or zeolites. The auther presents in this thesis that some new systems can catalyze epoxidation of propene with gaseous oxygen under photoirradiation; the highly dispersed niobium oxide on silica (chapter 8), the highly dispersed magnesium on silica and bare silica (chapter 9).

Survey of Part III

Evolution of technology of catalysis would be made up by discovery of a new system and a new concept. As for metathesis reaction, the active elements in the known catalytic systems are limited to transition metals, although some catalytic systems working on non-transition metals such as $EtAlCl_2$[19], Me_4Sn/Al_2O_3[20] and $MgCl_2$[21] have been discovered. In chapter 6,

the author presents metathesis reaction of alkenes over bare silica under irradiation; this is quite a new system. In chapter 7, the author shows the first catalytic activity of FSM-16 which has attracted much attention as a new silica material of highly ordered mesopores.[56, 57] These systems might have a potential to make a new field in metathesis reaction.

Concerning epoxidation of propene, the first success is presented in chapter 8; highly dispersed niobium oxide species on silica produce propylene oxide by using O_2. Although silica catalyzes metathesis reaction of propene without O_2 as described in chapter 6, in addition, another function of silica is revealed as described in chapter 9; propylene oxide was produced in the presence of O_2 (over silica). It is also mentioned that Mg ion promotes the activity to produce propylene oxide.

References

1 K. J. Ivin and J. C. Mol, *Olefin metathesis and metathesis polymerization* (Academic Press, San Diego, 1997).

2 W. L. Truett, D. R. Johnson, I. M. Robinson and B. A. Montague, *J. Am. Chem. Soc.*, 1960, **82**, 2337.

3 R. L. Banks and G. C. Bailey, *Ind. Eng. Chem., Prod. Res. Dev.*, 1964, **3**, 170.

4 N. Calderon, H. Y. Chen and K. W. Scott, *Tetrahedron Lett.*, 1967, **34**, 3327.

5 L. Phillips Petroleum, *Neth. Pat.*, 1964, 6400549.

6 R. L. Banks and R. B. Regier, *Ind. Eng. Chem., Prod. Res. Dev.*, 1971, **7**, 29.

7 L. British Petroleum, *Neth. Pat.*, 1966, 6511659.

8 N. Calderon, E. A. Ofstead, J. P. Ward, W. A. Judy and K. W. Scott, *J. Am. Chem. Soc.*, 1968, **90**, 4133.

9 N. Calderon, E. A. Ofstead and W. A. Judy, *J. Polymer Sci., A-1*, 1967, **5**, 2209.

10 J. C. Mol, J. A. Moulijin and C. Boelhouwer, *J. Chem. Soc., Chem. Commun.*, 1968, 633.

11 J.-L. Hérrison and Y. Chauvin, *Makromol. Chem.*, 1971, **141**, 161.

12 T. J. Katz, S. J. Lee and N. Acton, *Tetrahedron Lett.*, 1976, 4251.

13 R. R. Schrock, S. Rocklage, J. Wengrovius, G. Rupprecht and J. Fellmann, *J. Mol. Catal.*, 1980, **8**, 73.

14 K. H. Wengrovius, R. R. Schrock, M. R. Churchill, J. R. Missert and W. J. Youngs, *J. Am. Chem. Soc.*, 1980, **102**, 4515.
15 J. Kress, M. Wesolek and J. A. Osborn, *J. Chem. Soc., Chem. Commun.*, 1982, 514.
16 J. Kress, J. A. Osborn, R. M. E. Greene, K. J. Ivin and J. J. Rooney, *J. Chem. Soc., Chem. Commun.*, 1985, 874.
17 J. Kress, J. A. Osborn, R. M. E. Greene, K. J. Ivin and J. J. Rooney, *J. Am. Chem. Soc.*, 1987, **109**, 899.
18 J. Kress, J. A. Osborn, V. Amir-Ebrahimi, K. J. Ivin and J. J. Rooney, *J. Chem. Soc., Chem. Commun.*, 1988, 1164.
19 K. J. Ivin, J. J. Roony and C. D. Stewart, *J. Chem. Soc., Chem. Commun.*, 1978, 604.
20 H.-G. Ahn, K. Yamamoto, R. Nakamura and H. Niiyama, *Chem. Lett.*, 1992, 503.
21 P. Buchacher, W. Fischer, K. D. Aichholzer and F. Stelzer, *J. Mol. Catal.*, 1996, 163.
22 P. Günther, F. Haas, G. Marwede, K. Nützel, W. Oberkirch, G. Pampus, N. Schön and J. Witte, *Angew. Makromol. Chem.*, 1970, **14**, 87.
23 Y. Wada, C. Nakaoka and A. Morikawa, *Chem. Lett.*, 1988, 25.
24 M. Anpo, I. Tanahashi and Y. Kubokawa, *J. Chem. Soc., Faraday Trans. 1*, 1982, **78**, 2121.
25 M. Anpo, I. Tanahashi and Y. Kubokawa, *J. Catal.*, 1982, **75**, 204.
26 M. Anpo, M. Kondo, Y. Kubokawa, C. Louis and M. Che, *Chem. Express*, 1987, **2**, 65.
27 M. Anpo, M. Kondo, Y. Kubokawa, C. Louis and M. Che, *J. Chem. Soc., Faraday Trans. 1*, 1988, **84**, 2771.
28 M. Anpo, T. Suzuki, Y. Kubokawa, T. Fujii, K. Kuno and S. Suzuki, *Chem. Express*, 1986, **1**, 41.
29 T. E. Lefort, *French Pat. 729,952*, 1931,
30 R. A. vanSanten and H. P. C. E. Kuipers, *Adv. Catal.*, 1987, **35**, 265.
31 M. A. Barteau and R. J. Madix, in *The Chemical Physics of Solid Surfaces and Heterogeneous Catalysis* ed. D. A. King and P. Woodruff, Elsevier, 1982, vol. 4, p. 591.
32 D. Kondarides and Y. Iwasawa, *Hyomen*, 1994, **32**, 295.
33 H. A. Engelhardt and D. Menzel, *Surf. Sci.*, 1976, **57**, 591.
34 T. Hashizume, M. Taniguchi, K. Motai, H. Lu, K. Tanaka and T. Sakurai, *Surf. Sci.*, 1992, **266**, 282.
35 X. Bao, J. V. Bath, G. Lehmpfuhl, R. Schuster, Y. Uchida, R. Schlogl and G. Ertt, *Surf. Sci.*, 1993, **284**, 14.
36 S. Y. Yong and N. W. Cant, *Appl. Catal.*, 1989, **48**, 37.
37 J. T. Gleaves, A. G. Sault, R. J. Madix and J. R. Ebner, *J. Catal.*, 1990, **121**, 202.
38 R. Landau, G. A. Sullivan and D. Brown, *Chemtech*, 1979, 602.
39 A. Imamura and K. Hirao, *Bull. Chem. Soc. Jpn.*, 1979, **52**, 287.

40 K. Takehira, in *Shokubaikouza* ed. Catalysis Society of Japan, Kodansha, Tokyo, 1985, vol. 8, p. 172.
41 C. C. Su, J. W. Read and E. S. Gould, *Inorg. Chem.*, 1973, **12**, 337.
42 M. N. Sheng and J. G. Zajacek, *Adv. Chem. Ser.*, 1968, **76**, 418.
43 R. A. Sheldon, *Recl. Trav. Chim. Pays-Bas*, 1973, **92**, 253.
44 A. O. Chong and K. B. Sharpless, *J. Org. Chem.*, 1977, **42**, 1587.
45 F. D. Furia and G. Modena, *Pure Appl. Chem.*, 1982, **54**, 1982.
46 P. Chaumette, H. Mimoun, L. Saussine, J. Fisher and A. Mitschler, *J. Organomet. Chem.*, 1983, **250**, 291.
47 H. Mimoun, *J. Mol. Catal.*, 1980, **7**, 1.
48 H. Minoun, *Angrew. Chem. Int. Ed. Enbl.*, 1982, **2**, 734.
49 R. A. Sheldon, J. A. V. Doorn, C. W. A. Schram and A. J. De Jong, *J. Catal.*, 1973, **31**, 438 .
50 R. A. Sheldon, *J. Mol. Catal*, 1980, **7**, 107 .
51 M. G. Clerici, G. Bellussi and U. Romano, *J. Catal.*, 1991, **129**, 159.
52 U. Romano, A. Esposito, F. Maspero, C. Neri and M. G. Clerici, *Stud. Surf. Sci. Catal.*, 1990, **55**, 33.
53 B. Notari, *Stud. Surf. Sci. Catal.*, 1987, **37**, 413.
54 F. Blatter, H. Sun and H. Frei, *Catal. Lett.*, 1995, **35**, 1.
55 T. Tanaka, M. Ooe, T. Funabiki and S. Yoshida, *J. Chem. Soc., Faraday Trans.1*, 1986, **82**, 35.
56 S. Inagaki, Y. Fukushima and K. Kuroda, *J. Chem. Soc., Chem. Commun.*, 1993, 680.
57 S. Inagaki, A. Koiwai, N. Suzuki, Y. Fukushima and K. Kuroda, *Bull. Chem. Soc., Jpn.*, 1996, **69**, 1449.

Chapter 6

Photometathesis of alkenes over amorphous silica

Abstract

Silica, activated by evacuation at high temperatures, catalyses metathesis reactions of ethene and propene under photoirradiation.

Introduction

Metathesis reactions are known to be extremely useful for the synthesis of various alkenes. Therefore, many catalysts for such reactions have been extensively developed since the discovery of a molybdenum catalyst by Banks and Bailey[1] in a heterogeneous system and of a tungsten catalyst by Calderon *et al.*[2] in homogeneous system. Most of the catalysts contain transition metals such as Mo,[1] W,[2, 3] Re,[4] *etc.*, which can form metal carbene and metallacyclobutane intermediates.[5] Therefore, it was believed that these transition metals are necessary elements in catalysts for metathesis reactions.

Silica is a common material often used as a catalyst support, an adsorbent and so on, and generally it is inactive itself. However, silica can function as catalysts for some reactions,[6-12] in particular when it is activated by photoirradiation.[13-15] So far, there has been no report on catalysis by silica for metathesis. We report here the first discovery that silica can catalyse metathesis reactions of ethene and propene under photoirradiation.

Experimental

The silica sample employed was mainly Cab-osil M5, which was impregnated with water and dried, followed by calcination in flowing air at 773 K for 5 h. Before each reaction, it was heated in the presence of 50 Torr (1 Torr = 133.3 Pa) oxygen at the given temperature (Table 1) for 1h and evacuated at the same temperature for 1 h.

Results and discussion

Fig. 1 shows the time course of the reaction of propene over silica. Products were ethene (C_2), *trans*-but-2-ene (*trans*-C_4), *cis*-but-2-ene (*cis*-C_4) and a very small amount of but-1-ene

(1-C_4). The selectivity (ratio of the total moles of products to the moles of propene consumed) was 100 % within experimental error. Furthermore, the amount of ethene and butenes were approximately equimolar; the molar ratio of ethene to butenes (C_2:C_4) at each sampling of products in the gas phase was between 1.03 and 1.08, these values were comparable to theoretical value of 1.0, suggesting that a metathesis reaction of propene occurred in this system:

$$2\ CH_2{=}CHMe \rightarrow MeCH{=}CHMe + CH_2{=}CH_2 \qquad (1)$$

These results show that this system is as good as some of the best systems reported in the literature.[16] The high selectivity presents the potential for a photocatalytic system to promote a selective reaction. The conversion and product yields increased with time, and they seemed to achieve a specific composition, which is lower than the equilibrium conversion (42.3 % at 298 K- 47.8 % at 811 K).[16] The cause of saturation of conversion in this closed system might be photoadsorption of butenes onto the active sites of the silica surface. However, the following experiment proved that the cause of the saturated conversion in Fig. 1 was not catalyst deactivation. After the increase in conversion apparently stopped, the reactor and circulating part were evacuated at room temperature and propene was reintroduced to the system. The reaction proceed again under irradiation with virtually the same rate as the first run.

The reaction of ethene was also examined. In the case of ethene, if the only reaction was metathesis, then no new products should be observed. After the reaction under irradiation for 1 h on silica, nothing other than ethene was observed. When a mixture of $CH_2{=}CH_2$ and $CD_2{=}CD_2$ was introduced as reactant, the production of [$^2H_2$]ethene was observed. Neither [$^2H_1$]- nor [$^2H_3$]-ethene was found in the system, confirming that the only reaction occurring over the silica was metathesis:

$$CH_2{=}CH_2 + CD_2{=}CD_2 \rightarrow 2\ CH_2{=}CD_2 \qquad (2)$$

Fig. 2 indicates the response of the reaction to photoirradiation. It reveals that the reaction proceeded only under irradiation. The good response indicates clearly that the metathesis reaction was induced by irradiation. The dependence of the reaction upon the excitation wavelength was examined by using a UV filter, shown in Table 1 (entries 1-3). Irradiation with visible light only (entry 1), the reaction was limited to low conversion levels with a high ratio of C_2:C_4. On the other hand, irradiation with UV light (entries 2, 3), caused metathesis reaction to accelerate, indicating that UV light is required for the metathesis reaction on silica surface.

The effect of pretreatment temperature is shown in Table 1(entries 3-5). This silica is more activated by pretreatment at the higher temperature, suggesting that the desorption of the hydroxyl groups on the silica surface might relate to active sites.

We also examined other kinds of silica as catalysts; JRC-SIO-4(supplied from Catalysis Society of Japan) and some silica samples prepared by sol-gel method[17] from Si(OEt)4. The metathesis reaction was observed on each silica, except for an aged silica prepared by the sol-gel method thirty months ago. Among the silica samples prepared by the sol-gel method in the last three years, the newer sample exhibited the higher activity. This means that the number of active sites decreased with time. In order to reactivate a silica prepared twenty months ago, the sample was impregnated in water and dried, calcined in flowing air at 773 K before pretreatment at 1073 K. The refreshed silica exhibited higher activity, suggesting that this treatment restored the active site.

We tested other typical metal oxides such as MgO, Al_2O_3, SiO_2-AlO_2. On these oxides, although other reaction occurred to a small extent, the distribution of products was quite different from that for the metathesis reaction. The metathesis reaction under irradiation seems to be characteristic of silica surface among such typical metal oxides.

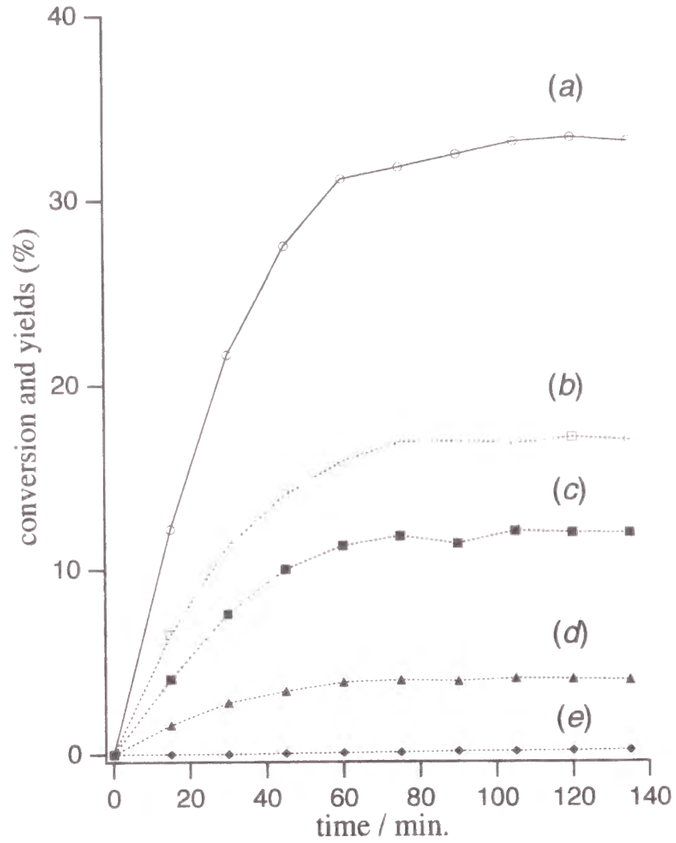

Fig. 1 Time course of the reaction: (*a*) conversion of propene and yields of (*b*) ethene, (*c*) *trans*-but-2-ene, (*d*) *cis*-but-2-ene and (*e*) but-1-ene. The reaction was carried out in a closed circulation system (250 ml; propene 200 μmol). The powder catalyst (400 mg) was spread on the flat bottom (12cm^2) of the quartz reactor irradiated from beneath by a 250 W Hg lamp. The pretreatment temperature was 1073 K. Products were analyzed by GC.

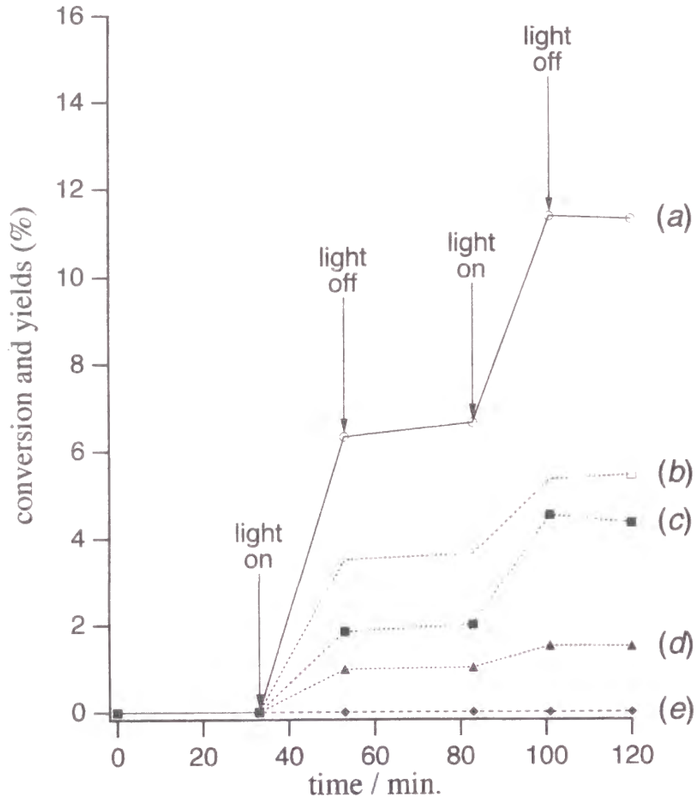

Fig. 2 Response of the reaction to the irradiation: (*a*) -(*e*) as in caption to Fig. 1

Table 1 Effects of pretreatment temperature and irradiation wavelength[a]

Entry	T / K	Filter	conv. (%)	C_2:C_4	Yields (%) C_2	*trans*-C_4	*cis*-C_4	1-C_4
1	1073	Y-43[b]	0.27	1.25	0.15	0.07	0.05	0.00
2	1073	UV-29[c]	4.75	1.05	2.43	1.59	0.73	0.01
3	1073	none	11.4	1.02	5.74	4.08	1.56	0.05
4	873	none	6.95	1.00	3.47	2.50	0.95	0.01
5	673	none	5.86	0.78	1.37	0.92	0.70	0.13

[a] The measurement was carried out under irradiation for 1 h using a 250 W Hg lamp after pretreatment in a closed static system (39.5 ml; sample 100 mg; propene 30 μmol; irradiated area of catalyst bed 12 cm^2).

[b] Y-43 filter admits light with $\lambda > 430$ nm.

[c] UV-29 filter admits light with $\lambda > 290$ nm.

Conclusion

From the results mentioned above, we conclude that silica catalyzed metathesis reactions of propene and ethene under photoirradiation, and it was activated by the treatment of impregnation in water and calcination in flowing air followed by evacuation at high temperatures.

References

1 R. L. Banks and G. C. Bailey, *Ind. Eng. Chem.*, 1964, **3**, 170.

2 N. Calderon, H. Y. Chen and K. W. Scott, *Tetrahedron Lett.*, 1967, **34**, 3327.

3 R. L. Banks and R. B. Regier, *Ind. Eng. Chem., Prod. Res. Dev.*, 1971, **7**, 29.

4 R. Nakamura, H. Iida and E. Echigoya, *Chem. Lett.*, 1972, 273.

5 J. L. Herrison and Y. Chauvin, *Makromol. Chem.*, 1971, **141**, 161.

6 J. N. Armor, *J. Catal.*, 1981, **70**, 72.

7 J. N. Armor and P. M. Zambri, *J. Catal.*, 1982, **73**, 57.

8 M. Lacroix, G. M. Pajonk and S. J. Teichner, *J. Catal.*, 1986, **101**, 314.

9 Y. Matsumura, K. Hashimoto and S. Yoshida, *J. Chem. Soc., Chem. Commun.*, 1987, 1599.

10 G. N. Kastanas, G. A. Tsigdinos and J. Schwank, *J. Appl. Catal.*, 1988, **44**, 33.

11 Y. Matsumura, K. Hashimoto and S. Yoshida, *J. Catal.*, 1989, **117**, 135.

12 E. W. Bittner, B. C. Bockrath and J. M. Solar, *J. Catal.*, 1994, **149**, 206.

13 A. Morikawa, M. Hattori, K. Yagi and K. Otsuka, *Z.Phys.Chem.,N.F.*, 1977, **104**, 309.

14 M. Anpo, C. Yun and Y. Kubokawa, *J. Catal.*, 1980, **61**, 267.

15 A. Ogata, A. Kazusaka and M. Enyo, *J. Phys. Chem.*, 1986, **90**, 5201.

16 J. C. Mol and J. A. Moulijn, *Adv. Catal.*, 1975, **24**, 131.

17 S. Yoshida, T. Matsuzaki, T. Kashiwazaki, K. Mori and K. Tarama, *Bull. Chem. Soc. Jpn.*, 1974, **47**, 1564.

Chapter 7

Photometathesis of propene over mesoporous silica

Abstract

Mesoporous silica (FSM-16) catalyses metathesis of propene under photoirradiation at a higher activity than amorphous silica whereas microporous silica crystals (silicalite-1) do not catalyse the reaction.

Introduction

Mesoporous silica materials such as MCM-41[1, 2] and FSM-16[3, 4] attract a great deal of attention as new materials and many applications are expected. Although the application of these materials for catalysis has been widely studied, attention has also been paid to the generation of catalytic activity through the introduction of other metal ions into the silica lattice, but not to the catalytic activity of unmodified mesoporous silica.

Here, we show that undecorated mesoporous silica (FSM-16) has a higher catalytic activity in the photometathesis of propene than does amorphous silica which was recently found to be catalytically active in this reaction.[5] To elucidate structural factors of mesoporous silica in this reaction, we compare the catalytic activities of other forms of SiO_2; amorphous silica, microporous crystalline silica (silicalite-1)[6] and high-silica zeolite (dealuminated mordenite).

Experimental

Amorphous silica (AMS) was prepared by the sol-gel method[7] by hydrolysis of tetraethylorthosilicate(TEOS) followed by calcination at 773 K for 5 h. FSM-16 was prepared essentially in the same manner as described by Inagaki *et al.*[3, 4] except that hexadecyltrimethylammonium bromide was used as a template and the resulting material was calcined at 873 K in an N_2 atmosphere for 1 h and subsequently in air for 5 h. Silicalite-1 was synthesized from TEOS and tetrapropylammonium bromide(TPABr) by hydrothermal synthesis(433 K, 24 h) followed by washing, drying and calcination at 823 K. Dealuminated mordenite(DM, SiO_2/Al_2O_3 = 328) was obtained by extraction (12×) of aluminium using 8 N HCl at 333 K for 24 h[8] from JRC-Z-HM15 (a reference catalyst,[9, 10] Catalysis Society of Japan). The structures of these samples were confirmed by XRD and N_2 adsorption-desorption isotherms.

Photocatalytic conversion of propene was carried out under irradiation for 1 h using a 250 W Hg lamp in a closed static system (120 ml; propene 100 μmol) at room temperature. The powdered catalyst (200 mg) was spread on the flat bottom (12 cm^2) of a quartz reactor irradiated from beneath. Pretreatment of catalyst was performed at 873 K (or 1073 K) in air for 2 h and in the presence of 100 Torr oxygen for 1 h, followed by evacuation at the same temperature. After 1h reaction, products and unreacted propene were collected with a liquid-N_2 trap when the catalyst was under irradiation, and they were analysed by GC.

Results

The XRD patterns of the samples pretreated at 873 K and that of silicalite-1 pretreated at 1073 K are shown in Fig. 1. AMS (*a*) showed a very broad diffraction peak at 2θ *ca.* 22°, indicating its amorphous nature. The FSM-16 sample (*b*) exhibited low-angle diffraction peaks at 2θ 2.36, 4.06 and 4.68° and a very broad diffraction peak around at 2θ *ca.* 23° as reported,[3, 4] indicating that this material has ordered hexagonal mesopores with XRD amorphous walls. Silicalite-1 (*c*) and DM (*d*) were clearly assigned by comparison with their published structures.[6, 11] The structures of AMS, FSM-16 and DM were essentially unchanged upon calcination at 1073 K, while silicalite-1 calcined at 1073 K (*e*) gave an XRD pattern resembling that of amorphous silica.

The N_2 adsorption isotherms of AMS and FSM-16 were of type-IV, indicating the presence of mesopores; isotherms of silicalite-1 and DM were type I, also suggesting microporous structures.

Table 1 shows the catalytic activities of the samples evacuated at 873 K for propene metathesis under photoirradiation. AMS catalysed the metathesis reaction quite slowly, the activity roughly corresponded to that reported previously.[5] By contrast, FSM-16 showed a much higher metathesis activity than AMS. It should be noted that FSM-16 seemed to exhibit a higher specific activity than AMS. This is because the ratio of catalytic activity of FSM-16 to that of AMS is larger than the ratio of BET surface area (1170 and 580 $m^2\ g^{-1}$ for FSM-16 and

AMS, respectively). The C_2/C_4 ratio on FSM-16 was closed to unity, indicating the metathesis reaction proceeded selectively. In contrast, silicalite-1 showed no activity, indicating its microporous structure is of no advantage under the reaction conditions. DM also give no gaseous products and judging from the color of DM after reaction, propene appears to have been adsorbed and polymerized on acid sites of DM.

Upon evacuation at higher temperature (1073 K), the activities of AMS and FSM-16 greatly increased, while DM produced no gaseous products, as shown in Table 1. Activation of amorphous silica upon evacuation at high temperature is in agreement with a previous report.[5]

Upon evacuation at 1073 K the zeolite structure of silicalite-1 was destroyed and became XRD amorphous (BET surface area: 7.5 m^2g^{-1}). This amorphous sample gave no metathesis products even after 30 h reaction.

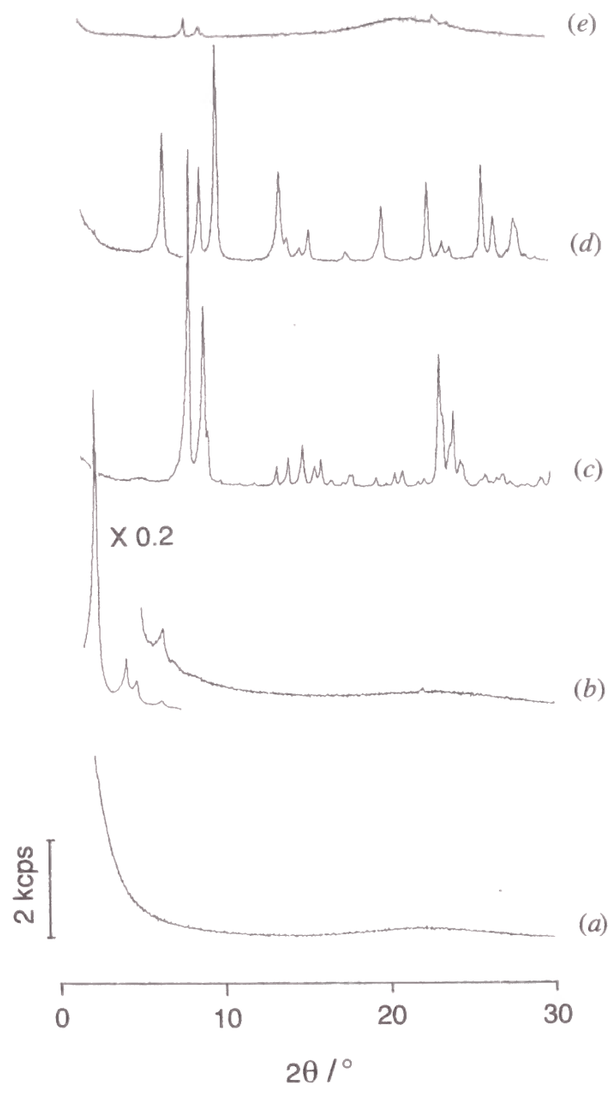

Fig. 1 XRD patterns of porous silica materials: (*a*) amorphous silica(AMS), (*b*) FSM-16, (*c*) and (*e*) silicalite-1 and (*d*) dealuminated mordenite (DM). Samples (*a*)-(*d*) were calcined at 873 K and (*e*) at 1073 K. Intensity of low angle part of (*b*) is reduced to 1/5.

Table 1 Results of tests for propene photometathesis on silica materials

pretreatment temperature/K	Sample	Yields(%)					Conv.(%) to metathesis	C_2/C_4 ratio
		C_2 [a]	*trans*-C4	*cis*-C4	1-C4	Adsorbed		
873	AMS	1.4	1.0	0.7	0.0	1.0	3.1	0.82
	FSM-16	8.2	5.7	2.8	0.3	5.8	16.9	0.94
	silicalite-1	0.0	0.0	0.0	0.0	2.3	0.0	-
	DM	0.0	0.0	0.0	0.0	100.0	0.0	-
1073	AMS	16.8	11.8	4.4	0.0	2.0	33.0 [b]	1.04
	FSM-16	16.2	12.0	4.7	0.4	5.6	33.3 [b]	0.95
	silicalite-1	0.0	0.0	0.0	0.0	1.3	0.0	-
	DM	0.0	0.0	0.0	0.0	98.7	0.0	-

[a] C_2 = ethene, C4 = butene. [b] The conversions on amorphous silica and FSM-16 reached equilibrium under the reaction conditions.[5]

Discussion

It is suggested from the results on the catalyst samples evacuated at 873 K that an amorphous phase of silica might be necessary for photometathesis on silica since reaction did not proceed on microporous crystalline silica, but only on amorphous silica (AMS) and on FSM-16 whose walls are amorphous.[2, 12] The results on the catalysis evacuated at 1073 K, however, indicated that catalytic activity is governed by the other factors, since amorphous samples produced by evacuation of silicalite-1 showed no activity.

Another distinguishable factor between these samples is the concentration of surface hydroxyl groups: microporous crystals have few hydroxy groups, while amorphous silica surfaces such as AMS and FSM-16 would possess a large amount of hydroxy groups. The increase of activity of AMS and FSM-16 evacuated at higher temperature indicates that this process produces active sites on the samples. Therefore it is suggested that sites produced by desorption of hydroxy groups would regulate the activity. For silicalite-1, there are only a small number of hydroxy groups prior to evacuation. Therefore, silicalite-1 evacuated at high temperature possesses few active sites, despite its amorphous surface.

There are two possibilities why FSM-16 exhibits higher activity than AMS. One is that FSM-16 has a larger number of surface hydroxy groups than AMS. The second is that the nature of the active sites differs from that of AMS as a consequence of the characteristic walls of FSM-16 which consist of double SiO_4 tetrahedral layers.[13]

Conclusion

In conclusion, the catalytic activity of unmodified mesoporous silica (FSM-16) has been investigated. FSM-16 exhibits higher photocatalytic activity for propene metathesis than amorphous silica. The key point is that FSM-16 has many hydroxyl groups on the amorphous walls which constitute the hexagonal mesopore structure. The active sites are proposed to be produced by desorption of hydroxy groups from the amorphous surface of silica.

References

1 C. T. Kresge, M. E. Leonowicz, W. J. Roth, J. C. Vartuli and J. S. Beck, *Nature*, 1992, **359**, 710.

2 J. S. Beck, J. C. Vartuli, W. J. Roth, M. E. Leonowicz, C. T. Kresge, K. D. Schmitt, C. T.-W. Chu, D. H. Olson, E. W. Sheppard, S. B. McCullen, J. B. Higgins and J. L. Schlenker, *J. Am. Chem. Soc.*, 1992, **114**, 10834.

3 S. Inagaki, Y. Fukushima and K. Kuroda, *J. Chem. Soc., Chem. Commun.*, 1993, 680.

4 S. Inagaki, A. Koiwai, N. Suzuki, Y. Fukushima and K. Kuroda, *Bull. Chem. Soc., Jpn.*, 1996, **69**, 1449.

5 H. Yoshida, T. Tanaka, S. Matsuo, T. Funabiki and S. Yoshida, *J. Chem. Soc., Chem.Commun.*, 1995, 761.

6 E. M. Flanigen, J. M. Bennett, R. W. Grose, J. P. Cohen, R. L. Patton, R. M. Kirchner and J. V. Smith, *Nature*, 1978, **271**, 512.

7 S. Yoshida, T. Matsuzaki, T. Kashiwazaki, K. Mori and K. Tarama, *Bull. Chem. Soc. Jpn.*, 1974, **47**, 1564.

8 A. Satsuma, T. Ishikura, T. Shimizu, M. Niwa, T. Hattori and Y. Murakami, *Kagaku Kogaku Ronbunshu*, 1995, **21**, 1120.

9 T. Hattori, H. Matsumoto and Y. Murakami, *Stud. Surf. Sci. Catal.*, 1987, **31**, 815 .

10 T. Uchijima, in *the First Tokyo Conference on Advanced Catalytic Science and Technology* ed. S. Yoshida, N. Takezawa and T. Ono, Kodansha, VCH, Tokyo, 1991, vol. p. 393.

11 M. M. J. Treacy, J. B. Higgins and R. von Ballmoos, *Zeolites*, 1996, **16**, 323.

12 C.-Y. Chen, H.-X. Li and M. E. Davic, *Microporous Mater.*, 1993, **2**, 17.

13 S. Inagaki, Y. Sakamoto, Y. Fukushima and O. Terasaki, *Chem. Mater.*, 1996, **8**, 2089.

Chapter 8

Photoepoxidation of propene over Nb-loaded silica

Abstract

Two series of Nb_2O_5/SiO_2 catalysts are prepared by an equilibrium adsorption method (type A) and a conventional evaporation to dryness method (type E). The loading amounts of type A catalysts were low (< 0.2 wt% as Nb_2O_5) and those of type E catalysts were varied from 0.1 to 10 wt%. UV/VIS diffuse reflectance spectra of the catalyst samples show that micro particles of Nb_2O_5 are present on the catalysts with high-loading and monomeric or oligomeric niobate species are present on the catalysts with low-loading. By analyzing luminescence spectra of the low-loading samples, we conclude that the type A catalyst contains monomeric NbO_4 tetrahedra and the type E catalyst oligomeric NbO_4 tetrahedra. Propene photo-oxidation on type A catalysts yields propene oxide selectively, formed on monomeric NbO_4, whereas the photo-oxidation on the type E catalyst with low-loading yields propanal selectively. Propanal is the product in decomposition of propene oxide on oligomeric NbO_4 tetrahedra.

Introduction

Niobium oxide supported on silica catalyzes the photo-oxidation of propene to produce aldehydes as main products,[1] similarly to vanadium oxide on silica.[2, 3] However, the activity of Nb_2O_5(3.4 mol%)/SiO_2 was found to be considerably lower than that of V_2O_5(3.4 mol%)/SiO_2,[1] when the catalysts were prepared by a conventional evaporation to dryness method. XANES analysis of these catalysts[4, 5] has shown that niobium species in Nb_2O_5/SiO_2 is a mixture of octahedrally and tetrahedrally coordinated species, while the vanadium species in V_2O_5/SiO_2 is mainly composed of VO_4 tetrahedral species.

In the case of V_2O_5/SiO_2,[5] the higher the dispersion of surface vanadate is, the higher the specific activity is. Furthermore, the selectivity to propanal drastically increases in the photo-oxidation of propene. We have proposed that propanal in propene photo-oxidation is formed *via* propene oxide whose oxygen atom originates from a V=O bond in V_2O_5/SiO_2 catalyst.[6] By analogy with the results for V_2O_5/SiO_2, the niobium species with high catalytic activity are expected to be those of an isolated tetrahedral form. Our *ab initio* molecular orbital calculations of vanadium oxide and niobium oxide cluster models[1, 7] have predicted followings; (1) adsorption of olefins onto V=O is more facile than that onto Nb=O and (2) once olefins are adsorbed, the bond strength of Nb=O is weaker than that of V=O. Therefore, not only high activity but also favorable selectivity to propene oxide and analogs can be expected for the Nb_2O_5/SiO_2 catalyst with highly dispersed NbO_4 tetrahedra.

It is very likely that the local structure in the catalysts is influenced by the structure of niobate ions in the impregnation solution. The structure of niobate ions varies with the pH value of the solutions, as pointed out by Jehrig and Wachs.[8] In the present work, we prepared silica-supported niobium oxide catalysts by the equilibrium adsorption method using impregnation solutions with various pH under acidic condition and carried out the photo-oxidation of propene over these catalysts.

Experimental

Nb_2O_5/SiO_2, type A, was prepared by an equilibrium adsorption method: impregnation of silica with a niobic acid solution of a controlled pH containing oxalic acid at 298 K for 20 h, followed by filtration and calcination in the stream of dry air at 773K for 5 h. The pH value was adjusted by addition of an ammoniacal solution. The loaded amounts of Nb_2O_5 in type A samples determined by X-ray fluorescence intensities are listed in Table 1. For the comparison, we have prepared another type of catalysts, type E, by evaporation to dryness method using a niobic acid solution prepared by dissolving niobic acid in 0.1 M oxalic acid. The loaded amounts of Nb_2O_5 in type E samples were 10, 5, 1 and 0.1 wt%. Niobic acid was supplied from CBMM. Silica was prepared by hydrolysis of tetraethyl orthosilicate as described elsewhere.[9] In X-ray diffraction patterns, no appreciable lines were observed for all catalyst samples.

The photoluminescence spectra were recorded at 77 K with a Hitachi 850 fluorescence spectrometer using a UV filter (permitted wavelength $\lambda > 300$ nm) for removal of scattered light from the u.v.-source. The decay curves of phosphorescence were recorded by a spectrometer with a Xe flash lamp constructed by Professor M. Yamamoto *et al.* at Department of Polymer Chemistry, Kyoto University. UV/VIS diffuse reflectance spectra were taken by a Shimadzu MPS-2000 spectrometer, using an *in situ* cell.

The photo-oxidation of propene was performed with a conventional closed circulating system. The catalyst (500 mg) was placed in a catalyst bed made of quartz. A high pressure Hg lamp (250 W) was used for irradiation. Details of the procedure are described elsewhere.[1-3] Every reaction was carried out more than twice to examine the reproducibility of the data.

Table 1 Loaded amounts of Nb_2O_5 in type A samples[a]

sample entry	A(pH 0.8)	A(pH 2.4)	A(pH 4.0)
pH of solution[b]	0.78	2.35	4.02
loading[c]/ wt%	0.17	0.23	0.23

[a] See text. [b] pH value was kept during the impregnation. [c] as Nb_2O_5.

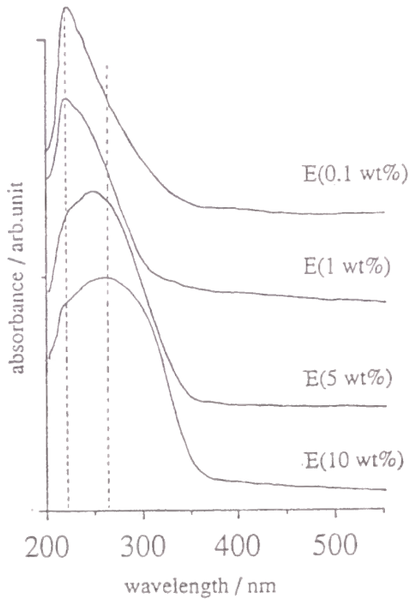

Fig. 1 UV/VIS diffuse reflectance spectra of type E catalysts.

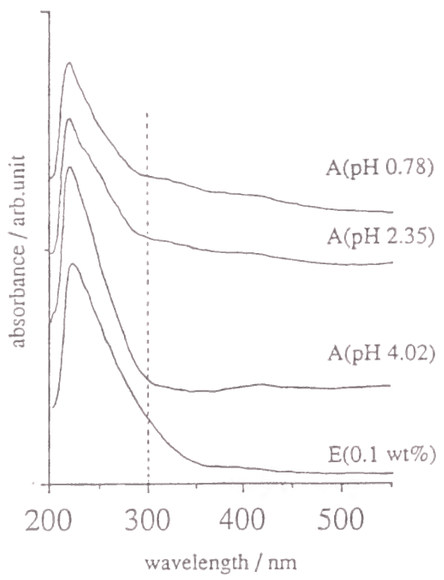

Fig. 2 UV/VIS diffuse reflectance spectra of type A catalysts.

Results and discussion

Characterization of catalyst samples

Fig. 1 shows the UV/VIS spectra of type E catalyst samples. With decreasing the loaded amount of Nb_2O_5, the peak position shifts to lower wavelength and the absorption band becomes narrower. In the case of E(10 wt%) sample, an absorption threshold is found at 350 nm, which is shorter than that corresponding to the band gap of Nb_2O_5 bulk (410 nm). The broadness of the band suggests that niobate species in E(10 wt%) sample is aggregated to form micro particles of Nb_2O_5 possessing energy band structure. Anpo *et al.* proposed that band energy gap position shifts to higher energy side with a decrease in the particle size of a semiconductor material.[10] In the present case, the energy shift of absorption threshold shows that the size of aggregated niobate particles is reduced with a decrease in the loaded amount. A sharp absorption band observed for E(0.1 wt%) suggests that the UV absorption is associated with local Nb-O bonds. Therefore, we can conclude that niobium oxides in E(0.1 wt%) involve monomeric and/or oligomeric species. On the other hand, as shown in Fig. 2, catalyst samples of type A exhibit similar spectra to that for E(0.1 wt%) although the loaded amount of Nb_2O_5 of type A samples is about twice as that of E(0.1 wt%). However, the absorption threshold for type A samples is found at higher energy side than that for E(0.1 wt%). These results indicate that fraction of monomeric or oligomeric niobium oxide is larger in the type A catalyst: highly dispersed catalyst can be prepared by the equilibrium adsorption method.

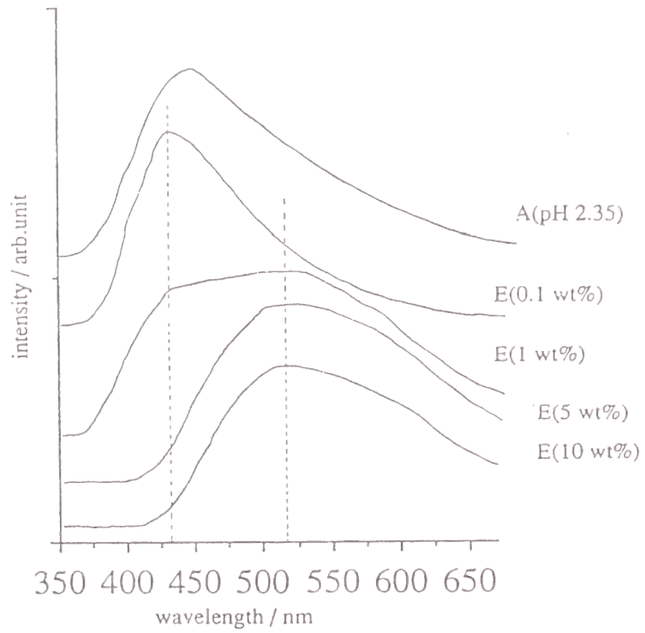

Fig. 3 Phosphorcence spectra of A(pH 2.35) and type E catalysts. A, E(0.1 wt%) and E(1 wt%), excitation: 260 nm. E(5 wt%) and E(10 wt%) excitation: 350 nm

It has been reported that V_2O_5,[2, 3, 11, 12] MoO_3[13] and MgO[14] dispersed on silica exhibit phosphorescent emission. This is also the case for the Nb_2O_5/SiO_2 catalyst.[1] Fig. 3 shows the emission spectra exhibited by A(pH 2.4) and type E catalyst samples. In the spectra of E(10 wt%) and E(5 wt%) samples, a broad emission is seen centered at 520 nm while in the spectra of E(0.1 wt%) and A(pH 2.35) samples, a single emission peak at 430 nm. The band by E(1 wt%) catalysts is composed of these bands. The results show that there are at least two kinds of emission sites and the relative ratio varies with the dispersion of surface niobate. It can be deduced from the result of UV/VIS spectroscopy that a site emitting 520 nm light, S520, lies on the aggregated niobium oxide particle and a site emitting 430 nm light, S430, is an Nb=O bond in monomeric or oligomeric niobate species. By the aid of XANES result,[4] we conclude that S430 and S520 are Nb=O bonds in an NbO_4 tetrahedron and an NbO_6 polymeric octahedra, respectively.

Fig. 4 shows the excitation spectra of type E catalyst samples monitoring emission intensity at 520 nm for E(5 wt%) and E(10 wt %) and at 430 nm for other low loading samples. The peak position shifts to lower wavelength with a decrease in the loaded amount of Nb_2O_5 as found in UV/VIS spectra. However, it should be noted that each peak is superimposed on a high background, indicating that emission is not caused only by excitation of specific bonds. Fig. 5 shows the excitation spectra of type A catalysts monitored at 430 nm. All the samples exhibit nearly the same spectra. The low back ground in this case suggests that excitation concerns a specific bond, presumably Nb=O in an NbO_4 tetrahedron.

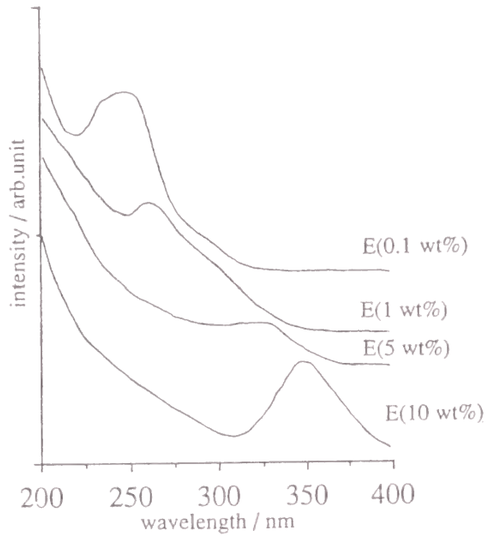

Fig. 4 Excitation spectra of E type catalysts. E(0.1 wt%) and E(1 wt%), monitored at 430 nm; E(5 wt%) and E(10 wt%), monitored at 530 nm.

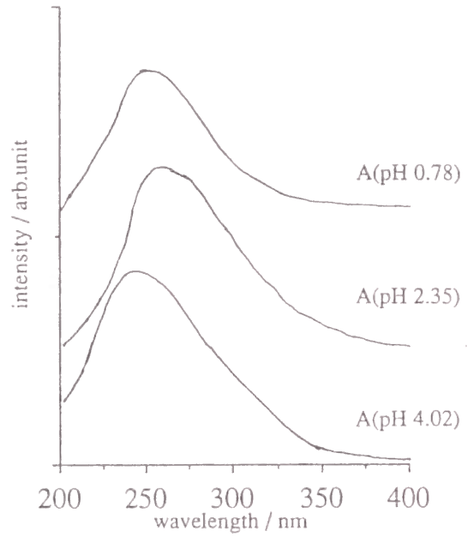

Fig. 5 Excitation spectra of A type catalysts monitored at 430 nm.

To obtain more detailed information from phosphorescent emission, we recorded decay curves for E(0.1 wt%) and A(pH 2.4) samples. The results are shown in Figures 6 and 7. In the case of E(0.1 wt%), emission decay (Fig. 6(a)) is much faster than in the case of A(pH 2.4) (Fig. 7(a)). This clearly shows that a process of radiationless deactivation of Nb=O bonds is very sluggish for A(pH 2.4) sample and indicates that cluster size of NbO_4 oligomer is quite small for the sample prepared by the equilibrium adsorption method. By a contact with 1 Torr of propene, emission is quenched more efficiently for A(pH 2.4) (Fig. 7(b)) than for E(0.1 wt%) (Fig. 6(b)). These dacay curves can not be simulated by assuming a single exponential curve. We found that these curves can be fit satisfactorily by three components of $\exp(-t/\tau)$ where τ is the lifetime. Table 2 shows the result of fitting. In the case of A(pH 2.4) sample, the long life component is predominant and much decreased by contact with propene, accompanied by a reduction in the lifetime. In a marked contrast, the composition of a long life component is small and lifetime (τ = 40 ms) is shorter for E(0.1 wt%) catalyst sample. No significant change in composition is found when propene is introduced. The emission site for E(0.1 wt%) and A(pH 2.4) catalysts is Nb=O in the slightly different structure of niobates. The oligomerization degree of niobium oxide species could be low for type A catalysts.

From the results mentioned above, we conclude that in the sample prepared by evaporation to dryness method, surface niobate species are aggregated: samples with loading of 5 and 10 wt% have the micro particles of niobium oxide similar to Nb_2O_5 bulk dominantly. The E(1 wt%) sample contains both micro particles like Nb_2O_5 bulk and niobium oxide oligomers which comprise NbO_4 tetrahedra. NbO_4 tetrahedra are dominant in E(0.1 wt%) sample and are presumably oligomerized to form pyroniobate or metaniobate form. In the sample prepared by the equilibrium adsorption method, NbO_4 tetrahedron monomer or the low-oligomer is preferentially present.

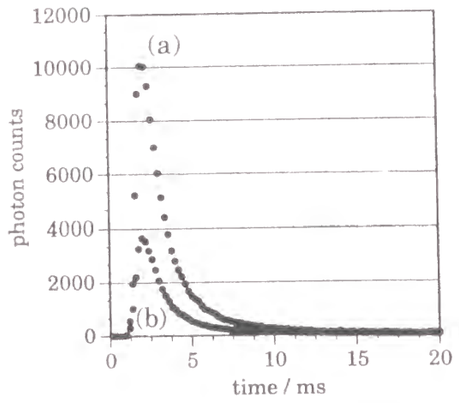

Fig. 6 Decay curves of emission by E(0.1 wt%). (*a*) in vacuo and (*b*) in contact with 1 Torr of propene.

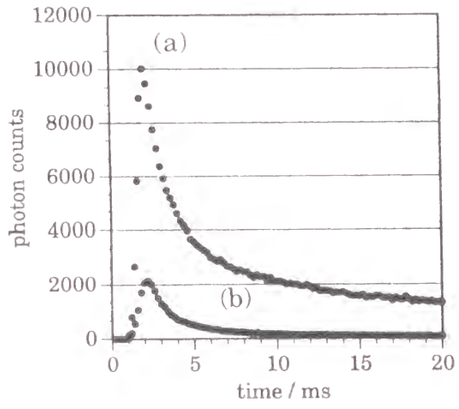

Fig. 7 Decay curves of emission by A(pH 2.4). (*a*) in vacuo and (*b*) in contact with 1 Torr propene.

Table 2 Deconvolution of decay curves in Figures 6 and 7

	in vacuo		contact with propene	
entry	lifetime / ms	composition / %	lifetime / ms	composition / %
A(pH 2.4)	1	5	1	19
	7	16	4	31
	61	79	36	49
E(0.1 wt%)	1	37	1	23
	3	42	3	46
	40	20	34	31

Photo-oxidation of propene

Propene photo-oxidation over type A and type E catalysts was carried out. Products were ethanal, propanal, acraldehyde, propanone and propene oxide. Carbon dioxde formed by total oxidation was scarcely observed. Fig. 8 shows the activity (1 h irradiation) of the catalysts normalized to niobium ions. With decreasing the loaded amount of Nb_2O_5, the normalized activity increases. This is considered to be due to the change in compostion of surface active species. In the case of type E catalyst, the decrease in the loaded amount less than 1 wt% is not effective to increase the normalized activity. Fig. 9 shows the change in selectivities with Nb_2O_5 loading for type E catalysts. The remarkable decrease in ethanal selectivity was found with decreasing the Nb_2O_5 loading from 10 wt% to 1 wt% and selectivities are constant with E(0.1 wt%) and E(1 wt%). Interestingly, propene oxide was found for E(0.1 wt%) and E(1 wt%). In our previous work on photo-oxidation over silica-supported vanadium oxide, we predicted the propene oxide formation as an intermediate to propanal and propanone.[6] Applying the conclusion obtained with V_2O_5/SiO_2 to Nb_2O_5/SiO_2, propene oxide formation relates closely to the presence of NbO_4 tetrahedral species. The type A catalysts have also NbO_4 tetrahedra and the fraction of monomeric or low-oligomeric NbO_4 is much higher than those in low-loaded type E catalysts, as mentioned in the preceding section. Such monomeric NbO_4 will exhibit a specific selectivity in the propene photo-oxidation. Fig. 10 shows the selectivity of type A catalysts together with those of E(0.1 wt%) catalysts. It should be noted that propene oxide formation is much enhanced and ethanal formation is reduced in comparison with E(0.1 wt%) catalyst. Provided that propanal and propanone are formed via propene oxide, the selectivity to propene oxide intermediate reaches over 60 % in the case of type A catalysts. The poor formation of C_3 oxygenates on the high loading type E catalysts can be attributed to the preferential presence of NbO_6 octahedral species as seen in the Nb_2O_5 bulk.

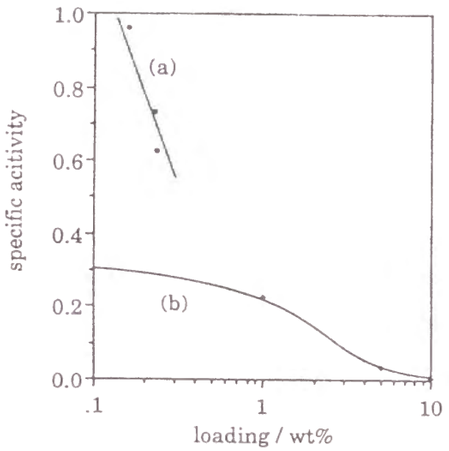

Fig. 8 Specific activity of (*a*) A-type catalysts and (*b*) E-type catalysts in photo-oxidation of propene. The specific activity was evaluated by normalization of total conversion of propene to the amount of niobium ions in the catalyst.

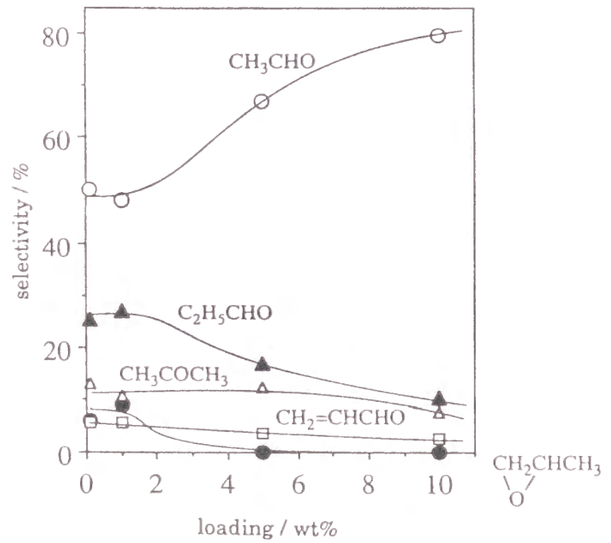

Fig. 9 Selectivities in photo-oxidation of propene over type E catalysts.

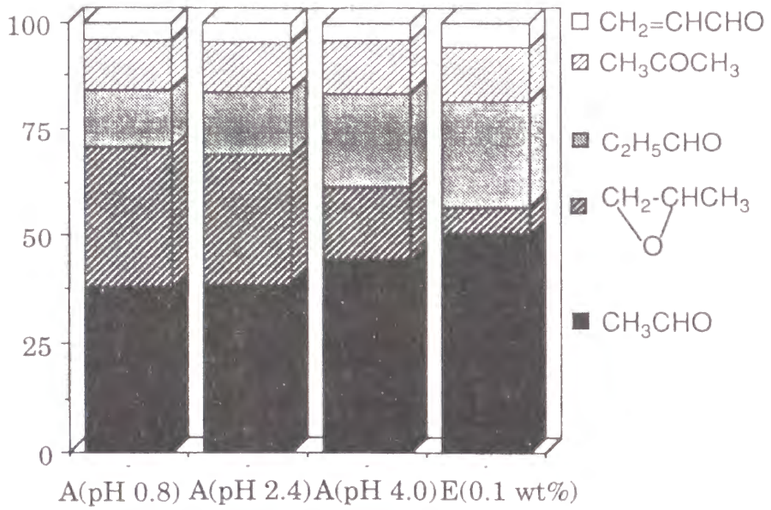

Fig. 10 Selectivity in the photo-oxidation of propene over type A catalyst and E(0.1 wt%) catalyst.

The results that ethanal formation is preferable over type E catalysts, especially over high loading catalyst, suggest the active sites for ethanal formation to be the polymeric NbO_6 octahedra. However, in a previous study of V_2O_5/SiO_2,[6] we found the ethanal formation via decomposition of propene oxide is inevitable. Thus, ethanal can be produced through both direct oxidative fission of a double bond of propene and the decomposition of propene oxide once formed. The difference of selectivity between E(0.1 wt%) and A type catalysts suggests that formation of propene oxide proceeds on both monomeric and oligomeric (aggregated) NbO_4, but is followed by decomposition of propene oxide on the latter by the attack of the adjacent excited Nb=O.

The lower activity and lower selectivity to propene oxide of A(pH 4.0) than those of A(pH 2.4) and A(pH 0.8) are due to the presence of higher amount of NbO_4 oligomers. In oxalic acid solution, niobium ion is present as a niobium oxalate. Jehrig and Wachs reported that in a low acidic condition,[8] oligomerization of niobium oxalate is brought about and precipitation of niobic acids starts. During the impregnation of silica with the solution of pH 4.0, niobium oligomer has already existed.

References

1 S. Yoshida, Y. Nishimura, T. Tanaka, H. Kanai and T. Funabiki, *Catalysis Today*, 1990, **8**, 67.

2 S. Yoshida, T. Tanaka, M. Okada and T. Funabiki, *J. Chem. Soc., Faraday Trans. 1*, 1984, **80**, 119.

3 S. Yoshida, Y. Magatani, S. Noda and T. Funabiki, *J. Chem. Soc., Chem. Commun.*, 1981, 601.

4 S. Yoshida, T. Tanaka, T. Hanada, T. Hiraiwa, H. Kanai and T. Funabiki, *Catal.Lett.*, 1992, **12**, 277.

5 T. Tanaka, Y. Nishimura, S. Kawasaki, M. Ooe, T. Funabiki and S. Yoshida, *J. Catal*, 1989, **118**, 327.

6 T. Tanaka, M. Ooe, T. Funabiki and S. Yoshida, *J. Chem. Soc., Faraday Trans.1*, 1986, **82**, 35.
7 H. Kobayashi, M. Yamaguchi, T. Tanaka, Y. Nishimura, H. Kawakami and S. Yoshida, *J. Phys. Chem.*, 1988, **92**, 2516.
8 J.-M. Jehng and I. E. Wachs, *J. Raman Spectroscopy*, 1991, **22**, 83.
9 S. Yoshida, T. Matsuzaki, T. Kashiwazaki, K. Mori and K. Tarama, *Bull. Chem. Soc. Jpn.*, 1974, **47**, 1564.
10 M. Anpo, N. Aikawa, Y. Kubokawa, M. Che, C. Louis and E. Giamello, *J. Phys. Chem.*, 1985, **89**, 5017.
11 A. M. Gritscov, V. A. Shvets and V. B. Kazansky, *Chem. Phys. Lett.*, 1975, **35**, 511.
12 M. Anpo, I. Tanahashi and Y. Kubokawa, *J. Phys. Chem.*, 1980, **84**, 3440.
13 T. Ono, M. Anpo and Y. Kubokawa, *J. Phys. Chem.*, 1980, **90**, 4780.
14 T. Tanaka, H. Yoshida, K. Nakatsuka, T. Funabiki and S. Yoshida, *J.Chem.Soc.Faraday Trans.*, 1992, **88**, 2297.

Chapter 9

Photoepoxidation of propene over silica and Mg-loaded silica

Abstract

Silica was found to promote the photooxidation of propene by molecular oxygen, yielding acetaldehyde, propylene oxide, and propionaldehyde. The yield of and selectivity to propylene oxide were improved significantly by modification of silica with 1 wt % magnesium oxide loading. The product selectivity was affected by the amount of magnesium and the preparation method. Mg *K*-edge XANES and phosphorescence spectra indicated that the active sites on the Mg-loaded silica for epoxidation of propene are highly dispersed and isolated magnesium oxide species. The photoactive sites on bare silica are briefly discussed.

Introduction

Epoxides are very important intermediates for many chemicals. Therefore, new heterogeneous catalytic processes producing epoxides directly from alkenes with gaseous oxygen are desirable. Epoxidation of ethene with gaseous oxygen over Ag catalysts was developed many years ago,[1] but the same reaction with propene has not been successful. Although Ti-containing zeolites[2-4] have recently attracted much interest as catalysts for epoxidation, the system must consume hydrogen peroxide as an oxidant. Gaseous oxygen is a more desirable oxidant for industrial use than hydrogen peroxide.

Silica is generally used as a support for catalysts and is usually regarded as a catalytically inactive material. However, it can function as a catalyst for some reactions,[5-8] in particular when it is activated by photoirradiation.[9-11] Some silica-based materials containing non-transition metal oxides were also found to be photoactive; e.g., highly dispersed magnesium oxide supported on silica has a function of photooxidation of CO[12, 13] and silica-alumina binary oxides are also photoactive.[14] These materials show photoemission spectra with fine structures similar to those of vanadium oxide dispersed on silica.[15] Tanaka *et al.* had already reported that an epoxide intermediate is formed in the photooxidation of light alkenes with O_2 over silica-supported vanadium oxide[16] and that highly dispersed niobium oxide on silica can catalyze epoxidation of propene with gaseous oxygen under photoirradiation.[17] In addition, a spectroscopic study was recently reported on the production of propylene oxide from propene and O_2 over Ba Y-zeolite irradiated with visible light.[18] These silica-based systems have some common factors; heteroatom species are highly dispersed and they become photoactive sites.

Previously, we found that silica showed an unexpected photocatalysis in metathesis reactions of light alkenes when it was evacuated at high temperatures,[19] and successively we discovered that the presence of gaseous oxygen causes partial oxidation of propene including epoxidation.[20] Furthermore,[20] we pointed out that the selectivity for propylene oxide was

doubled by loading magnesium oxide on the silica. However, the details on the promotion effect by loading Mg ions on silica have not been discussed. In the present study, we focus on the local structures of the active sites in Mg-loaded silica prepared by two different methods and discuss the correlation between the structure of the active sites and the epoxidation activity. The active sites of the bare silica are also discussed. The structure of magnesium species was studied by photoluminescence and Mg *K*-edge XANES spectra.

Experimental

The silica employed was prepared from $Si(OC_2H_5)_4$ by a sol-gel method, followed by calcination in air at 773 K.[21] BET surface area was 556 m^2g^{-1}. Mg-loaded silica was prepared by two methods as follows: (i) After impregnating the silica with a solution of $Mg(OCH_3)_2$ in methanol,[12] the mixture was filtered and the precipitation was dried at 343 K for 24 h, followed by calcination at 773 K in air for 5 h. (ii) After impregnating the silica with an aqueous $Mg(NO_3)_2$ solution, it was evaporated to dryness in water bath, followed by drying at 343 K for 24 h and calcination at 773 K in air for 5 h. These samples were referred to as (i) *x*MS-M (*x* stands for weight percent of MgO) and (ii) *x*MS-W hereafter. The magnesium oxide loadings were determined by XRF measurement. Bulk MgO was obtained from hydrolysis of a solution of $Mg(OCH_3)_2$ in methanol followed by calcination at 773 K.

Photoluminescence spectra were recorded at 77 K with a Hitachi F-3010 fluorescence spectrophotometer using a UV filter ($\lambda_{transmission} > 300$ nm) to remove scattered light from the UV source (Xe lamp), where the fluorescence emission was cut off mechanically to record phosphorescence spectra. Before recording spectra, the sample was treated with 60 Torr (1 Torr = 133.3 N m^{-2}) oxygen for 1 h at 1073 K, followed by 1 h evacuation at 1073 K. The optical cell was made of quartz, 5 mm diameter. The amount of the sample in the cell was ca. 150 mg.

X-ray absorption experiments were carried out on beamline BL-7A at UVSOR, Institute for Molecular Science, Okazaki, Japan, with a ring energy of 750 MeV and a stored current of 80-200 mA. Spectra were recorded at room temperature, using a beryl two-crystal monochromator in the total electron yield mode. The sample calcined at 1073 K was mixed with active carbon in dry hexane and was put on the first photocathode made of Cu-Be in the electron multiplier.[22, 23] We obtained only the spectra of higher-loaded samples with a loading above 5 wt% as MgO since low-loaded samples showed small ratios of signal to background (S/B) or signal to noise (S/N) in thier spectra.

Before reaction, the samples were heated under an oxygen atmosphere and subsequently evacuated at 1073 K. The photooxidation of propene[20] was carried out in a closed reaction vessel made of quartz (35 cm^3) at room temperature for 2 h as the standard condition. The reactants were propene (30 μmol) and oxygen (0 - 120 μmol; 60 μmol as standard). The catalyst (100 mg) was spread on the flat bottom (3.14 cm^2) of the vessel. A 250-W ultrahigh-pressure Hg lamp was used as a light source. The temperature of catalyst bed was elevated by ca. 10 K from room temperature by the photoirradiation. Products were collected in a part of the closed system by a liquid-N_2 trap when the catalyst bed was under irradiation. After that, the catalyst was heated in the dark to collect the adsorbed products on catalyst surface. Products were analyzed by GLC and GC-MS.

Results

Phosphorescence spectra

Figure 1 shows phosphorescence spectra of the silica and Mg-loaded silica samples. Silica (Fig. 1a) exhibited a broad emission centered around 440 nm, which can be assigned to surface hydroxy groups.[13] The 1 wt % MgO-loaded silica prepared from a solution of $Mg(OCH_3)_2$ in methanol, 1MS-M (Fig. 1b), showed an emission spectrum with fine structure centered at 525 nm. In the previous study,[12, 13] the site exhibiting the emission with fine

structure was assigned to highly dispersed magnesium oxide species on the silica surface. For this sample, 1MS-M, the broad band resulting from the surface hydroxy groups had disappeared, indicating that magnesium ions replace almost all the silanols remaining after evacuation at 1073 K.[13]

In the sample with high Mg loading, 6MS-M (Fig. 1c), the fine structure disappeared and a broad band centered at 450 nm appeared instead, indicating that magnesium oxide species in the sample are not highly dispersed. The peak position of the broad band of 450 nm was slightly different from that of hydroxy groups on silica of 440 nm. Since bulk MgO shows broad luminescence spectra,[24-27] the broad spectrum would result from crystallites or islands of magnesium oxides on silica.

In Fig. 2, the spectra of Mg-loaded silica samples prepared from aqueous solution (*x*MS-W samples) are shown. Fine structure on the spectrum resulting from the highly dispersed magnesium oxide species was observed most clearly in 5 wt % loaded sample, 5MS-W (Fig. 2b). The sample with low Mg loading, 1MS-W (Fig. 2a) showed a spectrum similar to that of silica; however, the spectrum contains a weak fine structure, indicating that there are both silanols and highly dispersed magnesium species on 1MS-W. A high-loaded sample, 20MS-W (Fig. 2c), shows only a broad emission centered at 460 nm. This broad spectrum is however different from that of 6MS-M in the line shape and peak position; the shape of the spectrum of 20MS-W is a little sharper than that of silica or 6MS-M, and the peak position shifts to *ca.* 10 nm higher wavelength than that of 6MS-M.

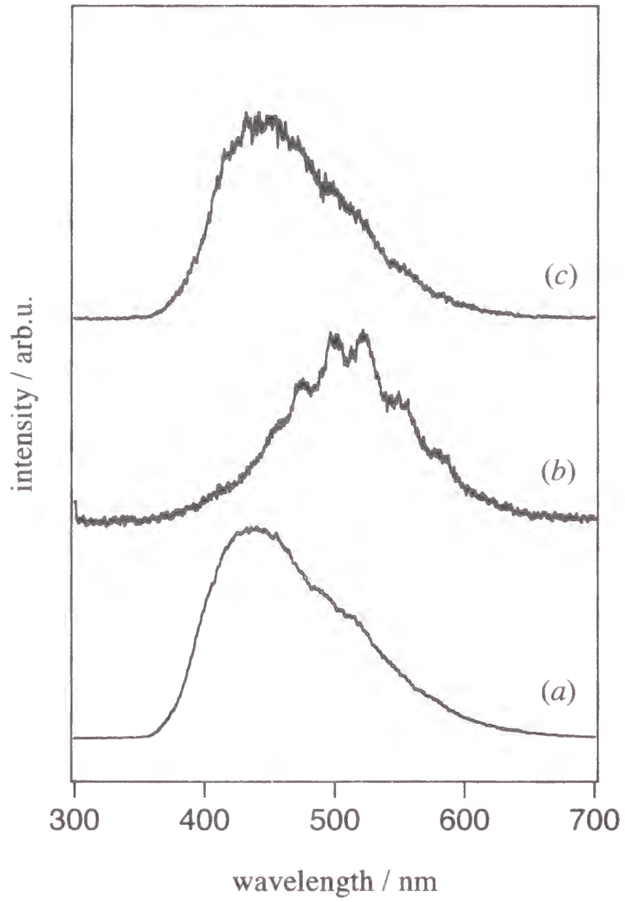

Fig. 1 Phosphorescence spectra of silica (*a*) and Mg-loaded silica, 1MS-M (*b*), 6MS-M (*c*). The excitation wavelength was 240 nm.

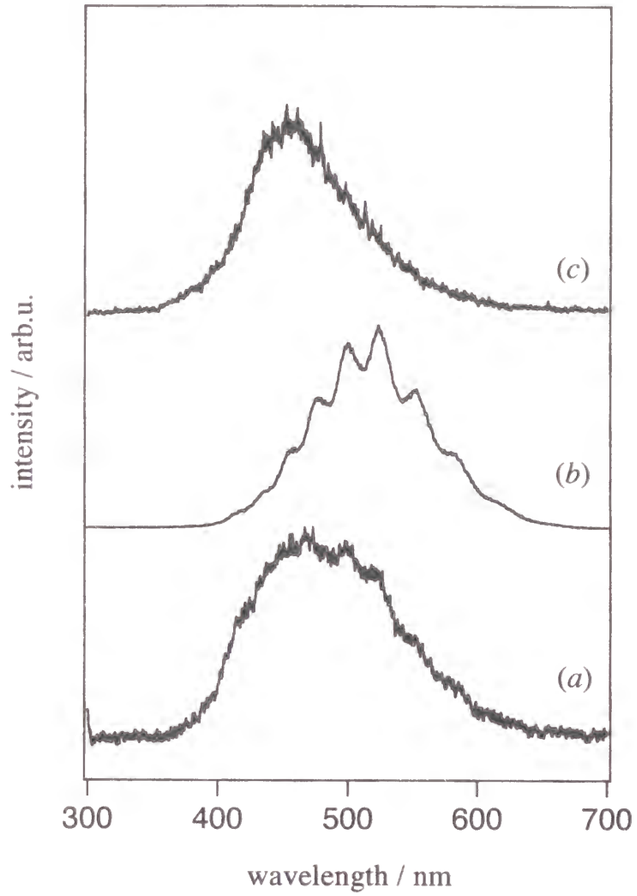

Fig. 2 Phosphorescence spectra of Mg-loaded silica, 1MS-W (*a*), 5MS-W (*b*) and 20MS-W (*c*). The excitation wavelength was 240 nm.

XANES spectra

The structure of magnesium oxide species in this system could not be analyzed by X-ray diffraction because no definite diffraction lines were detected. On the other hand, XANES spectra can offer us information about the local structure of a highly dispersed Mg species.[28]

Some normalized XANES spectra of MS-M and MS-W samples calcined at 1073 K are shown in Fig. 3. The XANES of 20MS-M (Fig.3b) is identical to that of bulk MgO of typical rock salt structure,[22, 23, 29] indicating that Mg ions exist in MgO particles; i.e., the Mg ion is surrounded by an oxygen octahedron. The XANES spectrum of 5MS-M (Fig.3a) is almost the same as that of MgO although the peak at 1315 eV is slightly larger. The *x*MS-M samples, prepared from a solution of $Mg(OCH_3)_2$ in methanol, exhibited almost the same XANES spectrum as that of MgO, indicating that MgO crystallites are formed on silica in this preparation method.[22, 28]

On the other hand, the XANES spectra of 5MS-W (Fig.3c) and 20MS-W (Fig.3d), samples prepared from a $Mg(NO_3)_2$ aqueous solution, are completely different from those of *x*MS-M samples, MgO and other compounds such as $Mg(OH)_2$, Mg_2SiO_4, $MgSiO_3$, and $Mg_2Si_3O_8$.[22, 28] This type of XANES spectra was assigned to highly dispersed magnesium oxide species on the silica surface.[28] Other *x*MS-W samples below the amount corresponding to a monolayer coverage (up to 30 wt % MgO) show also the same spectra. This indicates that impregnation with an aqueous solution of $Mg(NO_3)_2$ is more advantageous to disperse the magnesium ions on silica surface than impregnation with a solution of $Mg(OCH_3)_2$ in methanol.[28]

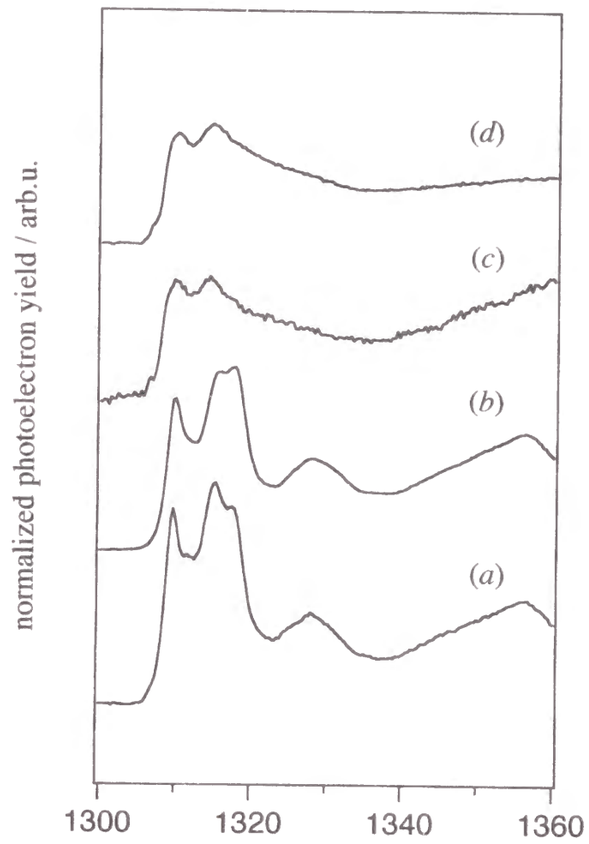

Fig. 3 Normalized Mg *K*-edge XANES spectra of Mg-loaded silica samples calcined at 1073 K; 5MS-M (*a*), 20MS-M (*b*), 5MS-W (*c*), 20MS-W (*d*).

Photooxidation

Table 1 shows the product yields in the photooxidation of propene in the presence of 60 μmol O_2 over silica, Mg-loaded silica samples, and MgO. The products were propylene oxide (PO; methyloxirane, or 1,2-epoxypropane), acetaldehyde (AA; ethanal), propionaldehyde (PA; propanal), acetone (AC; propanone), acrolein (AL; prop-2-enal), and alcohols (methanol, ethanol, and propan-2-ol). Although metathesis reaction of propene takes place in the absence of gaseous oxygen over silica,[19] the presence of gaseous oxygen inhibited the metathesis reaction completely. Heating the samples was necessary to desorb the products for full collection: in some cases, the adsorbed products amounted to half the whole product yield. The yields listed in Table 1 are the sum of the adsorbed and gaseous products.

On the silica sample (entry 1), acetaldehyde was main product with 0.62% yield, where propylene oxide was produced with 0.44 % yield and the selectivity for propylene oxide was 28.9 %. The production of acetaldehyde, propionaldehyde, and acrolein had been reported in the photooxidation over a kind of silica, porous Vycor glass.[30] However, the epoxidation of propene by gaseous oxygen over silica has not been reported.

Upon loading magnesium oxide on the silica, the oxidation activity (total yield) apparently was enhanced by ca. four times, regardless of the Mg-loading method and loading amount (entries 2 - 9). The selectivity to propylene oxide varied considerably with the loading amount and loading method. The highest yield of propylene oxide was 3.36 % on 1MS-M (entry 2) and 3.13 % on 1MS-W (entry 6). The best selectivity to propylene oxide in this study is 50.8 % on 1MS-M sample (entry 2). The Nb_2O_5/SiO_2 system also produces propylene oxide in the photooxidation of propene,[17] where the highest selectivity to propylene oxide was 33 %.
On high-loaded samples prepared with a solution of $Mg(OCH_3)_2$ in methanol, 4MS-M and 13MS-M (entries 3, 4), acetaldehyde was predominantly produced rather than propylene oxide. In the *x*MS-W samples prepared by an aqueous solution, the lower-loaded sample (entry 5) and the higher-loaded samples (entries 7-9) than 1MS-W showed lower selectivity to propylene oxide. The high-loaded sample such as 3MS-W, 6MS-W, and 13MS-W (entries 7-9) exhibited higher selectivity to propylene oxide than the corresponding samples prepared in

Table 1 The photooxidation of propene[a]

Entry	Sample	Products yield[b] (%)							Selec. to
		PO[c]	PA	AC	AL	AA	Alcohols	Total	PO (%)
1	SiO_2	0.44	0.33	0.11	0.02	0.62	0.00	1.52	28.9
2	1MS-M	3.36	0.70	0.40	0.00	1.66	0.50	6.62	50.8
3	4MS-M	0.23	0.82	1.11	0.07	2.25	1.43	5.91	3.9
4	13MS-M	0.07	1.43	1.66	0.07	2.86	1.00	7.09	1.0
5	0.3MS-W	2.02	0.40	0.91	0.17	1.20	0.80	5.50	36.7
6	1MS-W	3.13	0.83	1.03	0.17	2.33	0.30	7.79	40.2
7	3MS-W	2.05	0.70	0.76	0.06	1.61	0.84	6.02	34.1
8	6MS-W	1.68	0.86	1.33	0.07	2.01	0.99	6.94	24.2
9	13MS-W	0.25	0.85	1.15	0.11	2.36	0.97	5.69	4.4
10	MgO	0.03	0.03	0.00	0.03	0.03	0.00	0.12	25.0
11	1MS-M[d]	0.02	0.03	0.03	0.02	0.15	0.04	0.29	6.9
12	1MS-M[e]	0.00	0.04	0.01	0.11	0.12	0.20	0.46	0.0
13	1MS-M[f]	1.93	0.48	0.45	0.06	1.11	0.28	4.30	44.9

[a] O_2/Pr(mole ratio of O_2 to propene)=2, irradiation time, 2 h.
[b] Based on initial amount of propene.
[c] See text.
[d] By using a UV-cut filter. See text.
[e] Performed without Hg lamp in an electric furnace at 573 K for 1 h.
[f] Photoirradiation for 1 h in the presence of gaseous oxygen was carried out before starting the standard reaction experiment.

the other method such as 4MS-M and 13MS-M (entries 3, 4). On bulk MgO, the reaction hardly occurred (entry 10), suggesting that large particles of magnesium oxide are not efficient for photooxidation.

When the irradiation light was limited by using a UV cut filter ($\lambda_{transmission} > 310$ nm), the reaction proceeded very slowly and the selectivity to propylene oxide was low (entry 11). This indicates that the UV light is essential for the oxidation, particularly for oxidation to propylene oxide. Oxidation in the dark at 573 K proceeded very slowly, where propylene oxide was not detected (entry 12).

The presence of O_2 was also essential for the photooxidation over the silica and Mg-loaded silica. Figure 4 shows the dependence of the activity of 1MS-M on the O_2/propene ratio, where the amount of propene introduced was constant. Clearly, a high O_2/propene ratio is favorable for the photooxidation. In the absence of O_2, only oxidation of propene to acetaldehyde took place at a very slow rate under irradiation over 1MS-M, although metathesis reaction proceeded (the result is not shown). Photooxidation to propylene oxide progressed just in the presence of O_2. The optimal condition for the highest selectivity to propylene oxide in this study was O_2/propene = 2, although an excess oxygen seemed to promote other partial oxidation pathways.

To examine the oxygen photoactivation, the following test (entry 13) was carried out; after the pretreatment, the sample was irradiated for 1 h in the presence of gaseous oxygen without propene and subsequently the reaction started by the introduction of propene into the reactor. In comparison with the standard condition (entry 2), the yields of propylene oxide and others were not increased, or rather slightly decreased, suggesting that the first step in the reaction mechanism is the activation of propene by the photoexcited site rather than the activation of oxygen molecules. The activation of propene is supported by the activity for metathesis reaction over irradiated silica .

The dependence of product yields on the irradiation time was studied on 1MS-M sample (Table 2). A fresh sample was used at each run. The conversion, the total product yields, increased at longer reaction time, although it was not proportional to irradiation time. It would

be caused by the products adsorption on the active sites. The appropriate reaction time for the production of propylene oxide would be around 2 h in these conditions. The reduction of the selectivity for propylene oxide after the irradiation for 8 hours (Table 2) indicated that produced propylene oxide was converted to other products successively. To examine the reactivity of propylene oxide, propylene oxide (10 μmol) was introduced with oxygen (60 μmol) over 1MS-M sample. After irradiation for 2 h, 35 % of propylene oxide was converted into propionaldehyde (selectivity 33.5 %), propene (22 %) and others (ethene, acetaldehyde, acetone, etc.). This result confirmed that the produced propylene oxide was secondarily converted into other products. A large part of the propionaldehyde yield might come secondarily isomerized product from propylene oxide.

Table 2 Dependence of products yields on UV irradiation time over 1MS-M sample.[a]

Irradiation	Products yield[b] (%)							Selec.to
time (h)	PO[c]	PA	AC	AL	AA	Alcohols	Total	PO (%)
1	2.12	0.49	0.40	0.11	1.56	0.28	4.95	42.8
2	3.36	0.70	0.40	0.00	1.66	0.50	6.62	50.8
8	2.77	1.24	1.79	0.26	1.98	5.06	13.09	21.1

[a] O_2/Pr(mole ratio of O_2 to propene)=2,

[b] Based on initial amount of propene.

[c] See text.

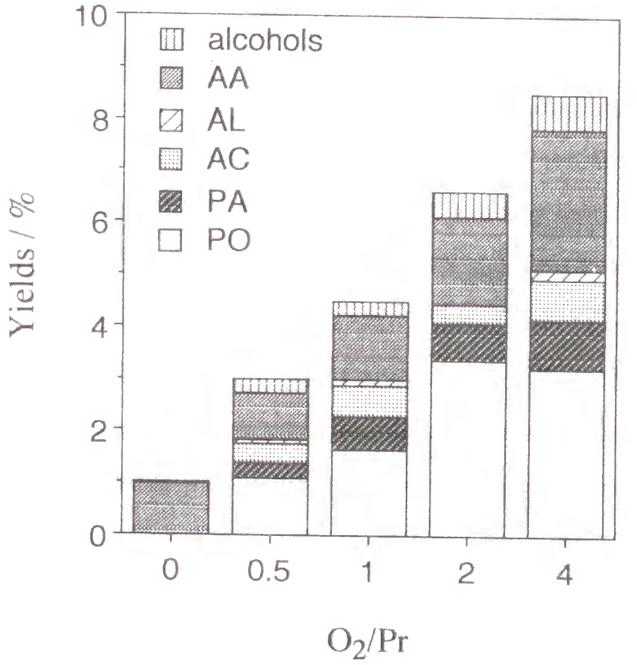

Fig. 4 Dependence of product yields on O_2/propene ratio in the photooxidation of propene over 1MS-M. Propene, 30 μmol constant; irradiation time, 2 h.

Discussion

Mg loading by using a $Mg(OCH_3)_2$ in methanol solution

The preparation method using $Mg(OCH_3)_2$ in methanol solution leads to the formation of small crystallites on silica[22, 28] and zeolite.[31] In this study, the high-loaded samples prepared in this method (xMS-M, $x > 5$) contain magnesium oxide crystallites, as indicated by XANES (Fig. 3a and 3b) and the broad phosphorescence spectrum (Fig. 1c) assigned to the MgO crystallites on which the hydroxy groups and/or unsaturated Mg-O pair emit.[24-27] The $Mg(OCH_3)_2$ should aggregate on the silica surface and MgO crystallites should be formed by calcination.

In the low-loaded sample such as 1MS-M, judging from the highest conversion and selectivity to propylene oxide and the phosphorescence spectrum with fine structure, the structure of magnesium species should be different from the MgO crystallites mentioned above. Although we cannot record XANES spectrum of such a low-loaded sample, we could presume that the strucure, i.e., magnesium oxide, should be highly dispersed on the silica surface. On the spectrum of 1MS-M, the broad band resulting from silanols [13] as shown in Fig. 1a disappeared completely while only the emission with fine structure as shown in Fig. 1b was observed instead, indicating that almost all the hydroxy groups on silica reacts with the $Mg(OCH_3)_2$ and that no aggregation of magnesium species would occurs. The loading of MgO in 1MS-M corresponds to 0.25 mmol g^{-1}, and the population of residual hydroxy groups on silica calcined at 773 K was evaluated to be 0.211 mmol g^{-1}.[13] These values correspond to 0.3 nm^{-1} on the silica surface. Therefore, the magnesium species on 1MS-M should be highly dispersed and isolated. Since the spectrum with the fine structure is observed when it is evacuated at high temperature, the emission site is suggested to be coordinatively unsaturated surface magnesium oxide species.[13, 14]

Since $Mg(OCH_3)_2$ easily reacts with water, $Mg(OCH_3)_2$ should react with surface hydroxy groups on silica in dry methanol:

$$Mg(OCH_3)_2 + [Si]\text{-}OH \rightarrow Mg(OCH_3)\text{-}O\text{-}[Si] + CH_3OH. \quad (1)$$

When the number of $Mg(OCH_3)_2$ molecules is comparable to (or less than) that of [Si]-OH, highly dispersed species would be formed on silica.

When there are more $Mg(OCH_3)_2$ molecules than that of [Si]-OH groups, they would be weakly adsorbed on silica surface under impregnation. By successive drying and calcination in air, the adsorbed magnesium species could aggregate. Magnesium oxide crystallites would be constructed on the surface after calcination.

In conclusion we can state that the local structures of magnesium oxide species in a low-loaded sample are obviously different from the high-loaded ones; magnesium oxide species on xMS-M samples are small crystallites of MgO of rock salt structure in the high-loaded samples ($x > 5$) and highly dispersed and isolated in a low-loaded sample ($x = 1$).

Mg-loading by using a $Mg(NO_3)_2$ aqueous solution

In the Mg-loaded silica samples prepared by using an aqueous solution of $Mg(NO_3)_2$, the dispersion of the magnesium oxide species is high as shown by XANES spectra (Fig. 3c and 3d). The local structure of magnesium oxide species was not changed with loading below the amount corresponding to a monolayer coverage (up to 30 wt % MgO). Although we cannot obtain XANES spectrum of 1MS-W, it is reasonable assumption that the local structure of these magnesium oxide species is also the same as in the other xMS-W samples, that is, highly dispersed. The local structure of the highly dispersed magnesium oxide species is strongly affected by silica tetrahedral structure, if the species is epitaxially constructed.

Phosphorescence emission spectra, however, varied with the magnesium oxide loading. The 1MS-W sample shows a broad emission accompanied by the spectrum with fine structure (Fig. 2a), indicating that there are both the silanol and highly dispersed magnesium oxide species on the surface. Since xMS-W samples were prepared by using an aqueous solution, the number of the surface hydroxy groups on the silica soaked in the impregnating solution

would be larger than that in a nonaqueous solution. Therefore, while in the 1MS-M preparation (non-aqueous solution), $Mg(OCH_3)_2$ molecules replace all the silanols that remains after evacuation at 1073 K,[13] the same number of Mg ions can replace with only part of the silanols formed in the 1MS-W preparation because of a large number of silanols formed in the aqueous solution. To exchange all such silanols completely by Mg ions in the aqueous impregnating solutions, in other words to prepare the sample exhibiting the phosphorescence spectrum with the fine structure (Fig. 2b), an amount of Mg ions corresponding to 5 wt % as MgO would be demanded. In this aspect, the local structure of magnesium oxide species in 1MS-W and 5MS-W are similar to each other, but the Mg ions in 1MS-W are more scattered and isolated than in 5MS-W.

The phosphorescence spectrum of the high-loaded sample exhibited a broad band (Fig. 2c), although the local structure of Mg is the same as the highly dispersed species, as shown in the XANES spectra (Fig. 3c and 3d). We suppose that there are islands or raft-like arrays of magnesium oxide species whose local structure is identical to that in the highly dispersed species. In this preparation method, the magnesium cations would be adsorbed on the silica surface, and the sintering of magnesium oxide species would not occur even under calcination. It is suggested that the luminescence is sensitively affected also by their second neighboring atoms of the sites; only the isolated magnesium species on the silica surface would exhibit the fine structure.

Activity and local structure of magnesium oxide species

The photooxidation activities of silica and Mg-loaded silica are reproduced in Fig. 5 from Table 1 to discuss the correlation between the local structures of magnesium oxide species and the activities. The results of *x*MS-M samples (Fig. 5a) show that only 1MS-M produced propylene oxide dominantly and that higher-loaded samples than 4 wt % produced mainly acetaldehyde. The results suggest that highly dispersed magnesium oxide species accelerate the oxidation to propylene oxide, while aggregated species and crystallites of magnesium oxide on silica are not responsible for the epoxidation. In the case of *x*MS-W (Fig. 5b), even 13MS-W

produced appreciable amounts propylene oxide. Since the magnesium oxide species in *x*MS-W samples are highly dispersed, *x*MS-W samples are available for the production of propylene oxide. Among *x*MS-W samples, the higher-loaded samples showed lower activities for epoxidation than 1MS-W, indicating that the highly dispersed and isolated magnesium oxide species are active for epoxidation. On the other hand, the species which existed as islands or raft-like arrangements are not so active for epoxidation; e.g., in 13MS-W, there would only be a small amount of isolated species which are active for photoepoxidation. Among *x*MS-W samples, the local structure of magnesium species is similar, but the scattering of the species (isolated or not) affect the selectivity for epoxidation. Judging from the photooxidation activity and the selectivity for propylene oxide, the local structure and dispersion of the magnesium oxide species on 1MS-W would be the same as that on 1MS-M; highly dispersed, isolated and coordinatively unsaturated.

It is important aspect that the isolated magnesium species which is put in silica network rather promote the epoxidation activity of the bare silica.

Highly dispersed niobium oxides supported on silica also produce propylene oxide in the photooxidation of propene.[17] In the system, highly dispersed species are responsible for propylene oxide production and aggregated species predominantly produce acetaldehyde. The correlation between the dispersion of metal oxide species and the selectivity in the niobium-silica system is similar to the present case of Mg-loaded silica. Highly dispersed heteroatoms on silica seem to be active site for propylene oxide production.

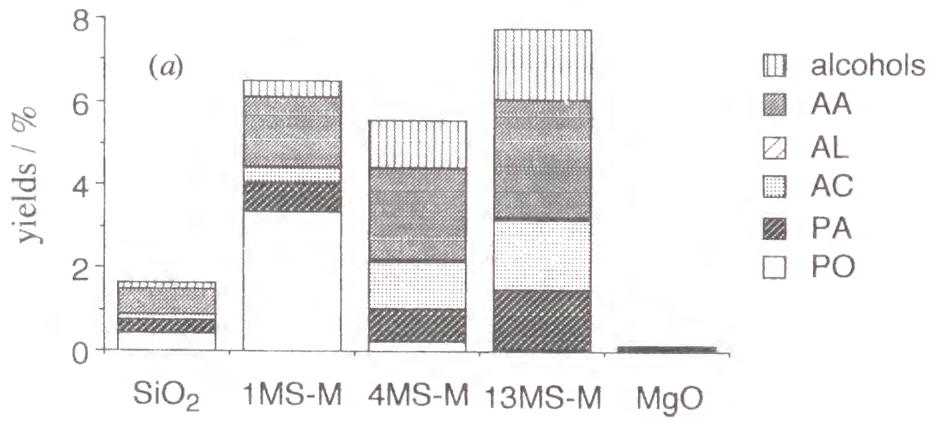

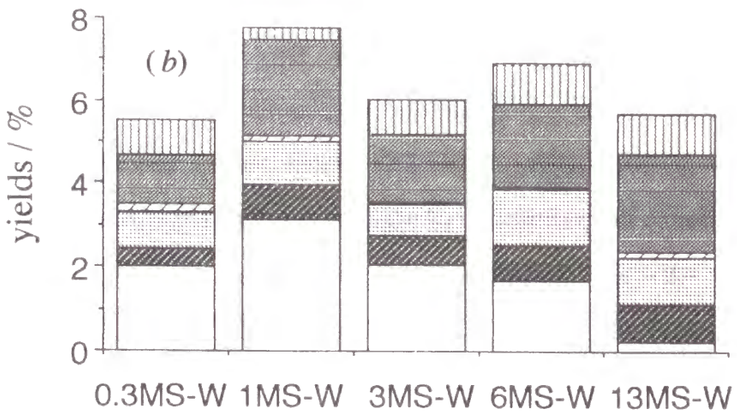

Fig. 5 Product yields over silica, *x*MS-M samples and MgO (*a*), and *x*MS-W samples (*b*).

Active sites of silica surface

Silica is usually used as catalyst support, since silica itself is considered to be inactive for catalytic reactions; in the studies of silica-supported catalysts,[16, 17, 32, 33] the photooxidation on pure silica was not reported. Supported vanadium oxides[16, 32, 33] or niobium oxides[17] were activated by lower pretreatment temperature such as 673 K. On the other hand, catalytic activities of silica for photooxidation[20] and for photometathesis[19] were generated when the silica samples were evacuated at a higher temperature (873 K or 1073 K). The key of the discovery seems to be evacuation at high temperature; e.g., in the previous study[19] the activity of silica for metathesis reaction was found to be increased with elevating temperature. In this study, the metathesis reaction hardly occurs in the presence of gaseous oxygen. Therefore, the active sites which are produced by evacuation at high temperature are the same in the two reactions, photometathesis and photooxidation.

Silica is known to exhibit broad photoemission spectra.[13, 14, 34, 35] The employed silica evacuated at 1073 K also exhibited a broad phosphorescence spectrum as shown in Fig. 1a, which results from surface hydroxy groups.[13] Although the active sites for the photooxidation might emit a specific luminescence, the spectrum would be concealed with the large broad spectrum resulting from silanols. On the other hand, when heteroatoms such as magnesium[12, 13] or aluminum[14] are on/in silica matrix, they easily show the phosphorescence spectra with the fine structure.

We treat here the heteroatoms as a clue to determine the active sites for the photooxidation on pure silica surface. The spectra of Mg-loaded silica and silica-alumina were only clearly observed on samples evacuated at high temperature such as 1073 K. The activation by evacuation at high temperature for photocatalysis[19] or photoluminescence[12-14] is explained by desorption of water molecules or hydroxy groups on the surface. The desorption of hydroxy groups would produce coordinatively unsaturated sites on the surface, and the sites would be concerned with photoexcitation. The photoexcitation sites on Mg-loaded silica and silica-alumina were proposed to be coordinatively unsaturated Mg and Al sites on the surface of the tetrahedral silica network[13, 14]. By analogy, in the case of silica surface, coordinatively

unsaturated surface sites such as Si-(O-Si)3 are suggested to be the photoactive sites. The spectrum of silica evacuated at 1073 K might seem to be slightly overlapped with the fine structure in the higher wavelength region (Fig. 1a). If the M-(O-Si)3 site model is acceptable, the differences on the photoactivity might be explained by the difference of the central atom of the M-(O-Si)3 unit.

Conclusion

It was found that silica catalyzed the partial oxidation of propene to acetaldehyde and propylene oxide under photoirradiation in the presence of O_2. Mg-loaded silica exhibited a higher activity for photooxidation than silica. Highly dispersed and isolated magnesium oxide species on silica, the local structure of which is proposed to be tetrahedral, promoted the epoxidation of propene by O_2 under irradiation selectively, while crystallites or island structure of magnesium oxide on silica promoted the photooxidation to acetaldehyde predominantly. The local structures of magnesium oxide species were controlled by the preparation method and loading amount of magnesium. The active sites on the bare silica would be coordinatively unsaturated sites which were produced by evacuation at high temperatures. The active sites are the same in photometathesis as well as photooxidation.

References

1 T. E. Lefort, *French Pat. 729,952*, 1931,

2 M. G. Clerici, G. Bellussi and U. Romano, *J. Catal.*, 1991, **129**, 159.

3 U. Romano, A. Esposito, F. Maspero, C. Neri and M. G. Clerici, *Stud. Surf. Sci. Catal.*, 1990, **55**, 33.

4 B. Notari, *Stud. Surf. Sci. Catal.*, 1987, **37**, 413.

5 J. N. Armor, *J. Catal.*, 1981, **70**, 72.

6 G. N. Kastanas, G. A. Tsigdinos and J. Schwank, *Appl. Catal.*, 1988, **44**, 33.

7 Y. Matsumura, K. Hashimoto and S. Yoshida, *J. Catal.*, 1989, **117**, 135.

8 A. Parmaliana, F. Frusteri, D. Miceli, A. Mezzapica, M. S. Scurrell and N. Giordano, *Appl. Catal.*, 1991, **78**, L7.

9 A. Morikawa, M. Hattori, K. Yagi and K. Otsuka, *Z. Phys. Chem., N.F.*, 1977, **104**, 309.

10 M. Anpo, C. Yun and Y. Kubokawa, *J. Catal.*, 1980, **61**, 267.

11 A. Ogata, A. Kazusaka and M. Enyo, *J. Phys. Chem.*, 1986, **90**, 5201.

12 T. Tanaka, H. Yoshida, K. Nakatsuka, T. Funabiki and S. Yoshida, *J. Chem. Soc. Faraday Trans.*, 1992, **88**, 2297.

13 H. Yoshida, T. Tanaka, T. Funabiki and S. Yoshida, *J. Chem. Soc. Faraday Trans.*, 1994, **90**, 2107.

14 H. Yoshida, T. Tanaka, A. Satauma, T. Hattori, T. Funabiki and S. Yoshida, *Chem. Commun.*, 1996, 1153.

15 A. M. Gritscov, V. A. Shvets and V. B. Kazansky, *Chem. Phys. Lett.*, 1975, **35**, 511.

16 T. Tanaka, M. Ooe, T. Funabiki and S. Yoshida, *J. Chem. Soc., Faraday Trans.1*, 1986, **82**, 35.

17 T. Tanaka, H. Nojima, H. Yoshida, H. Nakagawa, T. Funabiki and S. Yoshida, *Catal. Today*, 1993, **16**, 297.

18 F. Blatter, H. Sun and H. Frei, *Catal. Lett.*, 1995, **35**, 1.

19 H. Yoshida, T. Tanaka, S. Matsuo, T. Funabiki and S. Yoshida, *J. Chem. Soc., Chem.Commun.*, 1995, 761.

20 H. Yoshida, T. Tanaka, M. Yamamoto, T. Funabiki and S. Yoshida, *Chem.Commun.*, 1996, 2125.

21 S. Yoshida, T. Matsuzaki, T. Kashiwazaki, K. Mori and K. Tarama, *Bull. Chem. Soc. Jpn.*, 1974, **47**, 1564.

22 H. Yoshida, T. Tanaka, K. Nakatsuka, T. Funabiki and S. Yoshida, *Stud. Surf. Sci. Catal.*, 1994, **90**, 473.

23 T. Yoshida, T. Tanaka, H. Yoshida, T. Funabiki, S. Yoshida and T. Murata, *J. Phys. Chem.*, 1995, 10890.

24 A. J. Tench and G. T. Pott, *Chem. Phys. Lett.*, 1974, **26**, 590.

25 S. Coluccia, A. M. Deane and A. J. Tench, *J. Chem. Soc. Faraday Trans. 1*, 1978, **74**, 2913.

26 W. W. Duley, *J. Chem. Soc., Faraday Trans. I*, 1984, **80**, 1173.

27 M. Anpo, Y. Yamada, Y. Kubokawa, S. Coluccia, A. Zecchina and M. Che, *J. Chem. Soc., Faraday Trans. 1*, 1988, **84**, 751.

28 H. Yoshida, T. Yoshida, T. Tanaka, T. Funabiki, S. Yoshida, T. Abe, K. Kimura and T. Hattori, *Journal de Physique IV*, 1997, **7**, 911.

29 T. Yoshida, T. Tanaka, H. Yoshida, S. Takenaka, T. Funabiki, S. Yoshida and T. Murata, *Physica B*, 1995, **208&209**, 581.

30 Y. Kubokawa, M. Anpo and C. Yun, in *Proc. 7th Int. Congr. Catal.* ed. T. Seiyama and K. Tanabe, Kodansha, Tokyo, 1981, vol. B, p. 1170.

31 H. Tsuji, F. Yagi, H. Hattori and H. Kita, in *Proc.10th Intern. Congr. Catal.* ed. L. Guczi, F. Solymosi and P. Tetenyi, Akademiai Kiado, Budapest, 1993, vol. B, p. 1171.

32 S. Yoshida, Y. Magatani, S. Noda and T. Funabiki, *J. Chem. Soc., Chem. Commun.*, 1981, 601.

33 S. Yoshida, T. Tanaka, M. Okada and T. Funabiki, *J. Chem. Soc., Faraday Trans. 1*, 1984, **80**, 119.

34 C. Yun, M. Anpo and Y. Kubokawa, *J. Chem. Soc., Chem. Commum.*, 1977, 665.

35 M. Anpo, C. Yun and Y. Kubokawa, *J. Chem. Soc., Faraday Trans.I*, 1980, **76**, 1014.

Appendix

Chapter 10

Photooxidation of carbon monooxide over magnesium oxide on a silica-support

Abstract

Base sites and photoactive sites of fine particles of MgO dispersed on silica have been studied. In order to control the population of the coordinatively unsaturated surface Mg and O ions (Mg_{CUS} and O_{CUS}), some samples including magnesium oxide fine particles were prepared. These samples are well defined and have each specific amount of CUS ions by changing amount of loading on silica. Thus prepared samples were free from F+ center trapping an electron which have been proposed to be photoactive sites. From the correlation between the population of CUS ion pairs and the rate of photooxidation, we have concluded that the catalytic active sites for CO photooxidation are (Mg_{CUS}-O_{CUS}) pairs. Since a good relationship between the amount of base sites where CO_2 molecules are chemisorbed and the rate of photooxidation of CO is observed, base sites and photoactive sites are considered to be identical.

Introduction

MgO is a typical solid base catalyst.[1] Its active sites are thought to be associated to coordinatively unsaturated surface (CUS) O ions.[2] To elucidate surface structure of MgO, phosphorescent emission from UV-excited MgO is often used.[3,4] Excitation and emission wavelengths are closely related to the coordination circumstance of surface Mg and O ions,[4] because the process of excitation and emission involves the charge transfer between Mg_{CUS} and O_{CUS}. These ions are also admitted to play an important role in photocatalysis by MgO.[5] Some researchers[6] insist that photoemission sites are not Mg_{CUS} or O_{CUS} but F^+ centers trapping an electron. It is difficult to identify photocatalytic active sites to one of them because balk MgO usually includes both CUS ions and F^+ centers on the surface.

We have prepared the MgO/SiO_2 samples free from F^+ centers in the present work, and thus we have examined the role of CUS ions. On these samples, photocatalytic active sites would be restricted to CUS ions. The specific population of such surface ions would be controlled by changing the size of MgO particle dispersed on silica support. Furthermore, we have discussed a relation between the active sites for CO photooxidation and base sites.

Experimental

Samples (MgO/SiO_2, MS) were prepared in the manner described elsewhere.[7] A series of samples of different Mg^{2+} loading were prepared; 1MS (1 wt.% as MgO) to 20MS (20 wt.% as MgO). The loading amounts of MgO were determined by X-ray fluorescence analysis.

Chemisorbed amounts of CO2 on the base site at 273 K were estimated by extrapolation of adsorption isotherms to the zero pressure. X-band electron spin resonance (ESR) spectra were recorded at 77 K using a JEOL JES-PE ESR-spectrometer, and X-ray photoelectron spectra (XPS) were recorded with a Perkin Elmer Phi model 5500 spectrometer.

X-ray absorption spectra were recorded in a total electron yield mode at room temperature with the facility of the BL-7A station at UVSOR in Institute for Molecular Science for Mg *K*-edge with a beryl tow-crystal monochromator.[8] Energy calibration was made by using K-edge absorption of Al in beryl. Samples were mixed with active carbon in dry hexane and were pasted on the first photocathode made of CuBe of the electron multiplier.

Photooxidation of CO was carried out at room temperature in a closed circulating reaction system (250 cm^3). The initial amounts of CO and O_2 as reactants were respectively 200 μmol. Produced CO_2 was immediately frozen out in a liquid N_2 trap and the amount was evaluated by the decrease in pressure of the reaction system. A super high pressure 250 W Hg lamp was used as a light source.

Results and discussion

F^+ centers

ESR study was carried out to detect F^+ centers on the sample. F^+ centers and Mn ions as impurity were detected for a commercial MgO bulk sample evacuated at 673 K. Fig. 1(*a*) shows ESR signals due to F^+ centers of MgO bulk.

With UV-irradiation in vacuo, the signal intensity due to F^+ centers increased [Fig. 1(*b*)], but in the presence of O_2 the signal decreased significantly [Fig. 1(*c*)], indicating that the F^+ centers exist on the surface of bulk MgO.

On the contrary, 17MS sample did not exhibit such a signal. Only small unidentified signals were observed on the broad back ground due to the silica support. Back ground subtracted ESR spectra of 17MS sample are shown in Fig. 1(*d*)-(*f*). Since these small signals are characterized by different g values from those of F^+ centers mentioned above and were not affected by UV-irradiation [Fig. 1(*e*)] and were not quenched by O_2 molecules [Fig. 1(*f*)], these signals are different from that due to the F^+ centers. From these results, we have concluded that MS samples are free from F^+ centers. Even if they were other kinds of F^+

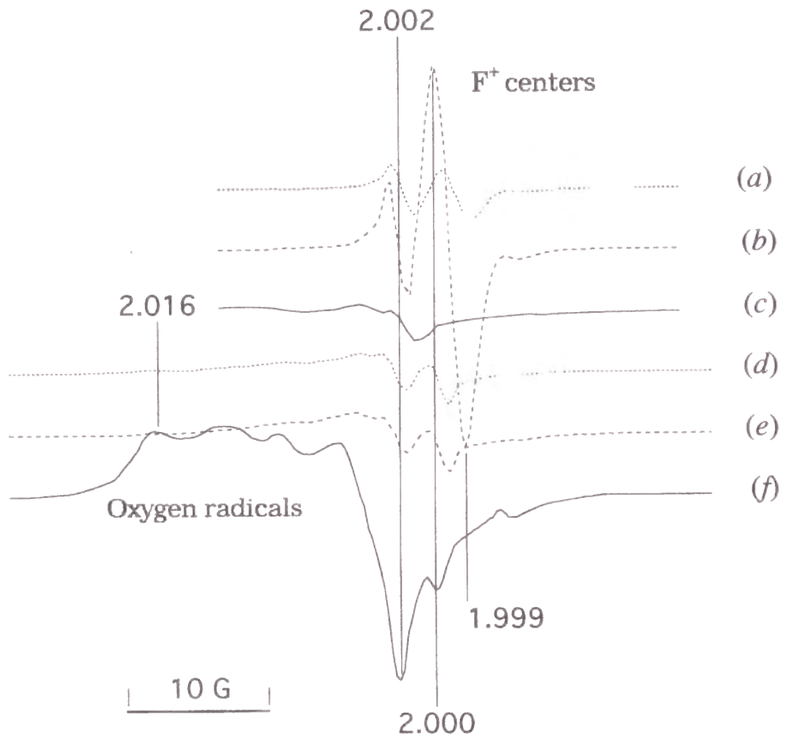

Fig. 1 ESR spectra of bulk MgO sample (*a*) *in vacuo*, (*b*) *in vacuo* under irradiation, (*c*) in the presence of O_2 under irradiation, and 17MS sample (*d*) *in vacuo*, (*e*) *in vacuo* under irradiation, (*f*) in the presence of O_2 under irradiation. Spectra were recorded at 77 K.

centers, these F^+ centers are not related to photooxidation because that they are not excited by irradiation [Fig. 1(*e*)].

In the presence of O_2 under UV-irradiation [Fig. 1(*f*)], some undefined signals by presumable oxygen radicals were obviously detected. It strongly suggests that these oxygen radicals would bring about the photooxidation on the MS samples.

Local structure and dispersion

In order to obtain fine particles of MgO, we prepared MS samples in which the loading amount of magnesium oxide were less than 20 wt.% as MgO. These samples exhibited no appreciable peaks in the XRD pattern. Therefore, XANES and XPS analyses were carried out to obtain information about the local structure and dispersion of magnesium oxide on silica.

XANES spectra are sensitive to coordination symmetry around the target atoms. Figure 2 shows XANES spectra of MS samples (*b*)-(*d*) together with that of bulk MgO and several compounds as references (*a*), (*e*)-(*i*). All MS samples gave approximately the same spectra regardless of the loadings. They are identical with that of MgO of a typical rock salt structure but different from that of other reference compounds. It indicates that Mg ions in MS samples are located at a center of a regular octahedron of oxygen ions.

It was possible that a compound such as $MgSiO_3$ or Mg_2SiO_4 were produced in MS samples. However, the XANES spectra of these compounds [Fig. 2(h),(i)] are quite different from that of MS samples, suggesting that there are no such compounds but magnesium oxide of rock salt structure in MS samples. Therefore, magnesium oxide particles in MS samples would possess the same characters as those of bulk MgO.

The surface concentration of MgO in MS samples estimated by XPS is shown in Fig. 3. The surface concentration increases linearly with the loading of magnesium oxide up to 5 wt.%, but the linearity did not hold above 5 wt.%. It suggests that MgO is highly dispersed as crystallite of raft-like structure in the samples up to 5 wt.% loading, and the crystallites have grown to large particles in the samples of loading above 5 wt.%.[9]

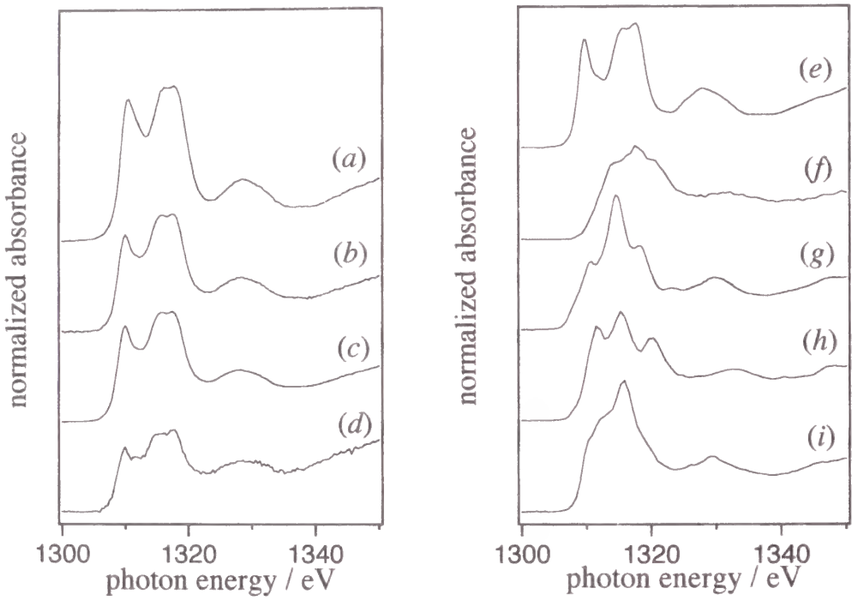

Fig. 2 Mg *K*-edge XANES of MS samples and references; (*a*) MgO prepared by calcination of $Mg(OCH_3)_2$, (*b*) 20MS, (*c*) 5MS, (*d*) 1MS, (*e*) pulverized MgO single crystal, (*f*) $Mg(OCH_3)_2$ extracted from methanol solution, (*g*) $Mg(OH)_2$ evacuated at 473 K, (*h*) $MgSiO_3$, (*i*) Mg_2SiO_4.

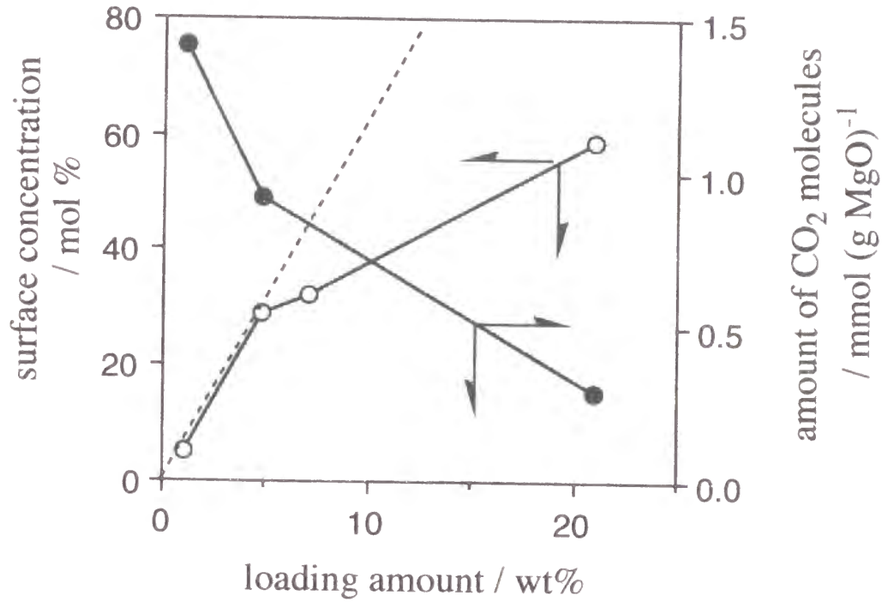

Fig. 3 Surface concentration of MgO in MS samples estimated by XPS, and amount of CO_2 molecules adsorbed on the base sites of MgO.

The results mentioned above indicate that MgO crystallites sizes were controlled by changing amount of loading of MS samples, so that specific population of CUS ions could be controlled.

Amount of base sites

We estimated specific population of base sites on MgO surface using the characteristic property of CO_2 molecules which are adsorbed selectively on the base sites.[1] As shown in Fig. 3, the smaller loading amount of MgO is, the larger amount of chemisorption normalized to one gram of MgO is. This shows that normalized amount of base sites on the surface of magnesium oxide in these samples decreases with an increase in loading amount of MgO, even in the case of that MgO crystallites present as the raft-like structure. Since specific population of CUS ions on magnesium oxide is larger in MS samples of low loading, it suggests that base sites relate to CUS ions.

Photooxidation of CO

The amount of catalysts for CO photooxidation was adjusted as that the equal amount of MgO crystallites (5 mg, 125 μmol) is contained, therefore, the conversion of CO is proportional to the specific activity of the MgO crystallites. The time course of photooxidation is shown in Fig. 4. Each sample exhibited an induction period about for 40 minutes. After the induction period, the conversion increased with time linearly. The reaction did not proceed in the dark, indicating it was photocatalytic oxidation. The photooxidation took place very slowly on silica without magnesium oxide loading, suggesting that photocatalytic active sites exist on the MgO crystallites.

Obviously in Fig. 4, a lower loading MS sample exhibits higher activity. Since the lower loading sample is supposed to have higher specific population of CUS ion pairs, it is indicated that the photoactive sites are the CUS ions on magnesium oxide fine particle.

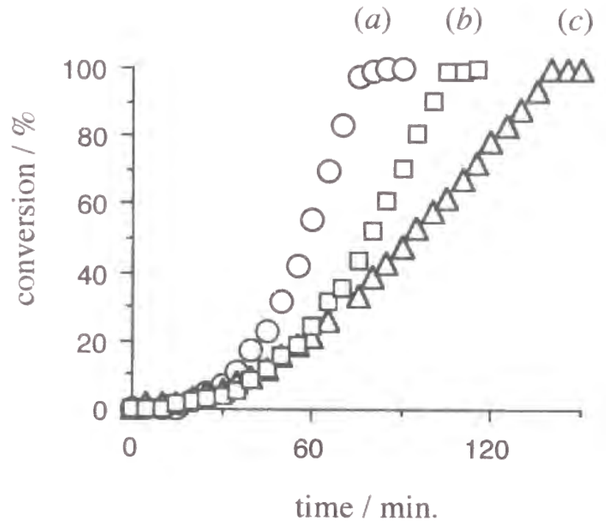

Fig. 4 Time course of CO photooxidation on MS samples; (*a*) 1MS, (*b*) 5MS and (*c*) 20MS.

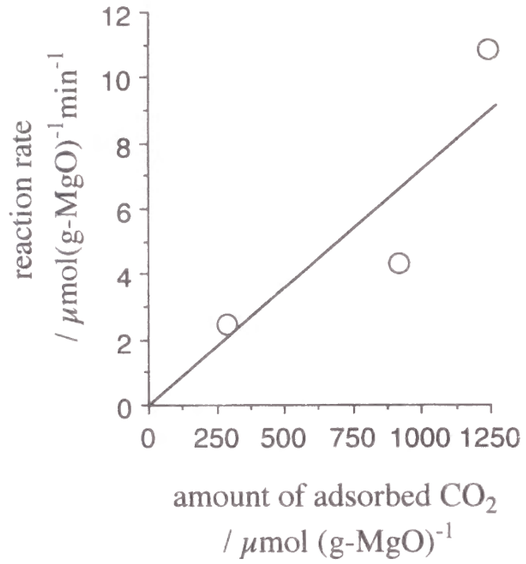

Fig. 5 Relation between reaction rate of CO photooxidation and the amount of chemisorbed CO_2 on MS samples.

Fig. 5 shows a relationship between reaction rate of CO photooxidation and the amount of chemisorbed CO_2 on MS samples. The reaction rate was evaluated from the region of the last 20 minutes. This good correlation between amount of chemisorbed CO_2 and reaction rate indicates that base site and photoactive site are identical. Since the photoactive sites are (Mg_{CUS}-O_{CUS}) pairs, we have concluded that base sites are the O_{CUS} ions in the pairs.

Conclusion

As a conclusion, the coordinatively unsaturated surface Mg and O ion pairs on the magnesium oxide fine particle in the MgO/SiO_2 samples function as catalytic active sites in the photooxidation of CO. The base sites on the magnesium oxide detected as adsorption sites of CO2 coincide with such CUS ion pairs.

References

1 K. Tanabe, M. Misono, Y. Ono, H. Hattori, *New Solid Acids and Bases* , Kodansha, Tokyo, 1989.

2 H. Kawakami and S. Yoshida, *J. Chem. Soc., Faraday Trans. 2*, 1984, **80**, 921.

3 A. J. Tench and G. T. Pott, *Chem. Phys. Lett.*, 1974, **26**, 590.

4 S. Coluccia, A. M. Deane and A. J. Tench, *J. Chem. Soc., Faraday Trans. 1*, 1978, **74**, 2913; S. Coluccia and A. J. Tench, *J. Chem. Soc., Faraday Trans. 1*, 1979, **75**, 1769; S. Coluccia and A. J. Tench, *Proc. 7th Int. Congr. Catal.*, Kodansha, Tokyo, 1981, p. 1154; S. Coluccia, A. Barton and A. J. Tench, *J. Chem. Soc., Faraday Trans. 1*, 1981, **77**, 2203; M. Anpo, Y. Yamada, S. Coluccia, A. Zecchina and M. Che, *J. Chem. Soc., Faraday Trans. 1*, 1989, **85**, 609.

5 M. Anpo, Y. Yamada, S. Coluccia, A. Zecchina and M. Che, *J. Chem. Soc., Faraday Trans. 1*, 1989, **85**, 609.

6 V. A. Shvets, A. V. Kuznetsov, V. A. Fenin and V. B. Kazansky, *J. Chem. Soc., Faraday Trans. 1*, 1985, **81**, 2913.

7 T. Tanaka, H. Yoshida, K. Nakatsuka, T. Funabiki and S. Yoshida, *J. Chem. Soc., Faraday Trans.*, 1992, **88**, 2297.

8 T. Murata, T. Matsukata, M. Mori, M. Obashi, S. Naoe, H. Terauchi, Y. Nishihata, O. Matsudo and J. Yamazaki, *J. de Phys.* 1986, **C8**, 135; T, Murata, T. Matsukawa, S. Naoe, T. Horigome, O. Matsudo and M. Watanabe, *Rev. Sci. Instrum.*, 1992, **63**, 1309.

9 F. P. J. M. Kerkhof and J. A. Moulijn, *J. Phys. Chem.*, 1979, **83**, 1612.

Summary

In part I, preparation chemistries of silica-based catalysts are described, and following main results were obtained.

In chapter 1, preparation chemistry of niobium oxide species on silica-support in the equilibrium adsorption method is discussed. The Nb K-edge XAFS study clarified the local structures of niobium complexes in the impregnating solution of niobium oxalate and those of niobium species supported on silica, and provided the following conclusions. Almost all the niobium oxide species on the samples prepared in the equilibrium adsorption method were tetrahedral. The loading amount and dispersion of tetrahedral species of niobium oxide in the NbO_x/SiO_2 catalysts were essentially determined by the structures in the solution and the adsorption state of the niobium oxalate complexes, and they were controlled by adjusting the niobium and ammonia concentrations of impregnating solutions. The addition of ammonia to the impregnating solution affected not only the pH of the solution but also the states of the liquid-solid interface; the former influenced the structure and adsorption equilibrium of niobium oxalate complexes, while the latter changed the state of adsorption. The loading amount of niobium oxide species on silica could be controlled by adjusting the niobium and ammonia concentration of the impregnating solution in the preparation. Although at pH 0.8-4 the loading amount is determined only by the niobium concentration, when the solution was adjusted at pH 5, the loading amount increases more than two times on keeping a highly dispersion, where the tetrahedra species existed as small oligomers without much aggregation. When the samples were prepared from the solution of pH 0.8-4 in the presence of ammonia, a small oligomer composed of the tetrahedral species on silica was formed. The highest dispersion of niobium oxide species was obtained from the solution of pH 0.8 that did not contain ammonia. In the sample, niobium oxide species were highly dispersed monomeric tetrahedra.

In chapter 2, preparation chemistry of silica-magnesia systems is discussed. The Mg K-edge XAFS study clarified the local structure of silica-magnesia systems prepared by four ways; by impregnation of silica with an aqueous solution of magnesium nitrate or with a methanol solution of $Mg(OCH_3)_2$, and by sol-gel method with tetraethyl orthosilicate and magnesium solutions mentioned above. The structure of Mg species was dependent on the preparation method. MgO particles on silica, where a Mg ion is located octahedral site, were formed by the method of impregnation of silica with a methanol solution of $Mg(OCH_3)_2$. Highly dispersed Mg species on silica surface, which are strongly interacted with surface silica matrix, were obtained by impregnation of silica or sol-gel method with an aqueous solution of magnesium nitrate. When the sample was prepared by sol-gel method with tetraethyl orthosilicate and a methanol solution of $Mg(OCH_3)_2$, tetrahedral Mg species were dispersed in the silica matrix.

In part I, some examples of the modification method of silica (preparation method of silica-based catalysts) are presented. Especially the highly dispersed active species on the silica surface are prepared in these ways. In those ways, silica photocatalysts will be more improved in the near future.

In part II, silica and silica-based materials were characterized by means of phosphorescence spectroscopy, and some emission and excitation bands were assigned to surface species.

In chapter 3, MgO/SiO_2 catalysts were characterized by photoluminescent spectroscopy and it was found that new phosphorescent active species were formed on the silica surface. Mg-loaded silica evacuated at a high temperature (1073 K) exhibited the fine structure on the emission spectra. The fine structure was observed clearer for a lower-loaded sample than for a higher-loaded sample. Therefore, highly dispersed Mg species with Mg-O bonds interacting with the SiO_2 surface, would be related to the luminescence. The emission was quenched by contact with oxygen and CO. The activity for photooxidation of CO on the low-loaded sample evacuated at 1073 K was higher than that on the sample evacuated at 773 K, suggesting that the luminescent surface species are also photocatalytic active sites.

In chapter 4, photoluminescent excitation and emission spectra resulting from hydroxy groups were described. In this study, highly dispersed magnesium oxide supported on silica was employed. During preparation of the sample, the luminescence-active silanols were lost by the reaction with $Mg(OCH_3)_2$. Coordination states of hydroxy groups produced by the reaction of the Mg-O species with added H_2O were estimated from their photoluminescent excitation spectra. We concluded that hydroxy group attached to the surface Mg ion is excited by 255 nm light, and that hydroxy groups coordinated to Mg ions within the silica matrix are excited by 265 nm light. Other surface hydroxy groups or hydroxy groups of $Mg(OH)_2$ microcrystallites, that produced by addition of an excess H_2O, are excited by 260 nm light. The emission spectra relating to hydroxy groups show a broad band centered at 440 nm regardless of their coordination states.

In chapter 5, phosphorescence spectra of dehydrated silica-alumina binary oxides are presented. It was found that the fine structure was clearly observed in the phosphorescent emission spectra of silica-alumina evacuated at a high temperature (1073 K) and excited by 300 nm light, although it was not observed in silica or alumina alone. We concluded that the fine structure on the emission spectra is due to the coordinatively unsaturated sites on the surface linkage of M-O-Si (M: Al, Mg). It is also suggested that other heterolinkages on silica may be photoactive.

In part II, the phosphorescence spectroscopy is demonstrated to be useful for the characterization of photoactive sites on silica-based catalysts. The photoactive site would have a high possibility to be photocatalytic active site.

In part III, the photocatalysis, metathesis of olefins and oxidation (epoxidation) of propene, on silica and silica based catalysts are presented.

In chapter 6, the first findings about metathesis reactions of olefins over amorphous silica under UV-light irradiation are described. Propene was selectively converted into ethene and butene on amorphous silica evacuated at a high temperature (1073 K). Metathesis of ethene was also confirmed by using labeled ethene. The activity increased with an increase in the pretreatment temperature, indicating that the dehydration produces the active sites.

In chapter 7, it was found that the mesoporous silica material (FSM-16) catalyzed metathesis of propene under photoirradiation with a higher activity than amorphous silica, whereas microporous silica crystals (silicalite-1) did not catalyze the reaction. The key point would be that FSM-16 has many hydroxyl groups on the amorphous walls that constitute the hexagonal mesopore structure. The active sites are proposed to be produced by dehydration of the amorphous surface of silica.

In chapter 8, photooxidation over Nb_2O_5/SiO_2 catalyst was investigated and it was found that photoepoxidation of propene by O_2 proceeds over the catalysts. Nb_2O_5/SiO_2 catalysts were prepared by an equilibrium adsorption method (type A) and a conventional evaporation to dryness method (type E), and the correlation between the structure of niobium oxide species and photooxidation activity was discussed. Among low-loaded samples, the type A catalyst contains monomeric NbO_4 tetrahedra and the type E catalyst contains oligomeric NbO_4 tetrahedra. Propene photo-oxidation over monomeric NbO_4 species on the type A catalysts yields propene oxide selectively, whereas the photo-oxidation over oligomeric NbO_4 species on the type E catalyst with low-loading yields propanal selectively. Propanal is the product in decomposition of propene oxide on oligomeric NbO_4 tetrahedra.

In chapter 9, the results on photooxidation of propene by O_2 over silica and Mg-loaded silica evacuated at a high temperature (1073 K) are shown. Silica was found to promote the photooxidation of propene by molecular oxygen, yielding acetaldehyde, propylene oxide, propionaldehyde. The yield of and selectivity to propylene oxide were improved significantly by modification of silica with 1 wt % magnesium oxide loading. Mg K-edge XANES and phosphorescence spectra indicated that the active sites on the Mg-loaded silica for epoxidation of propene are highly dispersed and isolated magnesium oxide species. Small aggregates of magnesium oxide on silica promotes photooxidation to acetaldehyde predominantly. Since propene metathesis did not occur in the presence of gaseous oxygen, it is suggested that the active sites are the same in two reactions, photometathesis and photooxidation.

In part III, it was found that the photometathesis of olefins and photoepoxidation of propene by O_2 proceed over amorphous silica, mesoporous silica, Mg-loaded silica and Nb-

loaded silica. A new family of photocatalysts, the silica and silica-based catalysts, are presented here, although the details on the mechanism and the active sites are still unclear.

The author wishes that these studies compiled in this thesis will be followed by many investigations, and a family of the silica-based photocatalysts would be more developed.

List of publications

Part I

Chapter 1

1. *XAFS Study of Niobium Species Formed during the Preparation of Nb/SiO_2 Catalysts by the Equilibrium Adsorption Method*
   H. Yoshida, T. Tanaka, T. Yoshida, T. Funabiki and S. Yoshida,
   Physica B, 1995, **208&209**, 681-682.

2. *Control of the Structure of Niobium Oxide Species on Silica by the Equilibrium Adsorption Method*
   H. Yoshida, T. Tanaka, T. Yoshida, T. Funabiki and S. Yoshida,
   Catal.Today, 1996, **28**(1-2), 79-90.

Chapter 2

3. *Mg K-Edge XANES Study of Silica-Magnesia Systems*
   H. Yoshida, T. Yoshida, T. Tanaka, T. Funabiki, S. Yoshida, T. Abe, K. Kimura and T. Hattori
   J. Physique IV, 1997, **7**, C2-911.

Part II

Chapter 3

4. *Photoluminescence of Magnesium Oxide Species supported on Silica*
   T. Tanaka, H. Yoshida, K. Nakatsuka, T. Funabiki and S. Yoshida
   J. Chem. Soc., Faraday Trans., 1992, **88**(15), 2297-2298.

Chapter 4

5. *Photoluminescence Spectra Resulting from Hydroxyl Groups on Magnesium Oxide Supported on Silica*
   H. Yoshida, T. Tanaka, T. Funabiki and S. Yoshida,
   J. Chem. Soc., Faraday Trans., 1994, **90**(14), 2107-2111.

Chapter 5

6. *Fine Structure in Phosphorescence Spectra of Silica-Alumina*
   H. Yoshida, T. Tanaka, A. Satsuma, T. Hattori, T. Funabiki and S. Yoshida
   Chem.Commun., 1996, 1153-1154.

Part III

Chapter 6

7. *Alkene Metathesis on Photoirradiated Silica Surface*
   H. Yoshida, T. Tanaka, S. Matsuo, T. Funabiki and S. Yoshida,
   J. Chem. Soc., Chem.Commun., 1995, 761-762.

Chapter 7

8. *Catalytic Activity of FSM-16 for Photometathesis of Propene*
   H. Yoshida, K. Kimura, Y. Inaki and T. Hattori
   Chem.Commun., 1997, 129-130.

Chapter 8

9. *Preparation of Highly Dispersed Niobium Oxide on Silica by Equilibrium Adsorption Method*
   T. Tanaka, H. Nojima, H. Yoshida, H. Nakagawa, T. Funabiki and S. Yoshida
   Catal.Today, 1993, **16**(3-4), 297-307.

Chapter 9

10. *Photooxidation of Propylene by O_2 over Silica and Mg-Loaded Silica*
    H. Yoshida, T. Tanaka, M. Yamamoto, T. Funabiki and S. Yoshida
    Chem.Commun., 1996, 2125-2126.

11. *Epoxidation of Propene by Gaseous Oxygen over Silica and Mg-Loaded Silica under Photoirradiation*
    H. Yoshida, T. Tanaka, M. Yamamoto, T. Yoshida, T. Funabiki, and S. Yoshida
    J. Catal., 1997, **171**(2), 351-357.

Appendix

Chapter 10

12. *Base site of Magnesium Oxide Dispersed on Silica as Active Sites for CO Photooxidation*
    H. Yoshida, T. Tanaka, K. Nakatsuka, T. Funabiki and S. Yoshida,
    in *Acid-Base Catalalysis II*, Kodansha, Tokyo, 1994, 473-478.

The following papers are not included in this thesis.

13. *Na K-Edge XAFS Study of Sodium Loaded on Alumina*
    S. Hasegawa, M. Morooka, H. Aritani, H. Yoshida and T. Tanaka
    Jpn. J. Appl. Phys., 1993, **32**, 508-510.

14. *A XANES Study on the Dehydration Process of Magnesium Hydroxide*
    T. Yoshida, T. Tanaka, H. Yoshida, S. Takenaka, T. Funabiki, S. Yoshida and T. Murata,
    Physica B, 1995, **208&209**, 581-582.

15. *Study of Dehydration of Magnesium Hydroxide*
    T. Yoshida, T. Tanaka, H. Yoshida, T. Funabiki, S. Yoshida and T. Murata,
    J. Phys. Chem., 1995, **99**(27), 10890-10896.

16. *XAFS Study of Niobium Oxide on Alumina*
    T. Tanaka, T. Yoshida, H. Yoshida, H. Aritani, T. Funabiki, S. Yoshida, J.-M. Jehng and I. E. Wachs
    Catal.Today, 1996, **28**(1-2), 71-78.

17. *Study on the Dispersion of Nickel Ions in NiO-MgO System by X-Ray Absorption Fine Structure*
    T. Yoshida, T. Tanaka, H. Yoshida, T. Funabiki, and S. Yoshida,
    J. Phys. Chem., 1996, **100**, 2302-2309.

18. *Influence of Local Structure on the Catalytic Activity of Gallium Oxide for the NO Selective Reduction by CH_4*
    K. Shimizu, M. Takamatsu, K. Nishi, H. Yoshida, A. Satsuma and T. Hattori,
    Chem.Commun., 1996, 1827-1828.

19. *Structural Analysis of CoO-MgO System by XAFS*
    T. Yoshida, T. Tanaka, H. Yoshida, T. Funabiki, S. Yoshida and S. Hasegawa
    J. Physique IV, 1997, **7**, C2-1145.

20. *Novel Method for Preparation of High Surface Area SnO_2 -Solvent Replacement by Alcohol*
    K. Suzuki, A. Satsuma, H. Yoshida and T. Hattori
    Chem. Lett., 1997, 279.

21. *Olefin metathesis over UV-Iradiated Silica*
T. Tanaka, S. Matsuo, T. Maeda, H. Yoshida, T. Funabiki and S. Yoshida
Appl. Surf. Sci., in press.

22. *Formation of Multi-Branched-Chain Aliphatics in Methanol Conversion over Modified Mordenites*
K. Nishi, T. Shimizu, H. Yoshida, A. Satsuma and T. Hattori
Appl. Catal., in press.

23. *Surface Reaction of the Selective Reduction of NO with Propene over Na-H-Mordenite as Investigated by Dynamic FT/IR*
A. Satsuma, T. Enjoji, K. Shimizu, K. Sato, H. Yoshida and T. Hattori
J. Chem. Soc., Faraday Trans., in press.

24. *Performance of YB66 Soft X-ray Monochromator Crystal at the Wiggler Beam Line of the UVSOR Facility*
T. Kinoshita, Y. Takata, T. Matsukawa, H. Aritani, S. Matsuo, T.Yamamoto, M. Takahashi, H. Yoshida, T. Yoshida, Y. Ufuktepe, K. G. Nath, S. Kimura, H.Kumigashira and Y. Kitajima
J. Synchrotron Rad., in press.